BHP Iron Ore Pty Ltd
A.B.N. 46 008 700 981
City Square
125 St Georges Terrace
PERTH WA 6000

ENGINEERING DOCUMENT

# PROJECT REPORT	PAGE 1 of 83
NUMBER PREP-040-G-12127/0	
DESCRIPTION INDUSTRIAL FACILITIES - OREBODY 32 SERVICES - SURPLUS WATER MANAGEMENT DEFINITION PHASE STUDY CREEK DISCHARGE MODELLING REPORT	
OFFICE OF ORIGIN ADVISIAN **WRITTEN BY** YINGYUAN SHI / ANTHONY BARR **CHECKED BY** STEFAN BERGER **TITLE OF CHECKER** SENIOR ENGINEER	**CONTRACT:** FX00.O.90029

STATUS REVIEW BY BHPIO RESPONSIBLE MANAGER/ENGINEER

SIGNED

REVIEWED ....
(Alpha or Numeric)

REVIEWED AS NOTED ....
(Alpha or Numeric)

REVISE AND RESUBMIT ....
(Alpha or Numeric)

REVIEWED BY BHPIO RESPONSIBLE MANAGER
(Numeric)

....

Rev.	Date	Description	By	Checked	BHPIO
A	19/08/22	Issued for Internal Review	SB	AB	
B	13/09/22	Issued for Client Review	AB / YS	SB	
C	01/05/23	Issued for Study	AB / YS	SB	
0	01/12/23	Issued for Use	AB / YS	SB	
			Yingyuan Shi Digitally sign	Digitally signed by Stefan Berger Date: 2023.12.01 10:33:42 +08'00'	

TABLE OF CONTENTS

DESCRIPTION **PAGE No.**

Appendices

Units & Abbreviations

Abbreviation	Meaning
2D	Two-dimensional
5YP	Five-year plan
BoM	Bureau of Meteorology
BWT	Below water table
CAPEX	Capital expenditure
DEM	Digital elevation model
DPS	Definition Phase Study
ER	Eastern Ridge
ET	Evapotranspiration
FY	Financial year
GS	Gauging station
HPC	Heavily parallelised compute
ILCL	Initial Loss/Continuing Loss
IPR	Independent peer review
IPS	Identification Phase Study
LiDAR	Light Detection and Ranging
MAR	Managed aquifer recharge
MCA	Multi-criteria assessment
ML	Megalitre(s)
ML/d	Megalitres per day
mm/d	Millimetres per day
mm/h	Millimetres per hour
OPEX	Operational expenditure
OB32	Ore Body 32

Oph	Ophthalmia
SME	Subject matter expert
SPS	Selection Phase Study
TN	Turkey’s nest

1 EXECUTIVE SUMMARY

The existing TUFLOW and GoldSim models developed to simulate creek discharge during the Selection Phase Study (SPS) were calibrated based on the provision of additional data by BHP. The focus of the calibration was to refine the conceptualisation and parameterisation of the GoldSim groundwater model and ensure that both models replicated the timing and extent of the wetting front associated with monitored discharge events. Surface water flow was modelled with the TUFLOW Heavily Parallelised Compute (HPC) software package while water balance modelling was carried out using GoldSim. The two models were coupled to provide a link between surface and subsurface water flows.

A variety of different scenarios were simulated to estimate the time taken for the wetting front to reach downstream points of interest after being released from the proposed Homestead Creek discharge location. It is estimated that the wetting front associated with a continuous discharge rate of 60 ML/day would reach Jigalong Road after 1,807 days.

Steady state modelling was conducted by removing the influence of alluvial storage to determine the maximum continuous and pulsed discharge rates which could be adopted without the wetting front reaching Jigalong Road and Nullagine Road. It was found that a continuous discharge rate of 47.5 ML/d resulted in the TUFLOW model reaching steady state before the wetting front arrived at Jigalong Road. A continuous discharge rate of 82 ML/d resulted in the TUFLOW model reaching steady state before the wetting front arrived at Nullagine Road.

Once the TUFLOW model had reached steady state, a hydrograph representing 1:2-year annual exceedance probability (AEP), 72-hour event from the upstream Homestead Creek catchment was applied as an inflow. In the case of the 47.5 ML/day scenario, the model took 15 days return to steady state. For a discharge rate of 82 ML/d, the model took 27 days to return to steady state.

The optimised pulse scenarios to Jigalong Road and Nullagine Road were designed based on the results of the optimised continuous discharge scenarios. Starting from steady state conditions, it was found that a cycle of 30 days with no discharge followed by 12 days with discharge resulted in sufficient drying time to prevent the wetting front reaching Jigalong Road (60 ML/day rate) and Nullagine Road (120 ML/day rate).

Additional discharge scenarios were modelled, the results of which are presented and discussed in the body of the report.

2 INTRODUCTION

2.1 Project background

BHP operates the Eastern Ridge (ER) Mine in the Pilbara region of Western Australia. Surplus water generated from below water table (BWT) mining activities at ER is managed via the integrated Eastern Pilbara Surplus Water Management System servicing ER, Mt Whaleback, Ore Body 18, Ore Body 31, and Jimblebar.

Ore Body 32 (OB32) is a BWT deposit in the five-year mine plan (FY21 5YP). Dewatering of the ore body will produce large volumes of water, which will need to be transferred from the pit to local demand points or suitable discharge locations. The existing surplus water system at ER does not support OB32 and thus a new surplus water solution is required to enable mining of OB32 per the FY21 5YP.

The work detailed in this report forms part of the OB32 Surplus Water Definition Phase Study (DPS). This study follows on from the SPS, which was completed in August 2021.

The wetting front modelling conducted during the SPS involved a combination of surface water modelling (using TUFLOW) and water balance modelling (using GoldSim) to estimate the timing and extent of the potential wetting front associated with various creek discharge scenarios and locations. The preferred solution, selected during the Identification Phase Study (IPS) and refined in the SPS, requires additional surplus water management capability to discharge (nominally) 60 ML/d to Ophthalmia Dam with an off take to enable future creek discharge to Homestead Creek and Fortescue River.

2.2 Project location

OB32 is a deposit within BHP’s Newman East operations, a subset of Eastern Ridge approximately 6 km northeast of Newman (see

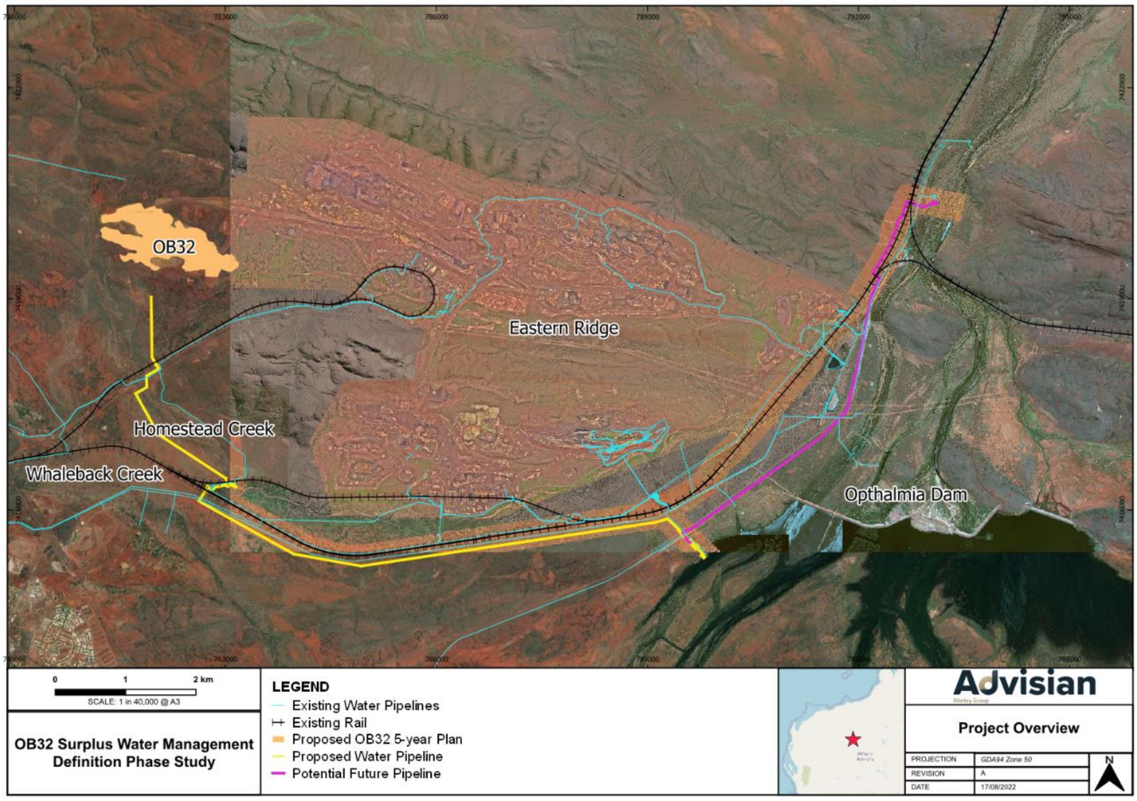

Figure 2-1).

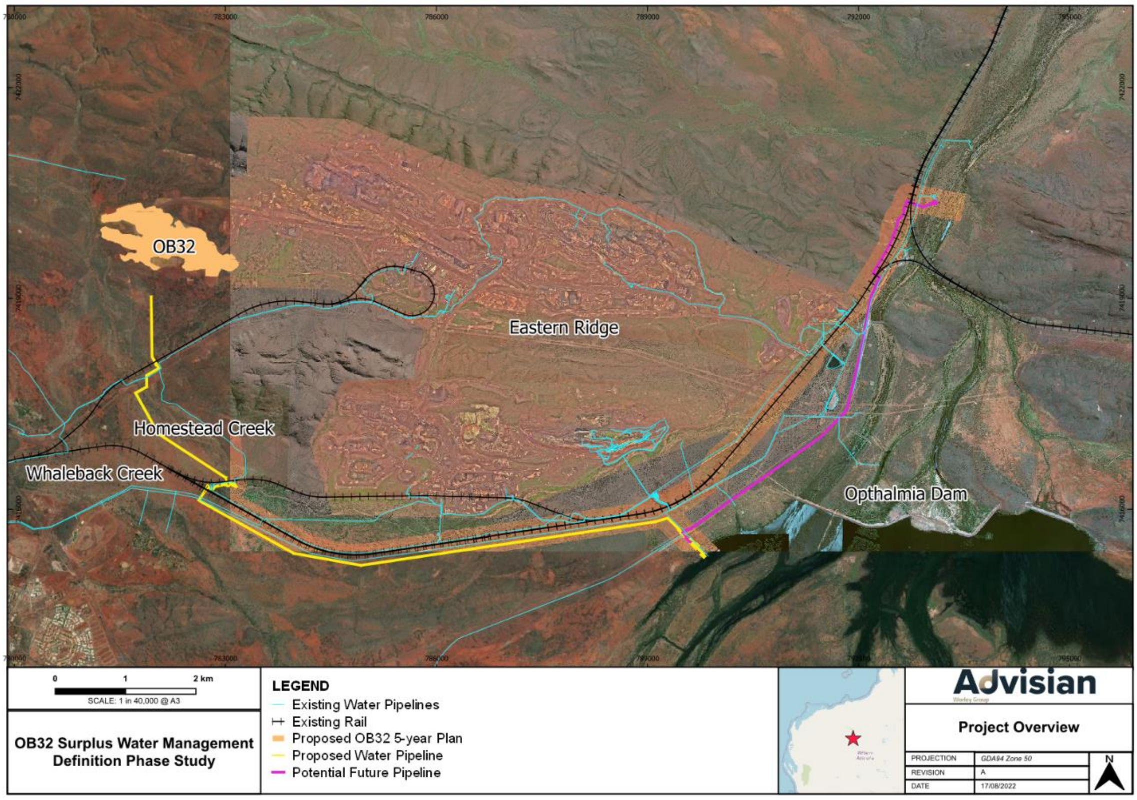

Figure 2-1: Project overview

2.3 Project scope

The scope of work for this project was to calibrate the existing TUFLOW and GoldSim models (from the SPS) with updated assumptions, based on the provision of additional geological, hydrogeological and discharge trial data, with a focus on refining the conceptualisation and parameterisation of the GoldSim goundwater model. The updated and calibrated models were required to determine the likely downstream wetting front extent and timing for various discharge rates applied to the creek system. This work was completed through a combination of 2D surface water and groundwater balance modelling using the software packages TUFLOW (BMT, 2022) and GoldSim (GoldSim Technology Group LLC, 2021).

The modelling was to account for the underlying geology of the creeks to include constraints pertaining to the available storage within geology strata and overlying alluvium in the creek bed. It also included simulation of how the wetting footprint, from surplus water discharge, extends and contracts during and following natural rainfall/creek flow events, to inform development of approval conditions regarding the wetting footprint limit.

A key component of the work included updating and calibrating of the models with reference to:

- Historical creek flow / loss data from gauging stations, and groundwater level responses to creek flow events from BHP’s existing monitoring network. A key output of this calibration was the improved conceptualisation and parameterisation (including a range of plausible hydraulic parameters) of the GoldSim groundwater model under both saturated (after prolonged creek discharge) and unsaturated conditions.

- Recent geological drill hole data north of Ethel Gorge.

Prior to undertaking model runs, a review of the most appropriate method for estimating infiltration losses was undertaken in conjunction with BHP. This ensured the adopted method was able to adequately reflect the key processes of infiltration along a narrow section of river, percolation down to the water table, filling of alluvial aquifer storage, and lateral propagation of water away from river channel. The technique for estimating evaporation and evapotranspiration was reviewed and agreed upon prior to commencing modelling. A technical memorandum (Doc No. 311012-00724-HY-MEM-001) outlining all model assumptions was provided to BHP prior to the commencement of modelling work.

The modelling of the wetting front under various discharge scenarios was required to:

1. Estimate the timing associated with propagation of the wetting front associated with specified discharge scenarios (outlined in Section 5.1);
2. Predict the likelihood of the wetting front reaching key locations such as Jigalong Road and Nullagine Road;
3. Assess the change in water balance of the creeks – pre-discharge ecological water availability with a comparison to post-discharge ecological water availability;
4. Characterise of the hydrological processes in the unsaturated zone and the associated storage in the unsaturated zone along Homestead Creek and Fortescue River;
5. Determine maximum continuous discharge rates that can be discharged from each discharge location without the wetting front arriving at (i) Jigalong Road and (ii) Nullagine Road;
6. Recommend proposed wetting / drying cycle times for pulsed discharge;
7. Assess the maximum groundwater levels at a BHP defined point (between Ethel Gorge and Kalgan Creek) before maximum continuous discharge rates (as determined through assessment required in Point 6) can be released; and
8. Report on water fluxes under steady state conditions to support understanding of key flow losses.

Upon the completion of the aforementioned assessments, Advisian undertook sensitivity analysis for:

- eight (8) variations of parameters at a selected discharge site for a specified discharge rate, and

- eight (8) variations of parameters at a selected discharge site for a target wetting front distance.

Variations in the hydraulic conductivity, which affects the infiltration rate and lateral flow away from the creek, the available storage (specific yield), which reflects the capacity of the alluvium to accept infiltration water, the initial depth to groundwater within the alluvium prior to discharge commencing, and external head (gradient) for lateral flow from alluvium to bedrock, formed parts of the sensitivity analysis.

Impacts to wetting front behaviour due to modified infiltration rates resulting from potential precipitate formation were also included in the assessment.

2.4 Purpose of report

The purpose of this report is to outline the methodology and assumptions adopted in the TUFLOW and GoldSim modelling, summarise the results and present recommendations with regards to the timing and duration of the various creek discharge options, provide guidance to minimise impacts to downstream locations of interest.

2.5 Data provided

BHP provided the following data to facilitate the modelling of surface and subsurface flows:

- Aerial survey imagery including:
  - Roy Hill, 2007;
  - Boolgeeda, 2014;
  - Ethel Gorge, 2016; and
  - Ethel Gorge, 2019.
- Alluvial material coverage (including base elevation and thickness of various lithologies) for the area adjacent to Ophthalmia Dam;
- Digital elevation model (DEM) for the Homestead Creek, Ophthalmia Dam, Whaleback Creek and Fortescue River areas;
- Raster dataset of water table elevation (Watertable.tif) supplied as part of a Leapfrog model of the Ophthalmia Dam;
- Infiltration rates taken from 20210805 Selection of Infiltration Rate for Fortescue River Discharge memorandum (Rea, 2021);
- Ophthalmia Dam site investigation data;
- Ethel Gorge hydrogeological investigation bore logs and aquifer testing results;
- Ethel Gorge and Ophthalmia Dam water level observation (both logged and manually dipped); and
- As-built drawings of Ophthalmia Dam (particularly 047-C-01502).

Figures 2-2 to 2-4 outline the coverage of the alluvium, DEM and water table elevation datasets, respectively.

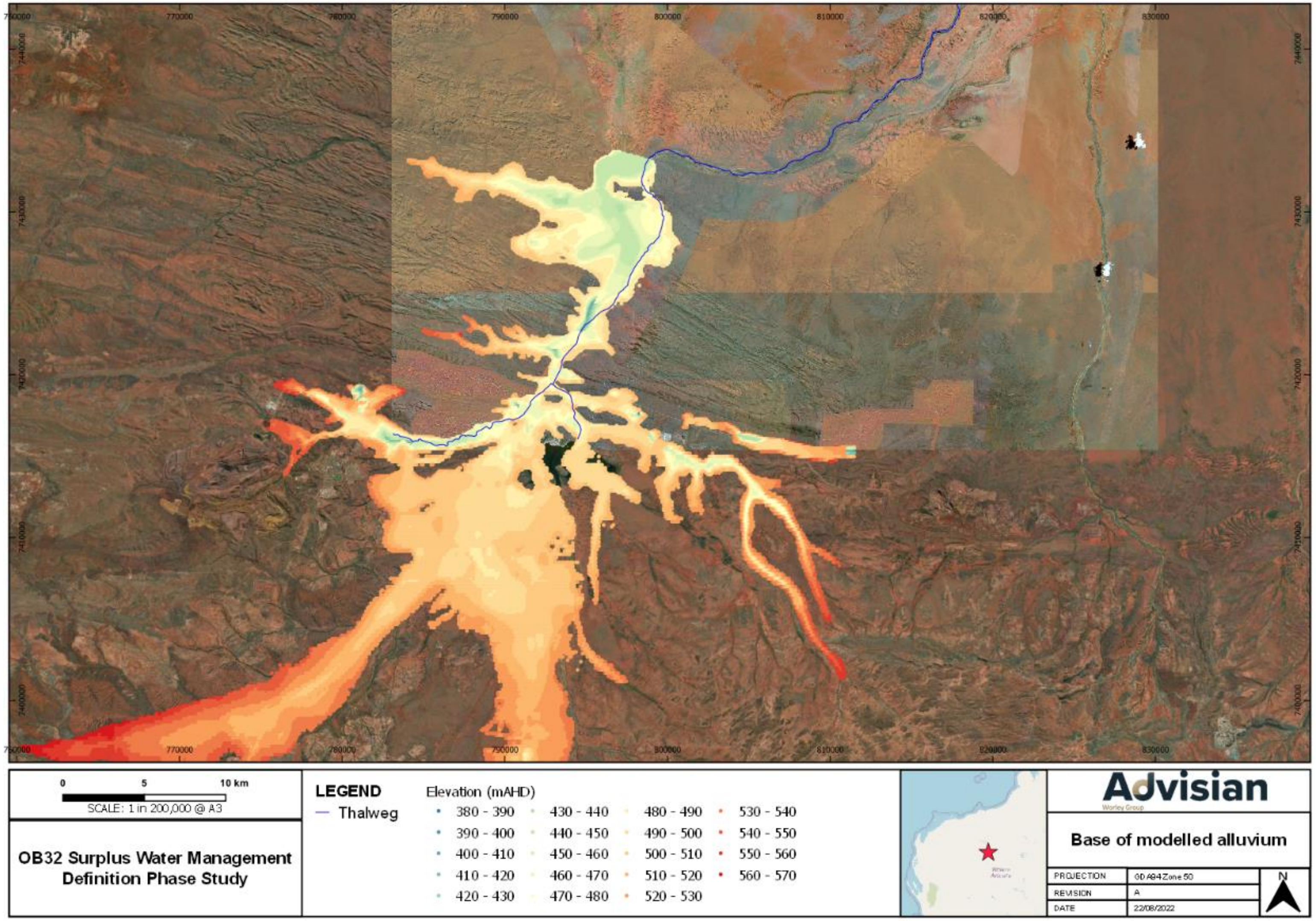

Figure 2-2: Elevation of base of alluvium

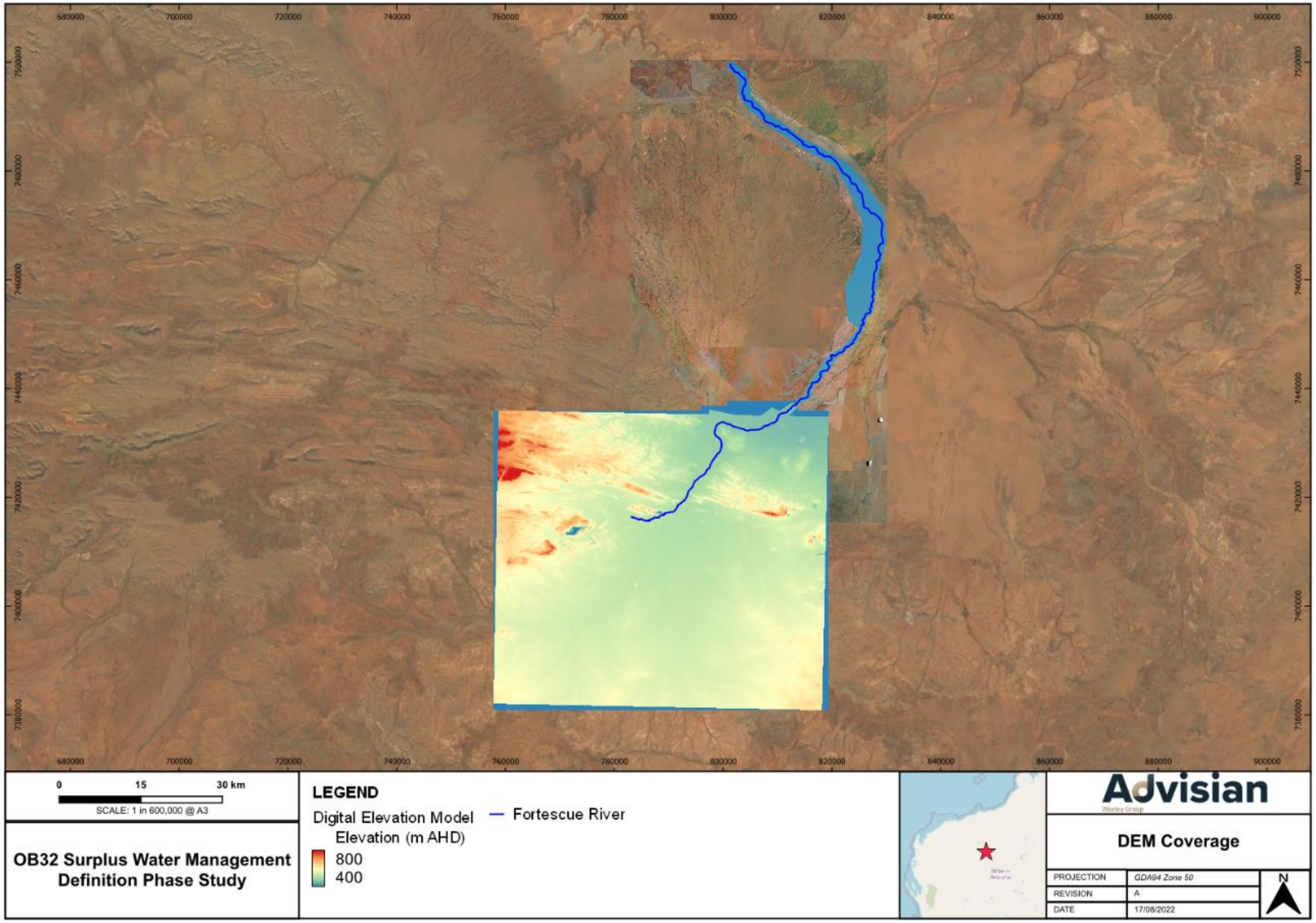

Figure 2-3: DEM coverage

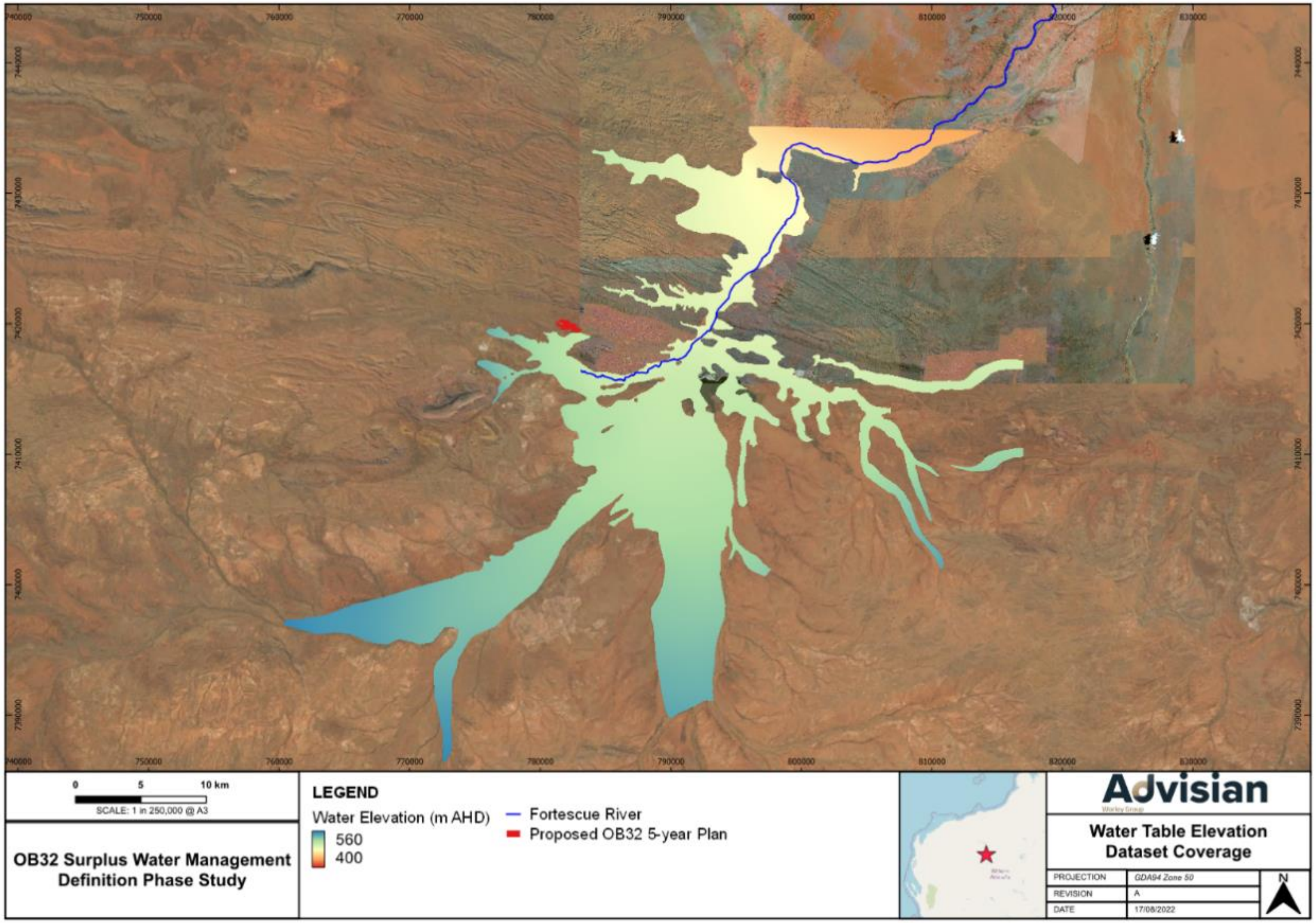

Figure 2-4: Water table elevation dataset coverage

3 WATER BALANCE MODELLING

3.1 Structure

The alluvium part of the water balance model was built in GoldSim version 14.0 (GoldSim Technology Group, LLC, 2021). GoldSim is a simulation package with suitable elements for representing data, time series, storages and interactions between elements. Here the platform is used to represent the shallow alluvial groundwater under a linear connection of reaches of the Homestead Creek-Fortescue River system. Each reach was selected according to local conditions based on hydrological and hydrogeological features. These reaches are shown in Figure 3-1 and described in Table 3-1.

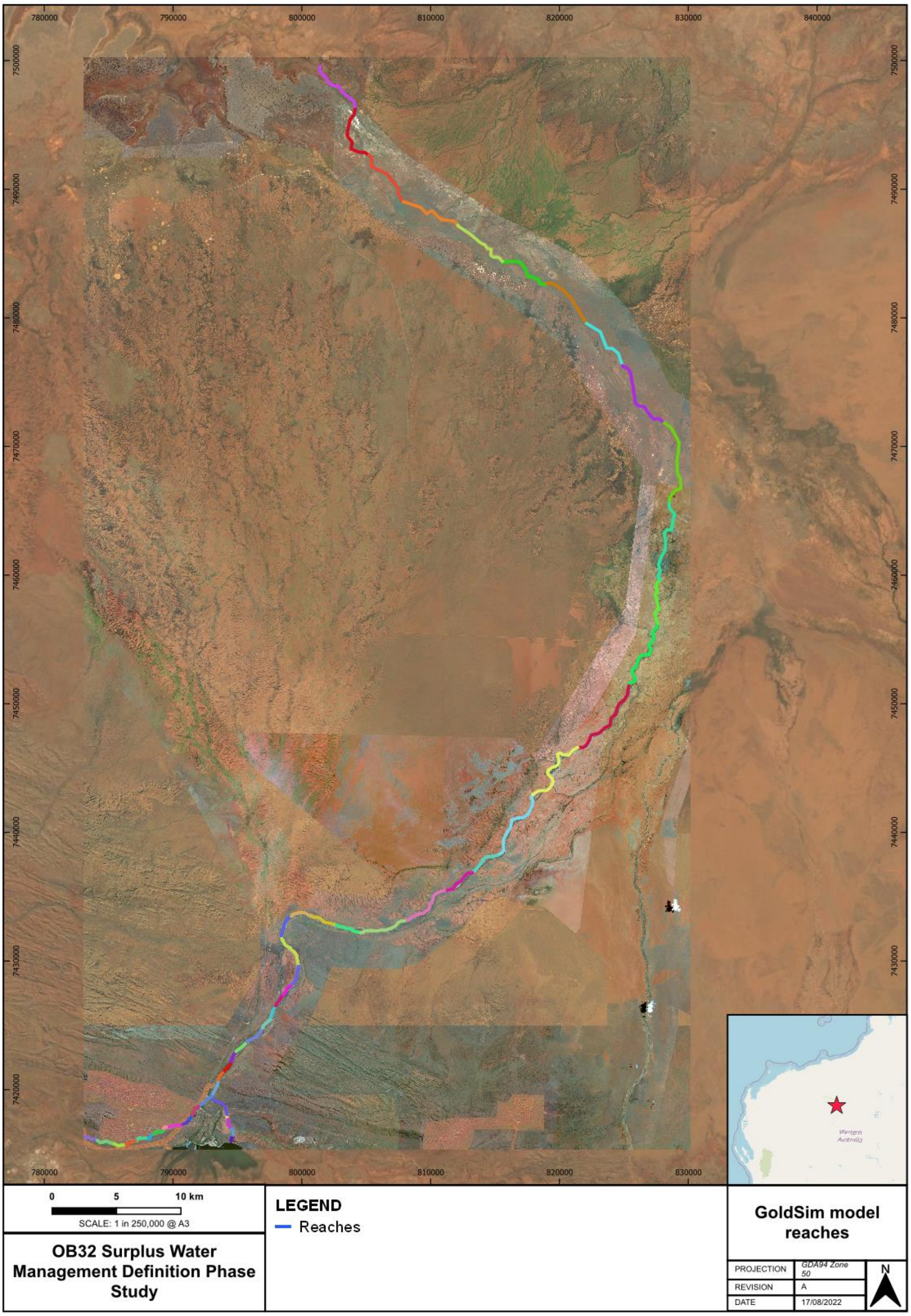

Figure 3-1: Homestead Creek-Fortescue River discharge reaches

Table 3-1: Reach descriptions

Reach ID	Waterway	Inflow(s)	Outflow	Description
1	Homestead Creek	Discharge from OB32	Reach 2	Homestead Creek immediately after discharge point
2	Homestead Creek	Reach 1	Reach 3	Homestead Creek adjacent to OB25 Pit 4 overburden
3	Homestead Creek	Reach 2	Reach 4	Homestead Creek near OB25 administration and workshops
4	Homestead Creek	Reach 3	Reach 5	Homestead Creek near OB25 ROM pad
5	Homestead Creek	Reach 4	Reach 6	Homestead Creek near west OB25 Pit 3 overburden
6	Homestead Creek	Reach 5	Reach 7	Homestead Creek near east OB25 Pit 3 overburden
7	Homestead Creek	Reach 6	Reach 8	Homestead Creek adjacent to OB25 Pit 3
8	Homestead Creek	Reach 7	Reach 9	Homestead Creek adjacent to northwest Ophthalmia Dam
9	Homestead Creek	Reach 8	Reach 10	Homestead Creek adjacent to Ophthalmia Dam Wall A
10	Homestead Creek	Reach 9	Reach 11	Homestead Creek adjacent to Fortescue River in Ethel Gorge to confluence with Fortescue River
11	Homestead Creek	Reach 10	Reach 12	Homestead Creek adjacent to Fortescue River in Ethel Gorge to confluence with Fortescue River, adjacent to upper infiltration basin
12	Homestead Creek	Reach 11	Reach 13	Homestead Creek adjacent to Fortescue River in Ethel Gorge to confluence with Fortescue River, adjacent to lower infiltration basin

13	Homestead Creek/Fortescue River/Shovelanna Creek	Reaches 12 and 18	Reach 19	Fortescue River in Ethel Gorge after confluence with Homestead Creek
14	Ophthalmia Wall C discharge creek	Discharge from Wall C Ophthalmia Dam	Reach 15	Ophthalmia Wall C creek discharge
15	Ophthalmia Wall C discharge creek	Reach 14	Reach 16	Ophthalmia Wall C creek discharge to Shovelanna Creek
16	Shovelanna Creek	Reach 15	Reach 17	Shovelanna Creek downstream of Wall C creek discharge
17	Shovelanna Creek	Reach 16	Reach 18	Shovelanna Creek downstream of Wall C creek discharge
18	Shovelanna Creek	Reach 17	Reach 13	Shovelanna Creek before confluence with Fortescue River
19	Fortescue River	Reach 13	Reach 20	Fortescue River in upper Ethel Gorge
20	Fortescue River	Reach 19	Reach 21	Fortescue River in upper Ethel Gorge
21	Fortescue River	Reach 20	Reach 22	Fortescue River in upper Ethel Gorge
22	Fortescue River	Reach 21	Reach 23	Fortescue River in upper Ethel Gorge
23	Fortescue River	Reach 22	Reach 24	Fortescue River in lower Ethel Gorge
24	Fortescue River	Reach 23	Reach 25	Fortescue River in lower Ethel Gorge
25	Fortescue River	Reach 24	Reach 26	Fortescue River in lower Ethel Gorge
26	Fortescue River	Reach 25	Reach 27	Fortescue River in lower Ethel Gorge
27	Fortescue River	Reach 26	Reach 28	Fortescue River in lower Ethel Gorge
28	Fortescue River	Reach 27	Reach 29	Fortescue River after Ethel Gorge
29	Fortescue River	Reach 28	Reach 30	Fortescue River after Ethel Gorge including confluence with Kalgan Creek

30	Fortescue River	Reach 29	Reach 31	Fortescue River after Ethel Gorge and confluence with Kalgan Creek
31	Fortescue River	Reach 30	Reach 32	Fortescue River eastern turn, with paleo Fortescue River continuing north
32	Fortescue River	Reach 31	Reach 33	Fortescue River heading eastward
33	Fortescue River	Reach 32	Reach 34	Fortescue River heading eastward
34	Fortescue River	Reach 33	Reach 35	Fortescue River heading eastward
35	Fortescue River	Reach 34	Reach 36	Fortescue River heading eastward
36	Fortescue River	Reach 35	Reach 37	Fortescue River heading northeastward
37	Fortescue River	Reach 36	Reach 38	Fortescue River heading northeastward
38	Fortescue River	Reach 37	Reach 39	Fortescue River heading northeastward
39	Fortescue River	Reach 38	Reach 40	Fortescue River heading NNE
40	Fortescue River	Reach 39	Reach 41	Fortescue River heading NNE
41	Fortescue River	Reach 40	Reach 42	Fortescue River heading NNE
42	Fortescue River	Reach 41	Reach 43	Fortescue River heading NNE
43	Fortescue River	Reach 42	Reach 44	Fortescue River heading north, Jigalong Rd crossing
44	Fortescue River	Reach 43	Reach 45	Fortescue River heading north
45	Fortescue River	Reach 44	Reach 46	Fortescue River heading north
46	Fortescue River	Reach 45	Reach 47	Fortescue River heading northwest
47	Fortescue River	Reach 46	Reach 48	Fortescue River heading northwest
48	Fortescue River	Reach 47	Reach 49	Fortescue River heading northwest

49	Fortescue River	Reach 48	Reach 50	Fortescue River heading WNW
50	Fortescue River	Reach 49	Reach 51	Fortescue River heading WNW
51	Fortescue River	Reach 50	Reach 52	Fortescue River heading WNW
52	Fortescue River	Reach 51	Reach 53	Fortescue River heading northwest
53	Fortescue River	Reach 52	Fortescue Marsh	Fortescue River heading NNW, Nullagine Rd crossing
54	Fortescue River	Reach 53	Fortescue Marsh	Fortescue River into Fortescue Marsh

3.2 Reaches

Each reach in the water balance model is based on a cross-section of the main water way and its bulk groundwater flow properties. The schematic applied in developing the GoldSim model is shown in Figure 3-2. This represents the initial conditions in the reach (no flow in the creek or river). Subsequent conditions when the discharge is flowing through the reach are shown in Figure 3-3. Lateral outflow to either the “left” or “right” (observing downstream) of each cross section is governed by the hydraulic gradient. These gradients are characterised by the differential water table elevation relative to the alluvial centre’s water table elevation as well as the corresponding reach lateral distance.

The modelling methodology for each reach accounts for inflows and outflows before calculating groundwater levels. The inflow is the leakage from the coupled TUFLOW model based on the number of equi-sized wet cells. Outflows are calculated as the increase in groundwater flow to adjacent (lateral) formations/areas and increase in evapotranspiration due to rising water table associated with the creek discharge. Groundwater levels are calculated based on the dimensions of each reach and the alluvial groundwater parameterisation.

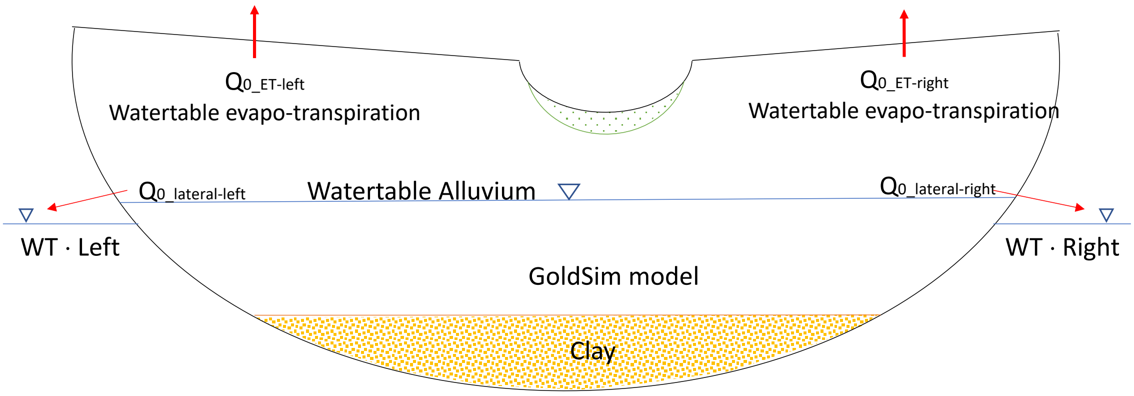

Figure 3-2: Schematic cross-section of a reach (initial conditions - dry)

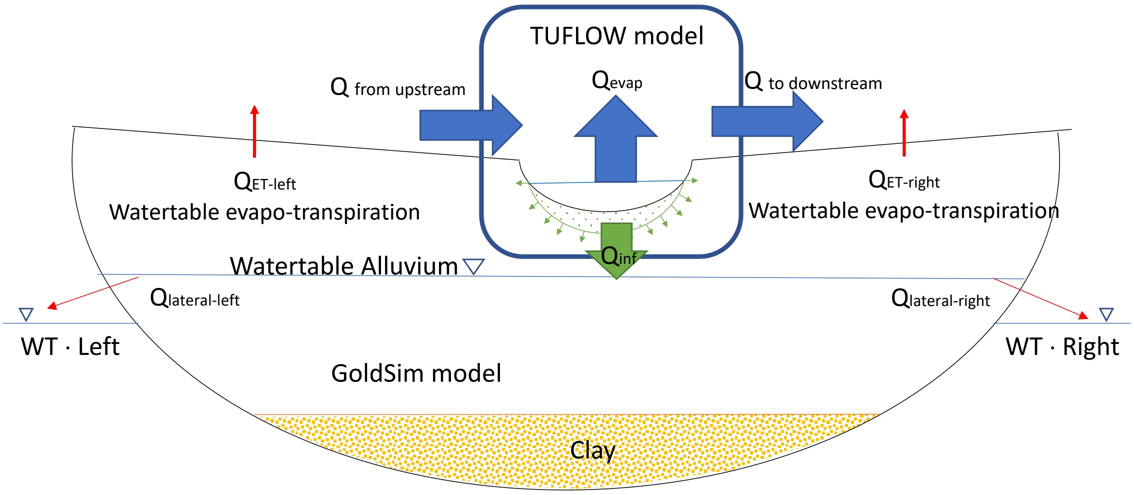

Figure 3-3: Schematic cross-section of a reach (creek discharge)

3.2.1 Geometry

The geometry of each reach consists of a base creek elevation, an initial water table elevation, a depth of active alluvium sediments (to the first aquitard in the alluvium) and the area of the reach.

The surface elevation was derived from BHP-supplied DEMs. The elevation of the water table was, for reaches 1 to 36, derived from a supplied raster of the water table. Lower reaches were interpolated from this location to an assumed 2 m depth to groundwater in the Fortescue Marsh. A minimum initial depth to groundwater of 2 m was used where shallower water tables were found.

The depth of the conductive alluvium in each of the reaches was estimated from the base of the waterway (from the DEM) to the top of the clay (CY2) or lignite clay (LT2) members of the Tertiary Detritals 2 (TD2) layer, whichever was the most elevated. The supplied BHP data lumped together all the surficial Quaternary and Tertiary Detritals 3 (TD3) members, so no upper alluvium discretisation was possible. Data was available for reaches 1 to 31, with the depths for the remaining reaches estimated.

The area of each reach was defined by the extent of alluvium as interpreted from BHP data and/or regional surficial geological maps. The geometry of each reach is listed in Table 3-2.

Table 3-2: Reach dimensions

Reach ID	Length (m)	Area (ha)	Creek bed elevation (m RL)	Water table elevation (m RL)	Alluvium depth (m)
1	1,112	114	522	509	40
2	1,175	100	520	507	40
3	966	67	518	505	40
4	1,164	77	515	502	40
5	1,101	92	512	499	40
6	609	62	510.5	498.5	20
7	827	89	509	497	20
8	717	72	507.5	497	20
9	892	56	506	496	20
10	680	66	504	494	20
11	604	105	500	494	25
12	867	52	499	494	25
13	1,750	98	498	494	30
14	612	41	504	502	20
15	660	63	503	501	20
16	681	60	501.5	499.5	20
17	421	69	501	499	20
18	1,758	106	500	498	20
19	1,573	85	494.8	490.8	30
20	835	80	494.5	490.5	30
21	1,046	111	493.9	489.9	30
22	1,739	112	492.7	488.7	30
23	1,359	163	490.4	486.4	25
24	1,318	138	488.6	485.6	25
25	1,148	146	487.2	485.2	25
26	1,713	143	485	482	25
27	2,051	147	483.9	481.9	25
28	2,559	239	482	479	30
29	3,007	302	479.7	476.7	30
30	2,441	237	477.6	474.6	30
31	1,995	177	475.5	469.5	30
32	1,527	210	474.3	468.3	30
33	1,994	275	472.2	466.2	30
34	1,994	284	470.7	464.7	30
35	8,035	712	467	460	30
36	7,364	818	462	453	30

37	3,431	589	459	448	30
38	4,477	610	456	444	30
39	7,719	1,809	452	441	30
40	8,030	2,147	449	439	30
41	6,887	2,641	446	438	30
42	6,194	2,098	443	435	30
43	4,171	1,485	440	433	30
44	6,967	2,421	437	430	30
45	7,013	2,282	433	427	30
46	6,232	2,235	430	424	30
47	4,653	1,429	427	422	30
48	4,831	1,244	422	417	30
49	4,265	944	419	414	30
50	4,823	728	417	413	30
51	5,064	865	415	411	30
52	4,917	1,107	413	410	30
53	5,117	1,107	411	409	30
54	4,484	704	410	408	30

3.2.2 Parameterisation

Parameters for the reaches were derived from information obtained from BHP data and previous experience. BHP provided data on multiple aquifer tests carried out in the area. A map of the tested bores with results is shown in Figure 3-4. Up to three tests were carried out at each bore, with both drawdown and recovery tests occurring at some of the bores. The range of transmissivities found in the bores is in Figure 3-5, with the hydraulic conductivity ranges shown in Figure 3-6. In these latter two figures, single values indicate only one test result available.

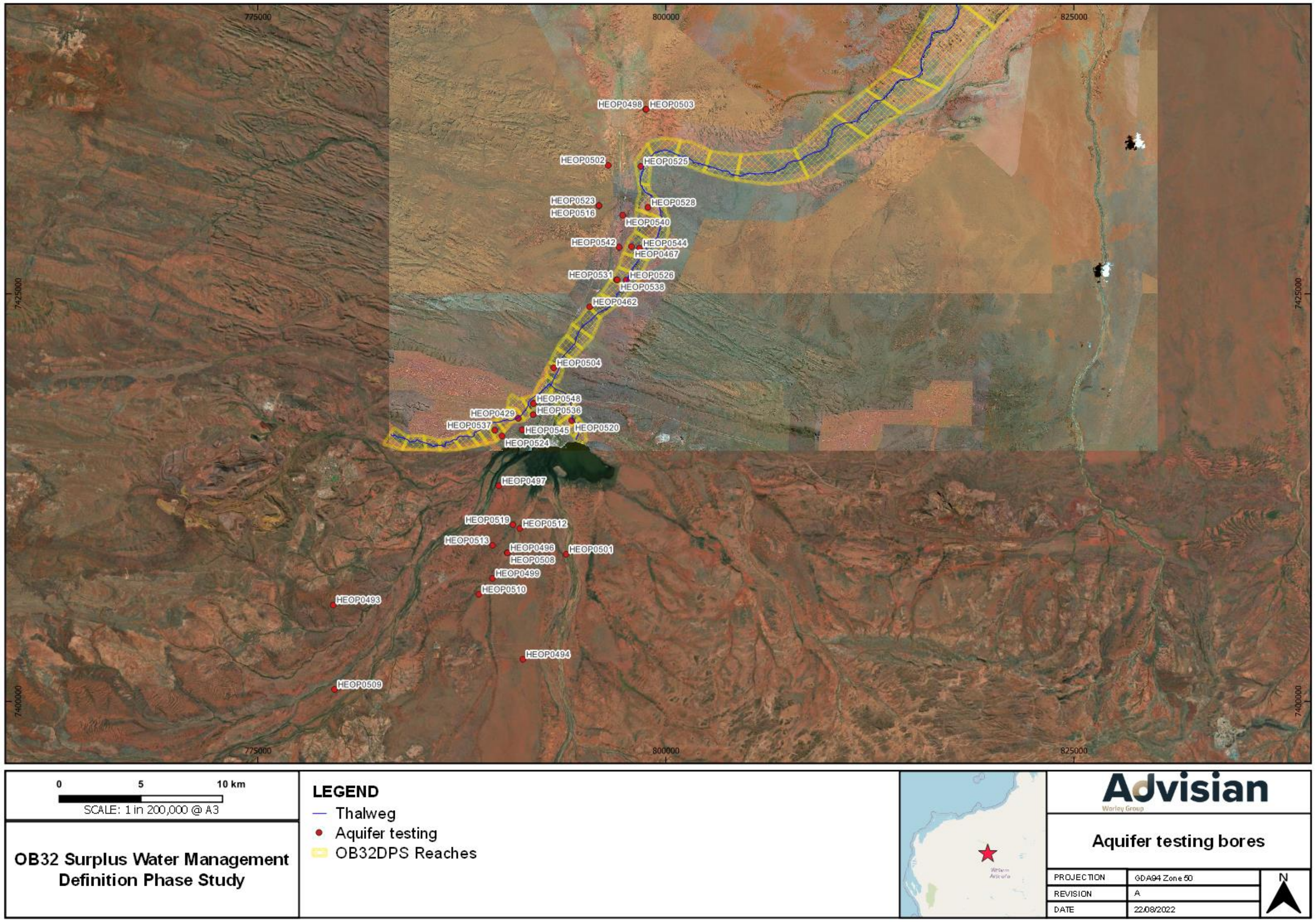

Figure 3-4: Aquifer testing bores

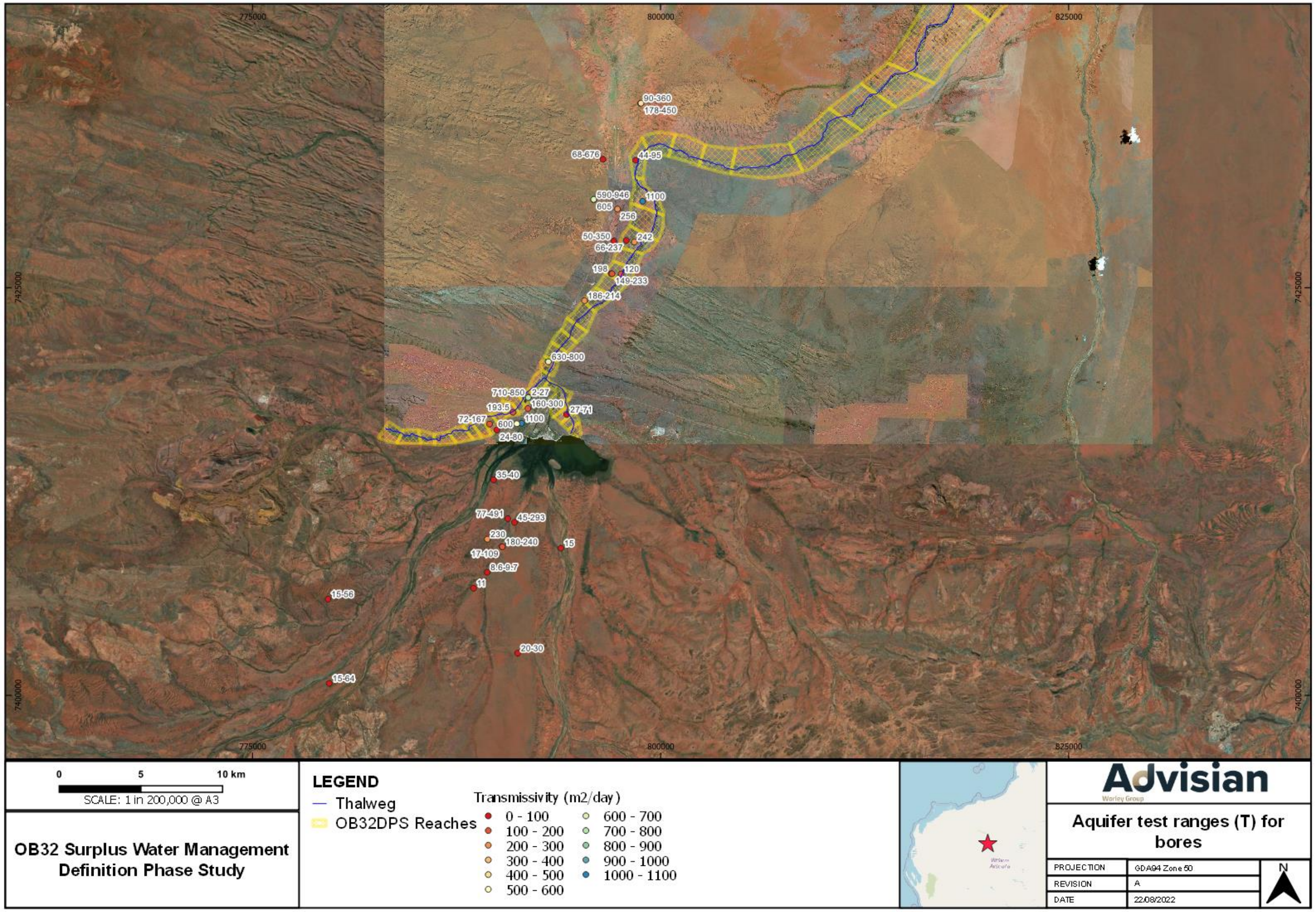

Figure 3-5: Aquifer testing: Range of transmissivities

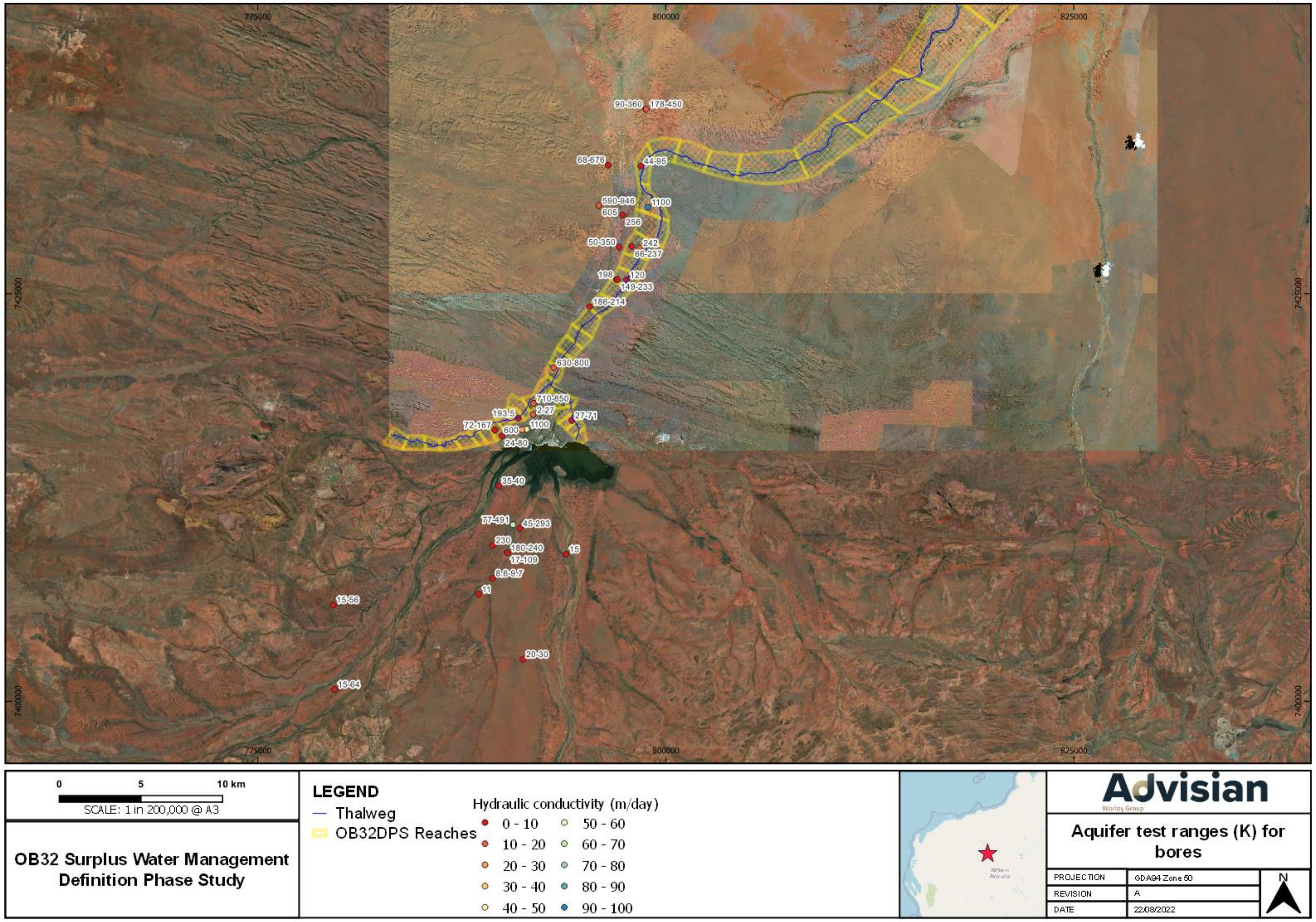

Figure 3-6: Aquifer testing: Range of hydraulic conductivities

The results of the aquifer testing indicate that the highest transmissivities and rates of hydraulic conductivity are observed close to Ophthalmia Dam and the confluence of Kalgan Creek and Fortescue River. It is noted that the screened interval for the abstraction and observation bores used to calculate these results may include deeper lithologies than included in the creek discharge modelling.

A summary of the parameters used for each reach is shown in Table 3-3.

Table 3-3: Reach parameters

Reach ID	Kv (m/day)	Sy (-)	Extinction depth (m)	Wetting Front Limit (%)
All reaches	0.45	0.2	4	90

3.2.3 Adjacent aquifers

External water table levels in the adjacent formations were evaluated by extrapolating from the supplied information or via estimation where no information was supplied/available. The distance to the external water table level was estimated as the distance at which the influence of any additional leakage from the alluvium would have minimal impact on the water table level in the adjacent formation. An exception to this was the external head on the left in reach 7, which was specified as the edge of the pit closest to Homestead Creek, where surface seepage occurs.

The hydraulic conductivity of the material surrounding the alluvium was estimated from BHP-supplied data (see Figure 3-6) and/or experience of similar material in the Pilbara (e.g., Advisian, 2021). The transmissivity for the interaction between the alluvium and the surrounding material was the product of this hydraulic conductivity and the thickness of the conductive alluvium layer. The flux from the alluvium to the surrounding material was calculated based on the head gradient between the water table in the alluvium and that in the adjacent aquifer, the transmissivity, and the active length of the reach.

A summary of the adjacent aquifer properties is in Table 3-4.

Lateral flows to the adjacent aquifers were calculated as the transmissivity of the saturated thickness in the alluvium multiplied by the length of the reach multiplied by the head difference between the alluvium and the adjacent aquifer.

Table 3-4: Reach lateral interaction

Reach ID	Top Alluvium Left (mAHD)	Distance Left (m)	Conductivity Left (m/day)	Top Alluvium Right (m AHD)	Distance Right (m)	Conductivity Right (m/day)
1	525.0	2000	0.1	524.5	2000	1.0
2	523.0	2000	0.1	522.5	2000	1.0
3	521.0	2000	0.1	520.5	2000	1.0
4	518.0	2000	0.1	517.5	2000	1.0
5	515.0	2000	0.1	514.5	2000	1.0
6	513.5	500	10	513.0	2000	1.0
7	512.0	500	10	511.5	2000	1.0
8	510.5	2000	0.1	510.0	2000	1.0
9	509.0	2000	0.1	508.5	2000	1.0
10	507.0	2000	0.1	506.5	2000	1.0
11	503.0	2000	0.1	502.5	1000	1.0
12	502.0	2000	0.1	501.5	1000	1.0
13	500.0	2000	0.1	499.5	2000	0.1
14	506.0	1000	1	505.5	2000	0.1
15	505.0	1000	1	504.5	2000	0.1
16	503.5	1000	1	503.0	2000	0.1
17	503.0	1000	1	502.5	2000	0.1
18	502.0	1000	1	501.5	2000	0.1
19	496.8	2000	0.1	496.3	2000	0.1
20	496.5	2000	0.1	496.0	2000	0.1
21	495.9	2000	0.1	495.4	2000	0.1
22	494.7	2000	0.1	494.2	2000	0.1
23	492.4	2000	0.1	491.9	2000	0.1
24	490.6	2000	0.1	490.1	2000	0.1
25	489.2	2000	1	488.7	2000	0.1
26	487.0	2000	5	486.5	2000	0.1
27	485.9	2000	10	485.4	2000	0.1
28	484.0	2000	10	483.5	2000	0.3
29	481.7	2000	10	481.2	2000	0.3
30	479.6	2000	10	479.1	2000	0.3
31	477.5	2000	10	477.0	2000	0.3
32	476.3	2000	10	475.8	2000	0.3
33	474.2	2000	5	473.7	2000	0.3
34	472.7	2000	2	472.2	2000	0.3
35	469.0	2000	1	468.5	2000	0.3
36	464.0	2000	1	463.5	2000	0.3
37	461.0	2000	1	460.5	2000	0.3
38	458.0	2000	1	457.5	2000	0.3
39	454.0	2000	0.3	453.5	2000	0.3

40	451.0	2000	0.3	450.5	2000	0.3
41	448.0	2000	0.3	447.5	2000	0.3
42	445.0	2000	0.3	444.5	2000	0.3
43	442.0	2000	0.3	441.5	2000	0.3
44	439.0	2000	0.3	438.5	2000	0.3
45	435.0	2000	0.3	434.5	2000	0.3
46	432.0	2000	0.3	431.5	2000	0.3
47	429.0	2000	0.3	428.5	2000	0.3
48	424.0	2000	0.3	423.5	2000	0.3
49	421.0	2000	0.3	420.5	2000	0.3
50	419.0	2000	0.3	418.5	2000	0.3
51	417.0	2000	0.3	416.5	2000	0.3
52	415.0	2000	0.3	414.5	2000	0.3
53	413.0	2000	0.3	412.5	2000	0.3
54	412.0	2000	0.3	411.5	2000	0.3

3.2.4 Evaporation from alluvium

The alluvium net evapotranspiration applied in the SPS (Advisian, 2021) was based on an assumed rate of evapotranspiration of 1 mm/day over the width of the alluvium. The revised method for the DPS calculates the evapotranspiration based on the following assumptions:

- The water table elevation is constant across the alluvium for each time step.
- The width (D) of the alluvium is defined. This will be an average width for each reach.
- The elevation of the base of the waterway in the reach is available.
- The elevation of the edge of the alluvium away from the waterway is available.
- An extinction depth for the evapotranspiration can be defined and is constant for the reach (Langevin, et al., 2017). Evapotranspiration is zero below the extinction depth.
- The evapotranspiration from the alluvium is a linear function of depth from the surface (at the supplied evaporation rate) to the extinction depth.
- Water tables below the extinction depth have an evapotranspiration rate of 0.
- The inundated area in a reach supplying potential infiltration is not included in the GoldSim calculation (this is part of the TUFLOW calculation) (see Figure 3-7).
- Evapotranspiration from water table above the ground surface (and not inundated by the waterway) is at the supplied evaporation rate.

- Where a pre-existing (initial) water table is above the extinction depth, the evapotranspiration used for the creek discharge modelling is the additional evapotranspiration that occurs as a result of a higher water table (Figure 3-8).

- The calculated evapotranspiration is multiplied by the wetted fraction of the reach if the wetting front is advancing, or the maximum extent of the wetting if the wetting front is receding

The loss from the alluvium water table through evapotranspiration was calculated over the area of the alluvium less any inundated area. A cross-sectional schematic of the evaporation and evapotranspiration from the alluvium is shown in Figure 3-7. If the initial water table in the reach was higher than the extinction depth, then the evaporative loss was the evapotranspiration calculated for the current water table elevation, less the evapotranspiration based on the initial water table elevation. As shown in Figure 3-8, this evapotranspiration is calculated over the uninundated area of the reach.

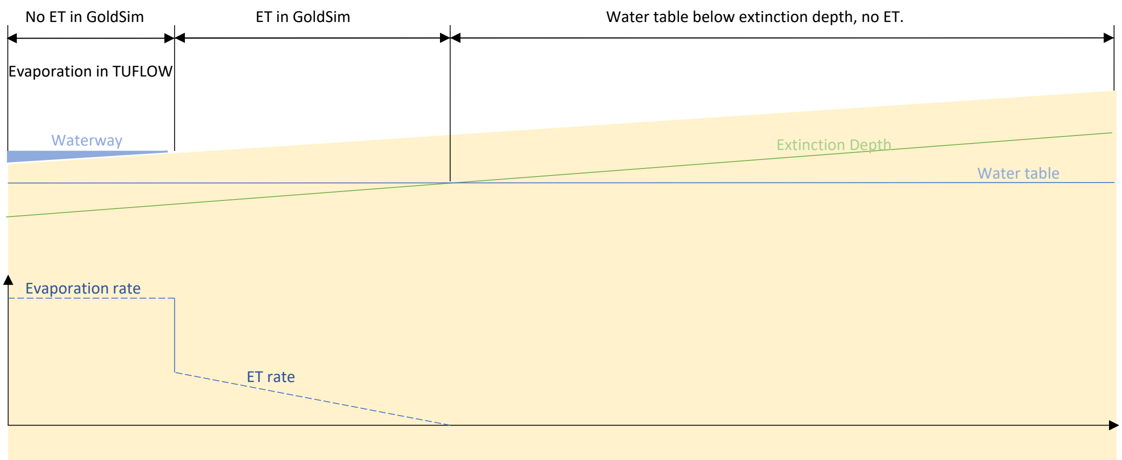

Figure 3-7: Creek discharge model evaporation and evapotranspiration

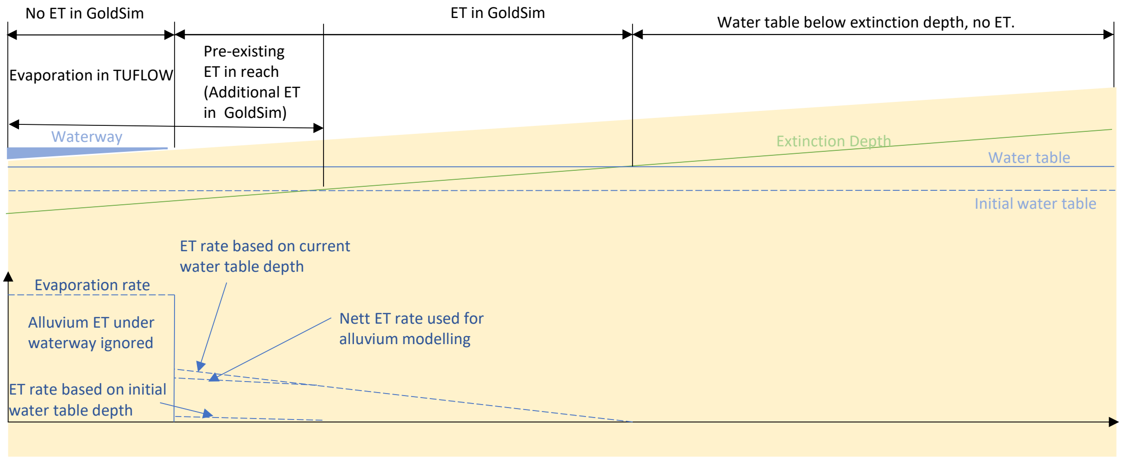

Figure 3-8: Creek discharge model - evapotranspiration calculation with initial high water table

The water table is assumed to be flat in each reach through the alluvium and is limited to the range between the initial water table and the base of the creek level. A reach with the water table at the base of the waterway can only accept leakage from the waterway at a maximum rate of the sum of the lateral losses and evapotranspiration.

The elevation of the lateral edge of the alluvium is listed in Table 3-4 with the extinction depth for each reach listed in Table 3-3.

3.2.5 Alluvium processes

The model calibration procedure found that unlimited infiltration at the vertical conductivity rate until the alluvial storage was filled resulted in slow surface flow of the discharge through the system. A numerical model was used to investigate the process of infiltration and lateral flow within the alluvium.

A groundwater model was constructed to examine the infiltration into the alluvium from the ‘flooded’ creek. The model consisted of a single row (1 m width) model with 100 m half-width aquifer (59 columns with column widths ranging from 0.5 m under creek to 2 m at edge of alluvium, and 40 1 m thick layers 0->40 m RL). The initial heads in the alluvium were set to 20 m RL.

The half-width of the ‘flooded’ creek was 5 m. Recharge was 0.5 m/day for the creek, representing the infiltration rates, and zero elsewhere. The outer alluvium boundary had a specified head of 20 m RL and a conductance of 0.001 m²/day. The model was created in MODFLOW-NWT (MODFLOW-2005) and used the unsaturated zone flow (UZF) package to simulate the initial infiltration through the unsaturated zone. This allowed the rejection of recharge (infiltration) that could not be accepted into the alluvium. The hydraulic conductivity was specified based on a vertical rate of 0.5 m/day, with horizontal hydraulic conductivity either 0.5 m/d (no anisotropy) or 5 m/d (order of magnitude anisotropy). The specific yield was specified as 0.2. The unsaturated zone parameters were a residual saturation of 0.02 and a B-Corey value of 0.5.

100 timesteps were used starting at 0.1 days and ending at 10 days stress periods (1 time step in each stress period) for a simulation length of 618 days.

The elevation of the water table was calculated for each stress period. Figure 3-9 and Figure 3-10 show the water table at various times for the no anisotropy and anisotropy (10x) cases respectively. These show the water table reaching the base of the creek at day 124 for the isotropic case (water table depth 0.16 m) and at day 179 (depth to water 0.1 m) for the anisotropy of 10. The water table gradient away from under the creek is much flatter for the anisotropic case (higher horizontal conductivity). In both cases the flat rise of water table under the creek can be seen. Note that the saturation may be less than 100% but close to 100% for a while before the water table reaches the base of the creek.

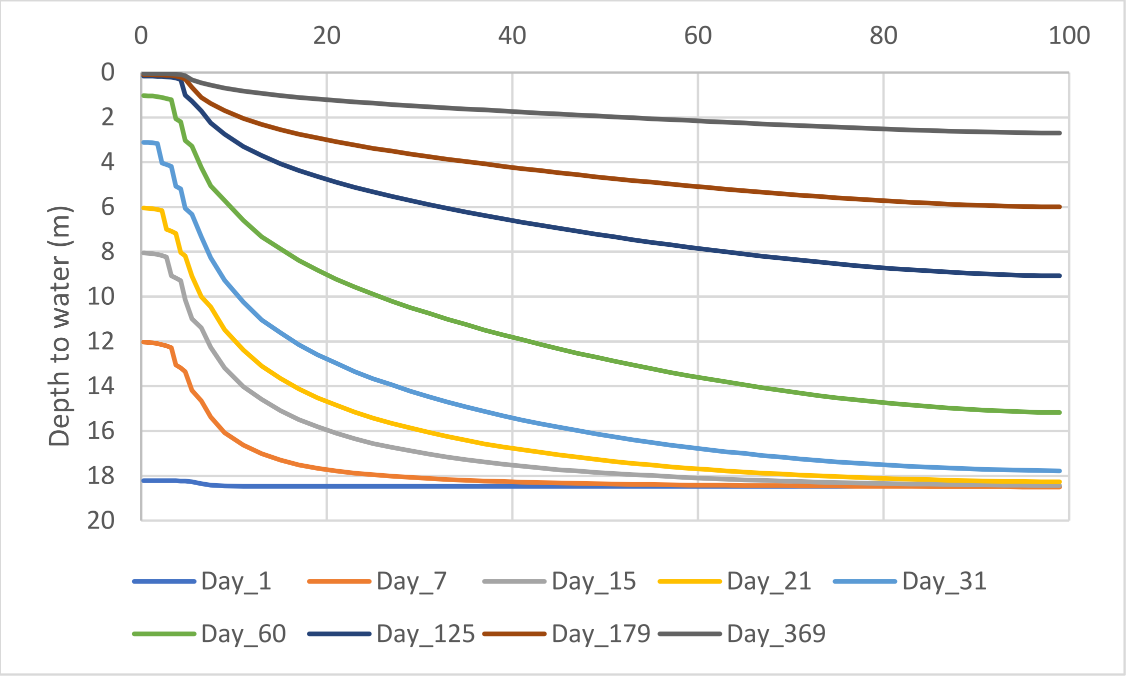

Figure 3-9: Simulated rising water table under an infiltrating creek for no anisotropy

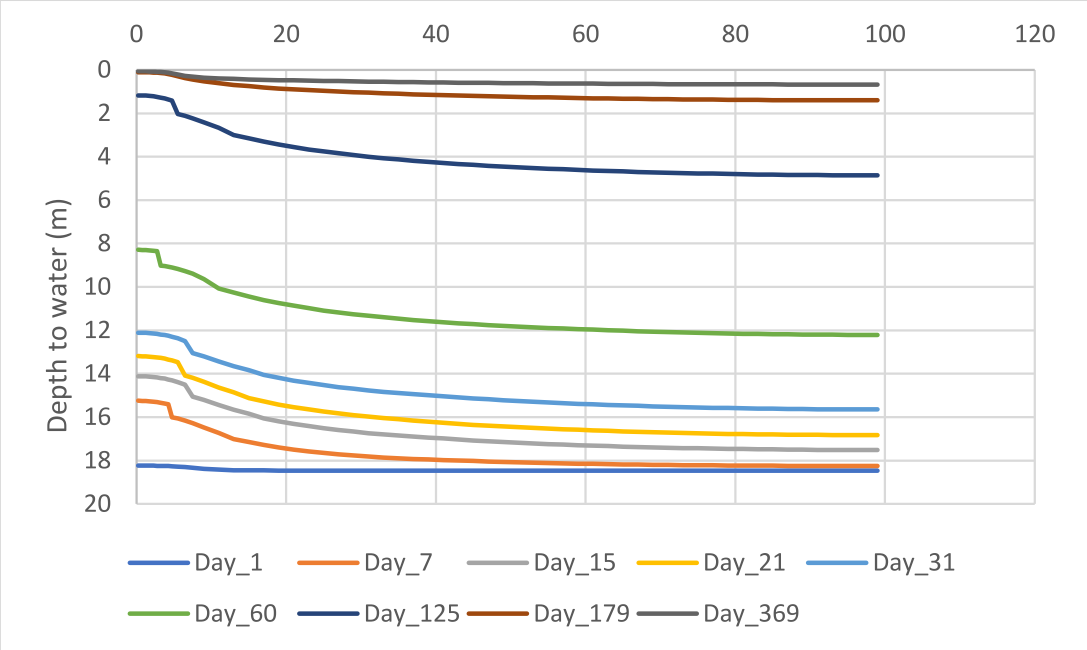

Figure 3-10: Simulated rising water table under an infiltrating creek for 10x anisotropy

Figure 3-11 and Figure 3-12 show the recharge flux for each of the simulations over time. These show a near-constant infiltration of 2.5 m3/d (0.5 m/day over 1 m x 5 m area) for a period after an initial lower start-up rate as the alluvium becomes more saturated. This is followed by a reduction in the rate as the water table approaches the base of the creek. The reduction in infiltration falls much faster (and later) for the anisotropic case. The recharge reduction is to around 10-15% of the original, i.e., only 85-90% of the potential infiltration occurs.

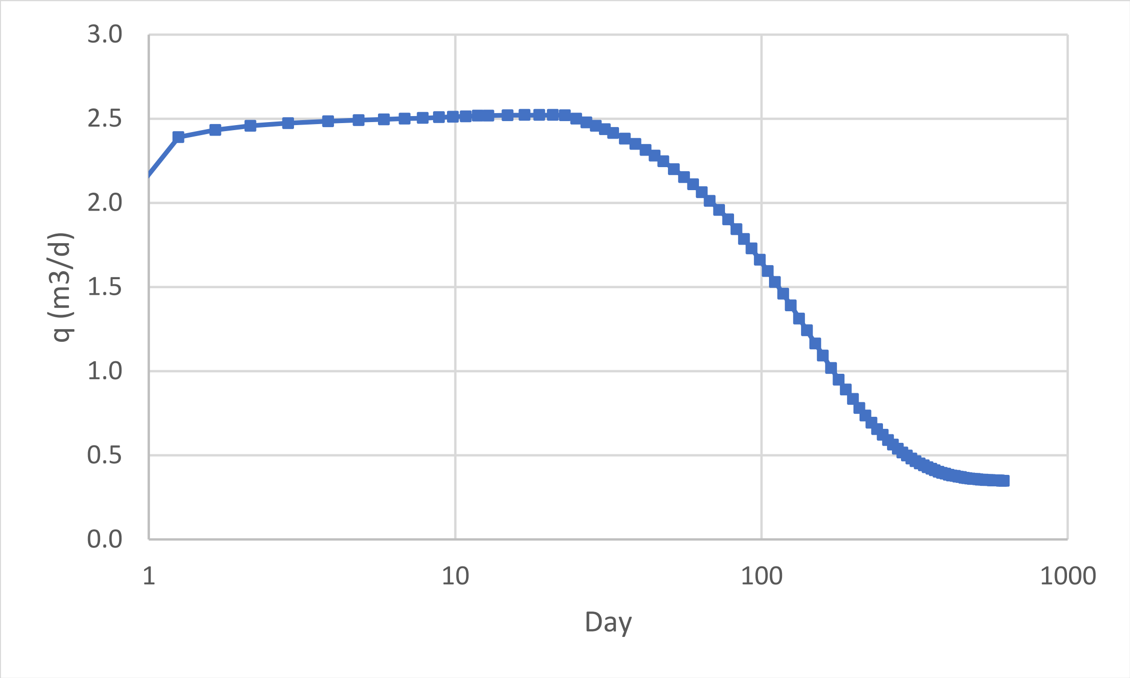

Figure 3-11: Simulated infiltration rate under the creek for no anisotropy

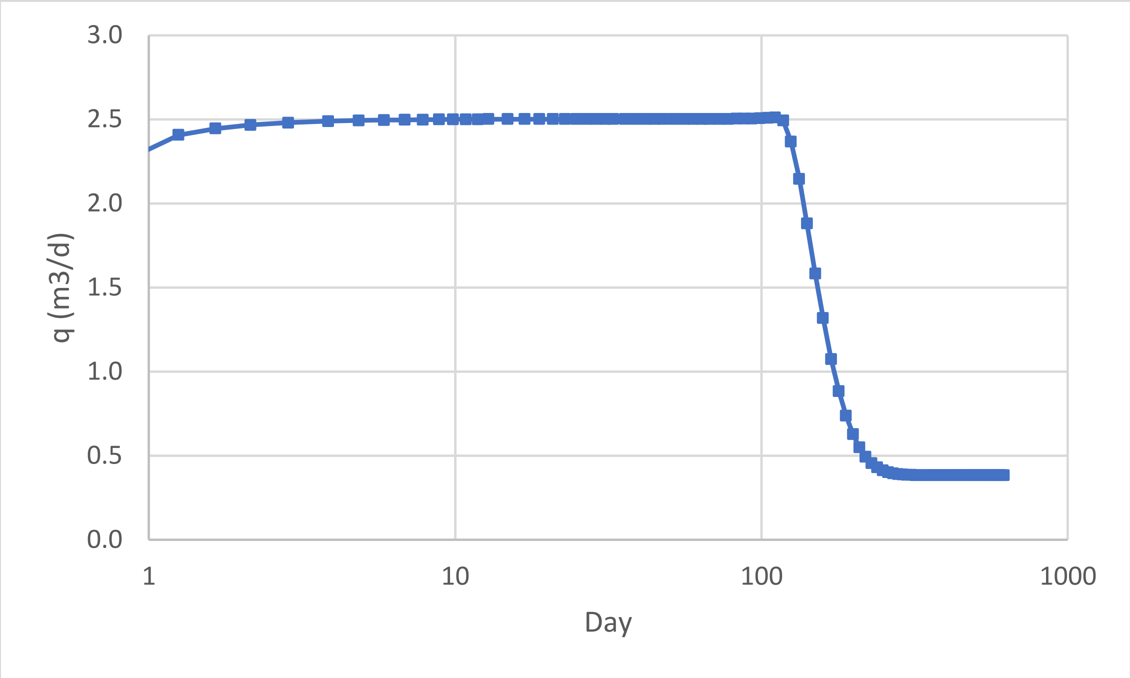

Figure 3-12: Simulated infiltration rate under the creek for 10 x anisotropy

Similar results were found for a 5 m width creek over a 1 km wide alluvial aquifer. These results indicate that a mound forms under the creek due to the infiltration and as the water table approaches the base of the creek there is a reduction in the infiltration rate from the creek.

To simulate this, an initial part of the alluvium was allowed to fill using the TUFLOW infiltration function. This was specified as a multiplier of 2.5 on the depth to the water table in each reach, akin to the isotropic case. This was limited to a maximum water table depth of 24 m. Then in the GoldSim model we used a multiplier factor (0.6) on subsequent infiltration into the reach until the whole reach became saturated. This additional leakage was added to the TUFLOW evaporation rate, along with any lateral leakage and evapotranspiration from the alluvium.

3.3 Calibration

BHP provided information about groundwater heads in the vicinity of Homestead Creek, Fortescue River and Ophthalmia Dam. This data consisted of logged water levels and manual groundwater dips. The intention was to use this data to assist in calibration of the model to the Ophthalmia Dam discharge between 23 January 2020 and 10 August 2020 (Rea, 2021). Information about additional discharges from Ophthalmia Dam was also provided. Rainfall data from the Bureau of Meteorology (BoM) was also obtained for the Newman Aero site (BoM Site ID 007176). Figure 3-13 shows the recorded Ophthalmia Dam discharge durations and average rates for the period 2016-2022 together with daily rainfall recorded greater than 10 mm. Most of the start of recorded discharge periods from the dam coincide with rainfall events, including a rainfall of 142.8 mm on 9 January 2020, prior to the commencement of the Rea (2021) discharge event.

Figure 3-14 shows a map of bores dipped since 2016 in the vicinity of the 2020 Ophthalmia Dam discharge period. Figure 3-15 shows the discharge periods, large rainfall events and all observations at an example bore (HEOP0574) since 2014. Figure 3-16 to Figure 3-20 compare the manually dipped bore observations with the heads from the calibration model. These bores were selected as within the alluvium area and with multiple observations during the Ophthalmia discharge.

HEOP0574 (Figure 3-15, Figure 3-16) shows that the observed water level responds strongly to the rainfall event prior to the start of discharge, and a decline in water levels after the discharge finishes. The simulated water levels rise to close to the observed water levels in the latter part of the discharge. Similarly, HEOP0504 (Figure 3-17) and HEOP0462 (Figure 3-18) show rises and steady levels during the simulation that are close to the observations. In bore HEOP0538 (Figure 3-19), there are only a few observations, but the simulated level is much higher than the observed levels, starting from a higher

level (the water table distribution (

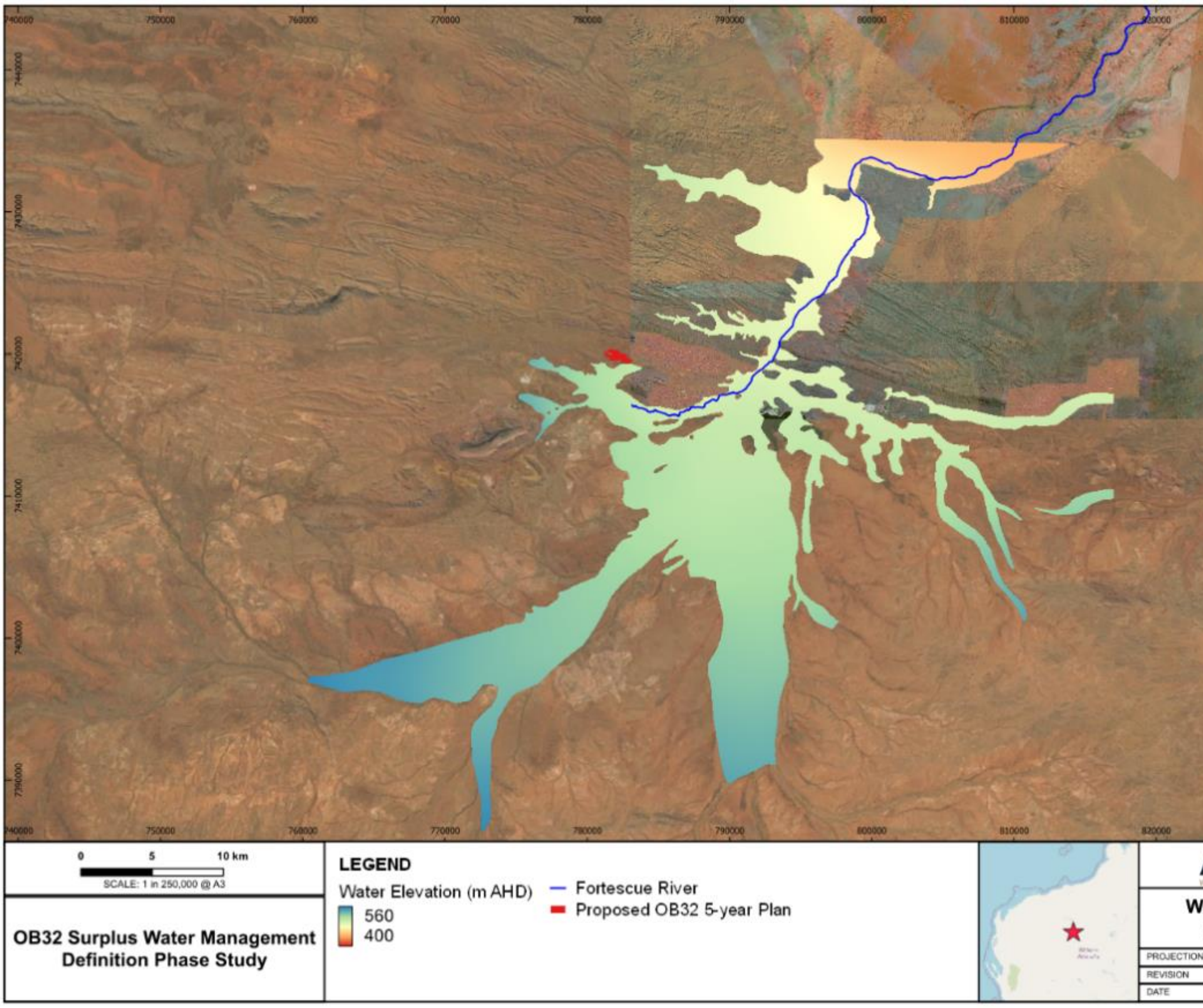

Figure 2-4) also has a higher head in this location than the observations). The observed and simulated water table levels in bore HEOP0467 (Figure 3-20) show higher observed than simulated, with observed levels almost constant during the discharge test with the simulated levels rising slowly.

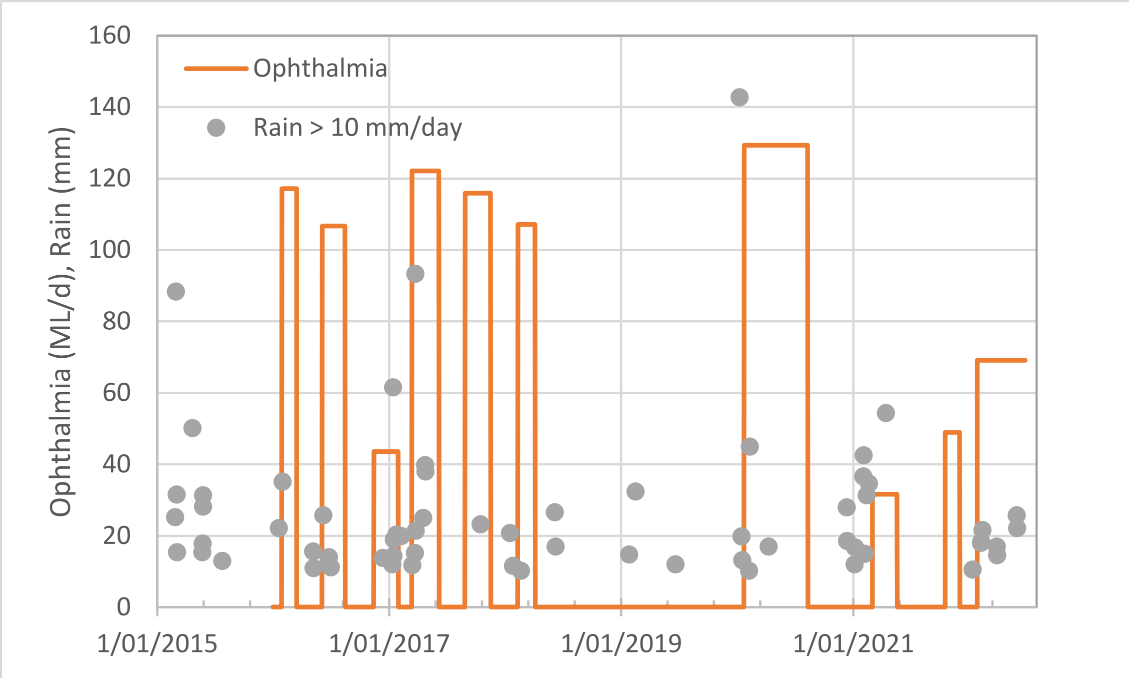

Figure 3-13: Ophthalmia discharge periods and rates with major rainy days at Newman Aero

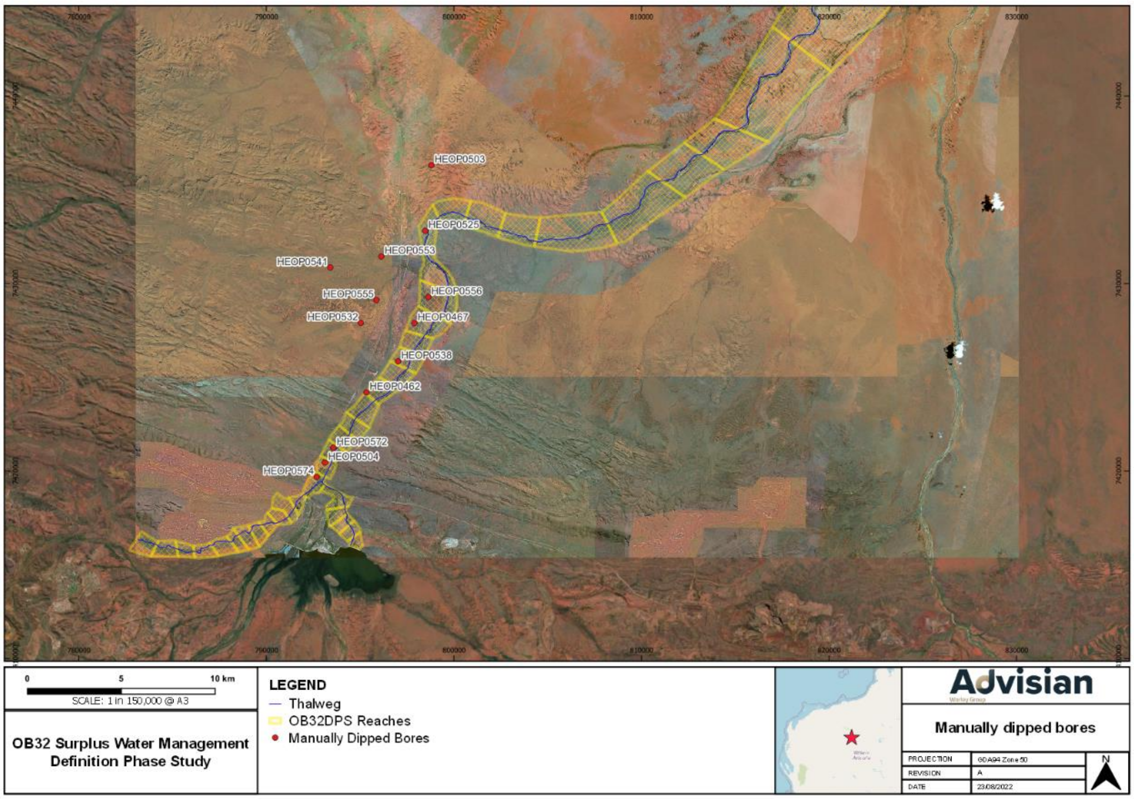

Figure 3-14: Locations of manually dipped bores with observations since end of 2016

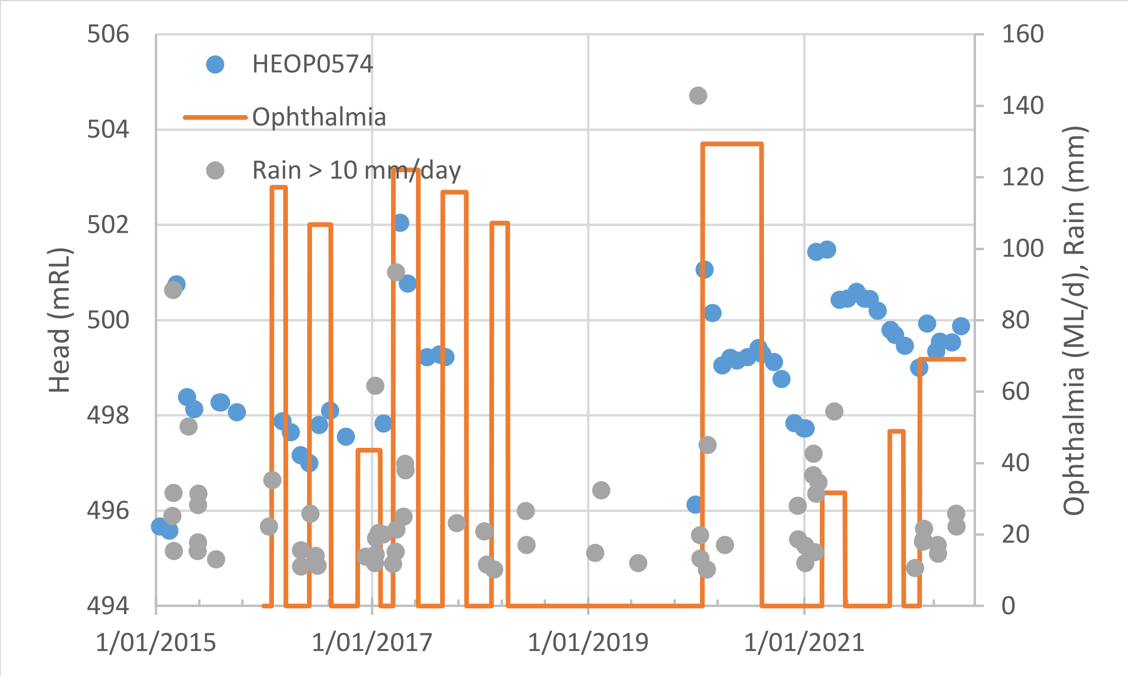

Figure 3-15: Manually dipped bore HEOP0574

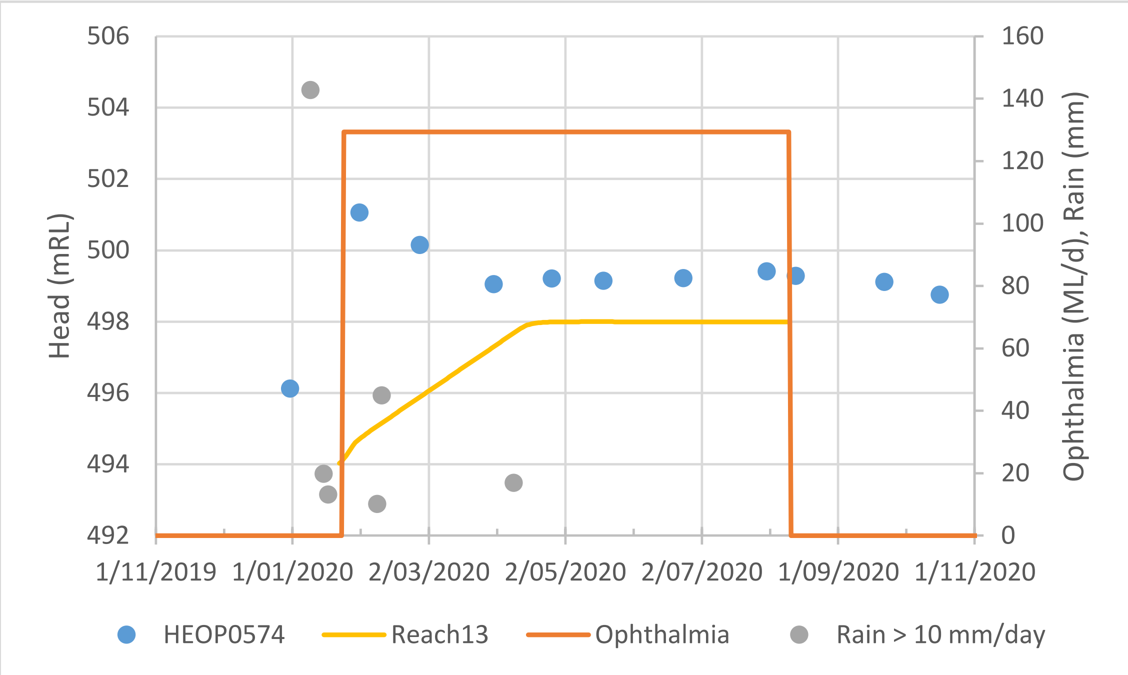

Figure 3-16: Manually dipped bore HEOP0574 during discharge calibration, 370 m from thalweg

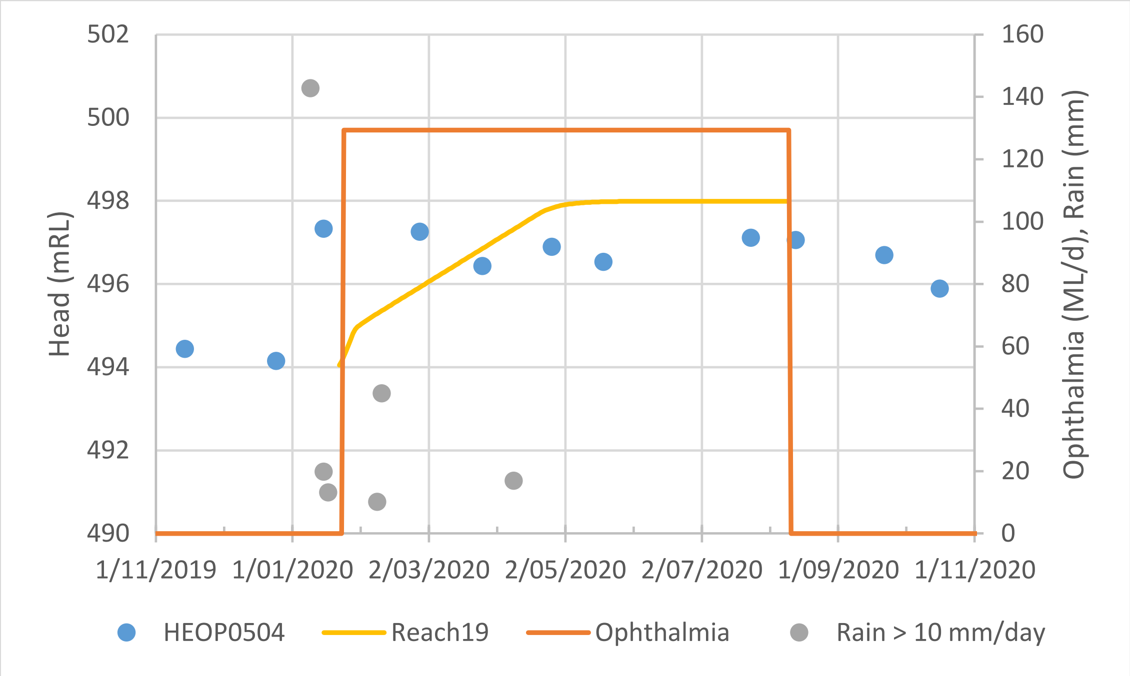

Figure 3-17: Manually dipped bore HEOP0504 during discharge calibration, 310 m from thalweg

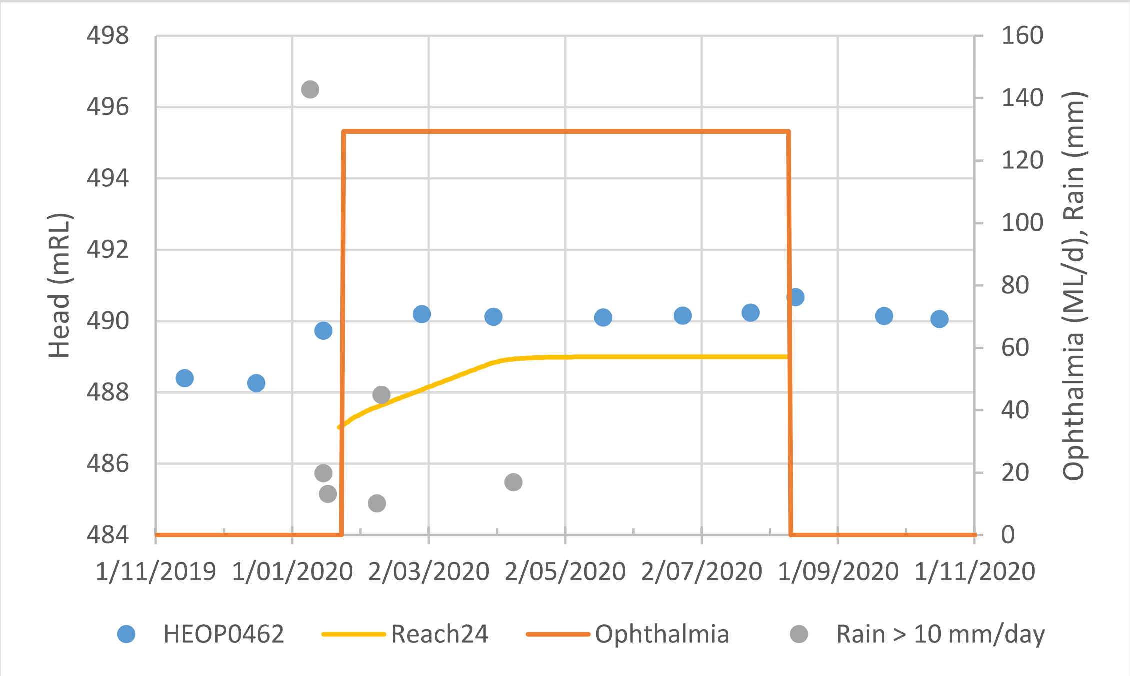

Figure 3-18: Manually dipped bore HEOP0462 during discharge calibration, 615 m from thalweg

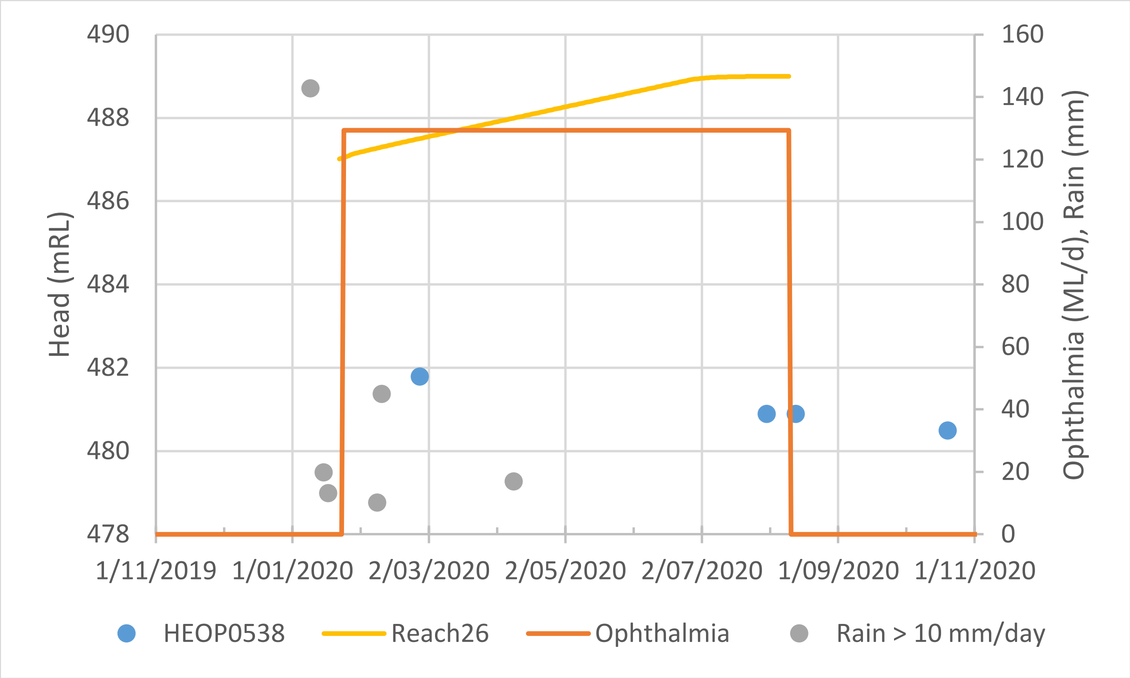

Figure 3-19: Manually dipped bore HEOP0538 during discharge calibration, 580 m from thalweg

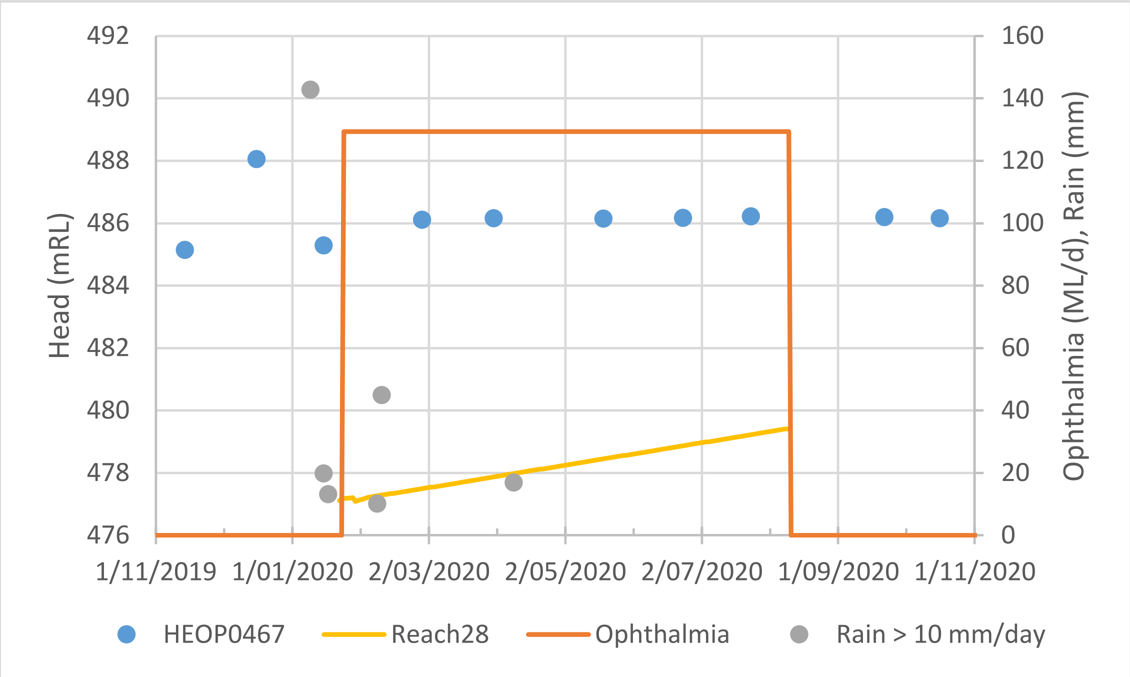

Figure 3-20: Manually dipped bore HEOP0467 during discharge calibration, 842 m from thalweg

A number of groundwater monitoring bores were logged during the discharge test. The logged hydrographs are shown in Figure 3-21 with the locations of the bores in Figure 3-22. HEQ0022M is located close to the north-western side of Ophthalmia Dam and may reflect the water level in the dam. It shows a steady decline in water level over the period of the discharge. Bore EEX0917M is located on reach 16 and bores HEA0137M and HEA0139M are located within reach 13, approximately 800 m upgradient of the confluence of Fortescue River and Shovelanna Creek. The remaining bores are located away from the discharge flow path and are not included in the following analysis. Figure 3-23 shows the response of the model and the logged water levels in EEX0917M. The model shows a similar response to the observed levels, with simulated heads approximately 1 m higher and an increasing water level through the discharge. Figure 3-24 shows the response in the adjacent bores HEA0137M and HEA0139M. The heads in these bores generally match the simulated levels with the maximum level simulated closely matching the observed level, with timing very close.

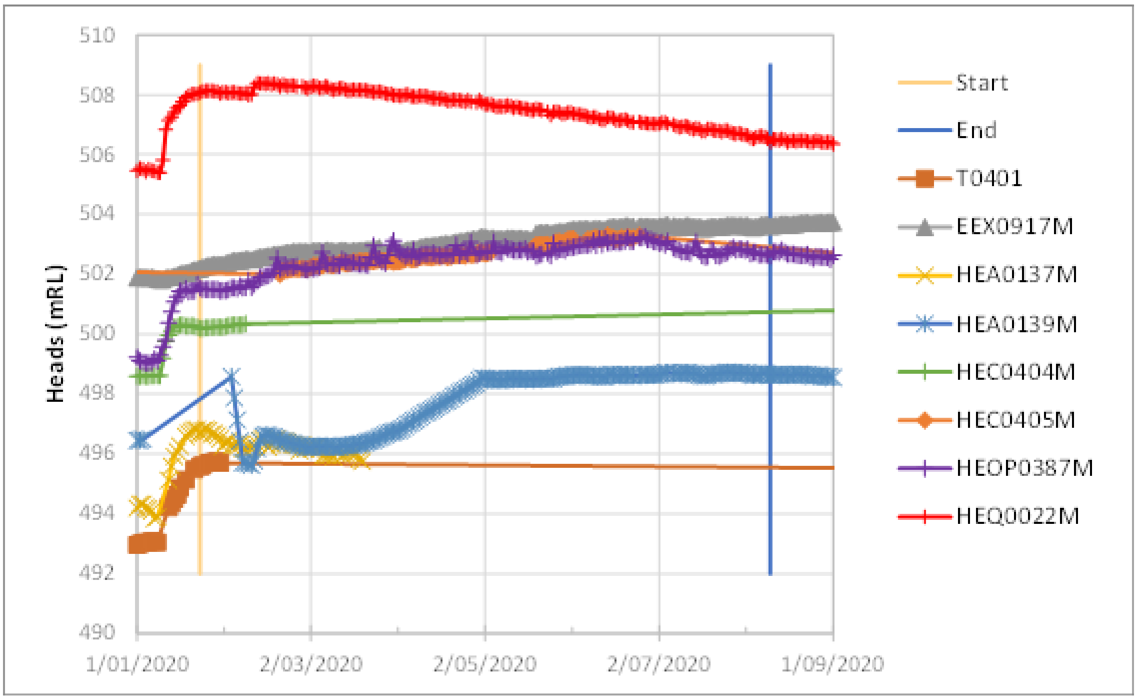

Figure 3-21: Logged observation bore hydrographs during discharge test

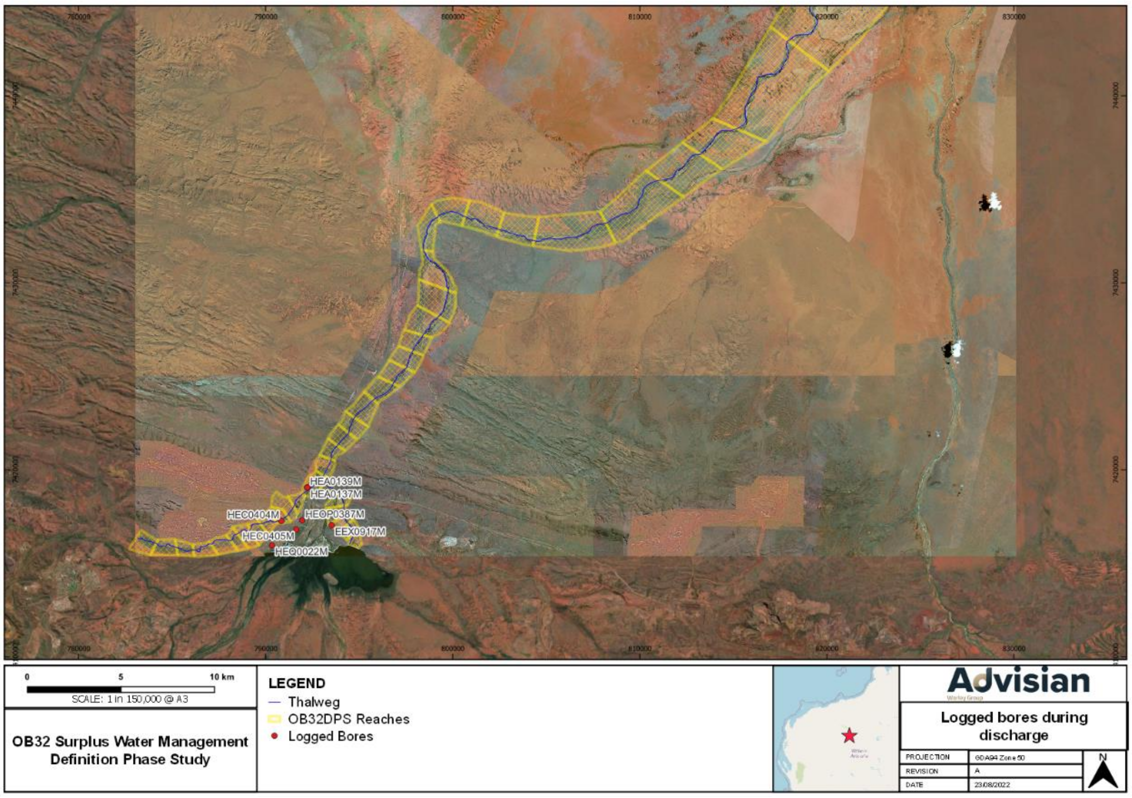

Figure 3-22: Locations of logged bores during discharge test

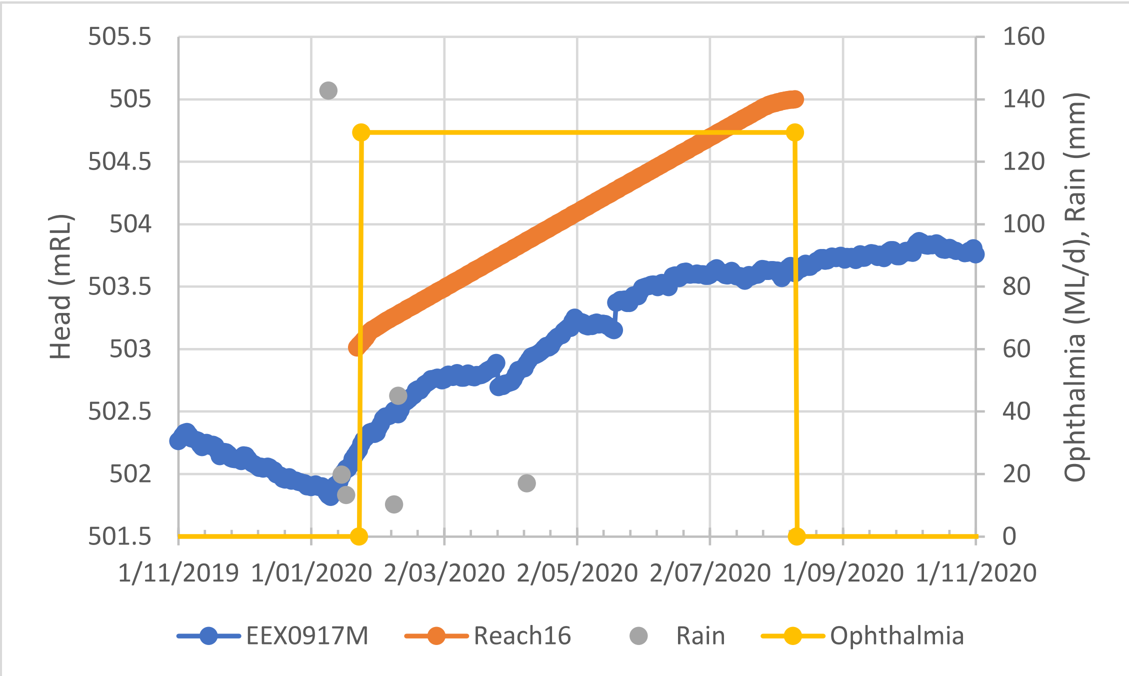

Figure 3-23: Logged hydrograph for bore EEX0917M during discharge calibration, 780 m from thalweg

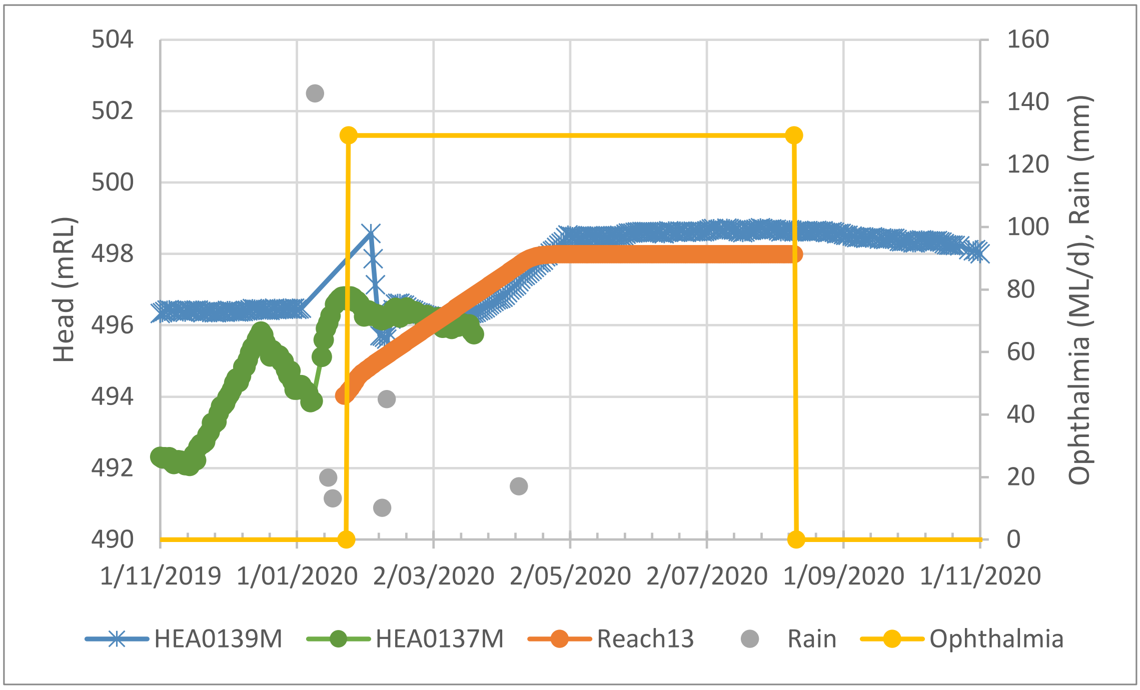

Figure 3-24: Logged hydrographs for bores HEA0137M and HEA0139M during discharge calibration, 800 m from thalweg

The comparison of the (calibration) model results and observations indicate that the model has a reasonable calibration. The large rainfall event (142 mm at Newman Aero on 9/1/2020) immediately preceding the discharge trial meant that the initial water table levels in the alluvium may have been higher than the (raster) distribution of water table levels, and, in some reaches, higher than the elevation of the thalweg. However, the model does show a sustained water table level in the alluvium close to that observed in a number of bores along the Fortescue River, with falling water table levels after the cessation of flow (Bores HEOP0574, HEA0139M in reach 13; HEOP0504, reach 19 in HEOP0462 in reach 23). This gives confidence that the model can represent the processes occurring in the alluvium as a result of sustained creek discharge to the Homestead Creek-Fortescue River system.

3.4 Available alluvium volume

An analysis was made using the initial conditions for the GoldSim model to estimate the time required for infiltration from the discharge to Homestead Creek to fill the underlying alluvium along the creek and Fortescue River. The analysis ignores any lateral flow from the alluvium into adjacent aquifers and evaporation form the waterway and evapotranspiration from the alluvium. The infiltration from the discharge fills each reach prior to flowing to the next reach. Figure 3-25 shows the time to fill the alluvium as a function of the distance from the discharge point on Homestead Creek. The upper reaches (1 to 32, without 14-18, distance 36.7 km) are filled relatively quickly (within 3 years), with the time increasing rapidly to fill the alluvium in the lower reaches of the (Upper) Fortescue River beyond the paleo-Fortescue River. It is noted that the length and area of the reaches increases further downstream.

The results indicate it would take a minimum of 22-23 years to fill the modelled alluvium system with a flow of 50 ML/day, and a minimum of 12-13 years to fill it for a discharge rate of 90 ML/day. Inclusion of evaporative loss from the surface flows and lateral and evapotranspiration from the alluvium would increase these times. It is noted that the creek discharge would flow downstream faster than the alluvium under the reaches could be filled, but this provides an indication of the minimum period for different discharge rates to reach steady-state taking alluvial storage into account.

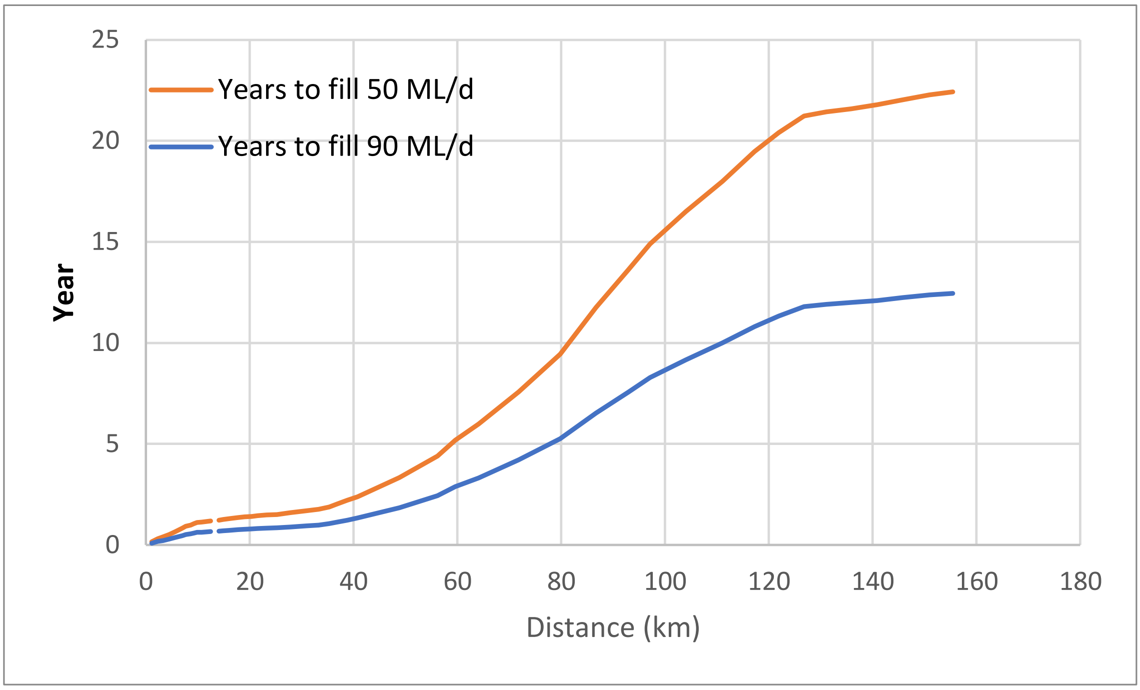

Figure 3-25: Minimum time to fill alluvial storage for 50 and 90 ML/day discharge

3.5 Interaction with surface water modelling

The results from this modelling were fed back to the surface flow modelling. This modelling used an assumed loss rate over the extent of surface water flow. Once the capacity of the alluvium was filled for a reach, only infiltration equivalent to the lateral and evapotranspiration losses from the reach were allowed. For the pulsed scenarios, these losses accumulated during the “dry” periods and the reach had capacity to accept increased infiltration when the flow restarted.

3.6 Discussion

The water balance modelling shows that there is considerable capacity in the alluvium to receive creek infiltration. However, the infiltration rates are large enough to fill most of the reaches within a short period of time once the flow spreads through the area. For the pulse scenarios, the net infiltration rate into the alluvium increases during the dry period as the wetted area decreases, and, when the discharge restarts, is followed by a decrease in the infiltration rate.

For the Homestead Creek discharge scenarios, high rates of lateral discharge to the left (travelling in a downstream direction) occur in reach 7. This is due to the high conductivity material in this vicinity and the low adjacent water table due to the dewatering of OB25 Pit 3. This lateral flow is likely to increase the dewatering requirements in this pit, or, if the dewatering is turned off, increase the rate of filling of the pit.

Other large lateral flows relative to the length of the waterway occur to the left in reaches 30, 31 and 32. This is because the Kalgan Creek tributary and paleo-Fortescue River have higher hydraulic conductivity than the surrounding material, making it a preferred conduit for groundwater flow to the west and north in this vicinity.

4 SURFACE WATER MODELLING

Two-dimensional (2D) modelling of the flow of surface water was carried out using the TUFLOW HPC software package (Version 2020-10-AD, BMT, 2022). TUFLOW HPC was selected due to its ability to accurately represent the channel hydraulics whilst also being able to incorporate a limited level of groundwater-surface water interaction. The results of the surface water modelling were fed into a GoldSim model to estimate the level of interaction between surface water and groundwater downstream of the proposed discharge point on Homestead Creek. The GoldSim modelling supplemented the limited groundwater/surface water interaction that can be modelled in TUFLOW.

An initial TUFLOW model which applied an assumed loss rate was used to decide the maximum wetted area in each reach. The number of equi-sized wet cells from the surface water modelling was then provided to the GoldSim modelling. The water balance for each reach was then calculated by the GoldSim modelling to decide the revised water table depth. The lateral losses and evapotranspiration due to rising water table were calculated and then included in the second iteration of the surface water modelling to determine the likely downstream extent.

4.1 Modelling philosophy

4.1.1 Surface water infiltration

The main processes that are expected to govern the extent and timing of the wetting front associated with the discharge of surplus water is the infiltration of water into the subsurface and the subsequent storage of said water. The same approach for surface water infiltration in the SPS was adopted in the DPS – refer to PREP-1210-C-12057 (Advisian, 2021) for further detail.

The soil parameters for the Green-Ampt loss model that were adopted in the 2D TUFLOW model were based on the available data and knowledge of the study area. They were split into two areas, covering Homestead Creek and Fortescue River.

The Green-Ampt parameters adopted in the TUFLOW model are shown in Table 4-1. The hydraulic conductivities for the two areas were based on an average of the expected hydraulic conductivities for the units along the waterway and were provided to Advisian by BHP. The infiltration rates associated with each reach were based primarily on analysis of hydrographs of rainfall events, and were calculated by BHP based on the loss of flow between the following stations:

- Fortescue River Mid (23.182°S, 119.919°E) – 19 km downstream of Ophthalmia Dam; and
- Fortescue River Downstream (22.903°S, 120.204°E) – 74 km downstream of Ophthalmia Dam.

Sensitivity analyses were conducted on a selection of the Green-Ampt parameters (see Section 5.3).

Table 4-1: Green-Ampt infiltration loss model inputs

Reach	Suction (mm)	Hydraulic Cond. (mm/hr)	Porosity Fraction	Initial Moisture Fraction
Homestead Creek	200	8.33	0.2	0
Fortescue River	200	18.75	0.2	0

4.1.2 Depth to groundwater

A groundwater elevation dataset (Watertable.tif) covering Homestead Creek, Ophthalmia Dam, Ethel Gorge and part of the Fortescue River was provided by BHP as part of a Leapfrog Geo model. It is understood that this dataset represents the typical groundwater elevation in 2019. The extent of the dataset is presented in Figure 2-4.

Advisian calculated the depth to groundwater for the area covered by the Watertable.tif dataset. There were areas immediately downstream of Ophthalmia Dam in the infiltration basins where the groundwater elevation was found to be above the ground level. By contrast, there were areas in Homestead Creek and the Fortescue River reaches, where the depth to groundwater was 10 m or more. Consultation with BHP subject matter experts (SMEs) with extensive knowledge of Ethel Gorge led to the adoption of a minimum depth to groundwater of 2 m throughout the model domain.

An assumption was required regarding the depth to groundwater for considerable area of the Fortescue River outside of the coverage of the Watertable.tif dataset (north of Salty Pools). Interpolation between the depth to groundwater based on the Watertable.tif dataset and the Fortescue Marsh region (where the water table is understood to be approximately 2 m below ground level) was used for the area where data was not available . The groundwater table and ground level profile comparison are depicted in Figure 4-1.

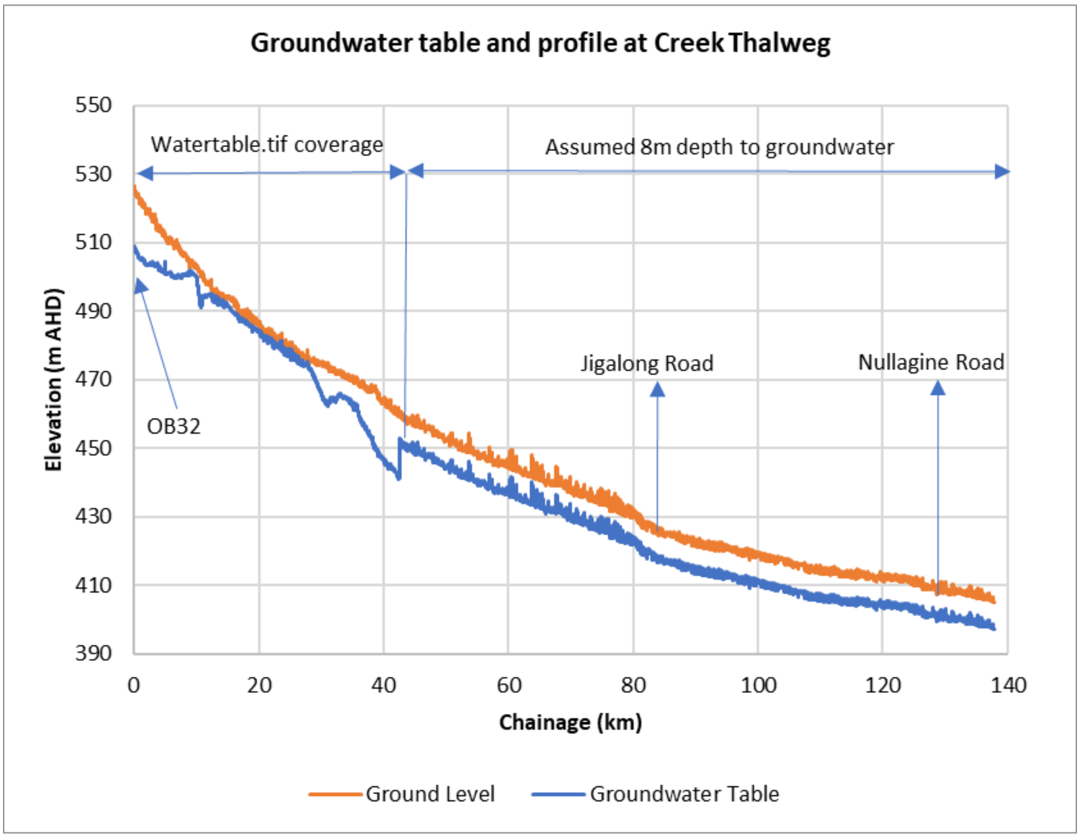

Figure 4-1: Groundwater table and ground level profile comparison

4.1.3 Subsurface storage and losses

As TUFLOW is a 2D surface water modelling program, there is no functionality to incorporate the lateral flow of groundwater. Each cell within the model domain can have a depth to groundwater associated with it, and thereby incorporate a level of subsurface water storage. The infiltration and storage of surface water into the subsurface is governed by the parameters outlined in Section 4.1. The available subsurface storage that is utilised in the TUFLOW model is a function of the number of wet cells, the depth to groundwater and the model cell size (i.e., alluvial storage is only activated if water flows over a cell). The actual alluvial storage available in the system is far greater than the product of the number of wet cells, depth to groundwater and cell size. Section 4.3 outlines the process that was undertaken to determine the appropriate factor to apply to the depth to groundwater to represent the actual available alluvial storage in the TUFLOW model.

There is no method in TUFLOW for removing the groundwater once the surface water has infiltrated into the subsurface. It is for this reason that the GoldSim modelling was required to capture the potential lateral groundwater migration based on the transmissivity of the local geology. The total lateral groundwater flux was then added to the evapotranspiration (see Section 4.1.4) to simulate the loss of groundwater from the subsurface to the surrounding areas.

Given the variability of the subsurface geology, different lateral groundwater losses were applied in accordance with the GoldSim model reaches (see Section 3.2). These reaches are shown in Figure 3-1.

4.1.4 Evapotranspiration

Point potential evapotranspiration data obtained from the Bureau of Meteorology (BoM) has been applied throughout the model domain (8.5 mm/day). This was similar to that in the Eastern Pilbara Water Resource Management Plan (BHP, 2018). This was applied as a negative rainfall in the TUFLOW model domain to simulate the evaporation and remove surface water from the model. If a negative rainfall is specified, it is treated as a loss in TUFLOW model. Negative rainfall is only applied to wet cells. As such, it is a good proxy for the evaporation process for the simulation of creek discharge.

4.1.5 Roughness

Examination of the available satellite and aerial images indicated that there is a mixture of heavily and sparsely vegetated areas in the braided and poorly defined main channel of the Fortescue River reach. This contrasts with the well-defined main channel of Homestead Creek, which is more incised and consequently has less vegetation by comparison. A single Manning’s n value of 0.04 was applied throughout the model domain to account for the average roughness across the two different geomorphic systems. It is acknowledged that this approach to roughness allocation is simplistic, but given the time scales over which the model was run, and as the simulated discharge rates were unlikely to overtop the banks of the main channel(s), it was deemed appropriate.

4.2 Modelling Methodology

The overall structure of the coupling between the GoldSim and TUFLOW models was developed in the previous phases and updated in the DPS. The modelling was performed using iterations between TUFLOW simulating the surface water flows and GoldSim simulating processes in the surrounding alluvium. The TUFLOW modelling used the Green-Ampt method to simulate the infiltration of water into the alluvium below wetted cells. The GoldSim model was used to simulate the alluvium as a series of reaches based on hydrogeological conditions. Losses and fluxes of groundwater in the GoldSim alluvium model in excess of the available TUFLOW storage were added (as negative values) to the existing evaporation from the surface flows.

The TUFLOW model increased the number of reaches to 54, which enabled greater resolution of the processes occurring, particularly around the wetting front extension and retraction.

4.2.1 Boundary conditions

The inflow boundary conditions associated with various surplus water discharge locations and model scenarios were implemented as source area polygons within the 2D model domain (see

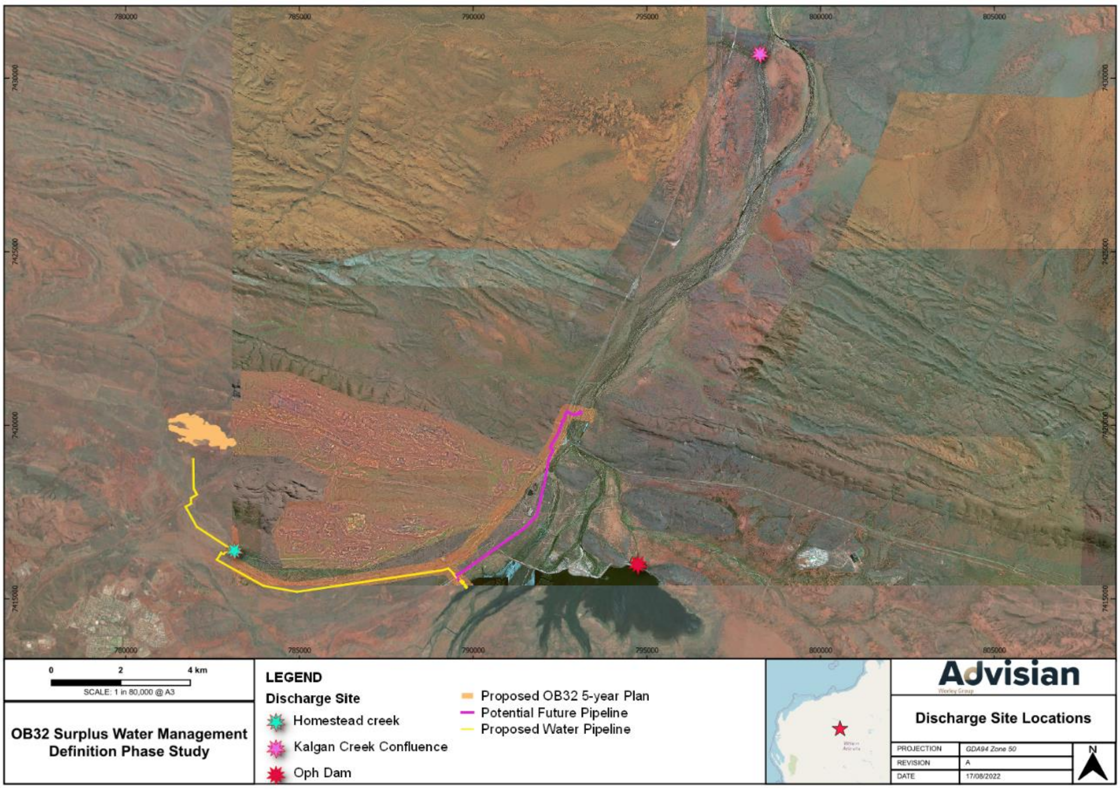

Figure 5-1). A 2% slope boundary condition was applied at the downstream end of the model to reduce the likelihood of backwater effects adjacent to the model outlet. The only other boundary condition applied was the negative rainfall representing evaporation and alluvium fluxes.

4.2.2 Model cell size

The 2D model base cell size was set to 25 m (with sub grid sampling of 5 m) to strike a balance between practical model run times whilst still providing meaningful results. Sub-grid sampling (SGS) stores and uses curves representing the sub-2D-cell terrain data of the DEMs and terrain modification shapes instead of each 2D cell and each 2D face having only one elevation.

Benchmarking has shown the benefits to be substantial for certain types of applications, for example:

- Catchment scale models flow much more effectively with water not being “trapped” by a coarse cell resolution, and cell size convergence (i.e. demonstration that by reducing the cell size(s) the model results do not demonstrably change) at much coarser cell sizes; and,

- Disturbed flow fields that can be apparent along a “saw-tooth” regular mesh wet-dry boundary disappear, with no spurious additional head losses generated and the results consistent with a well-designed flexible mesh. This has major benefits in that complex open channels, such as the braided Fortescue River can be accurately modelled using TUFLOW HPC using coarse cell sizes at any orientation to the channel.

The considerable size of the model domain equated to a total model size of approximately 6.4 million 25 m cells.

4.2.3 Interaction with water balance modelling

The TUFLOW modelling used the Green-Ampt method to simulate the infiltration of water into the alluvium below wet cells. An assumed loss rate over the extent of surface water flow was applied for the first iteration of the TUFLOW model run. The resulting number of wet cells per reach, per day were included in the GoldSim model to represent the time-varying influx of water into the subsurface storages via infiltration. The lateral losses were calculated in GoldSim based on the difference in head between the adjacent aquifers water table in the reach. Evapotranspiration was calculated as per the method outlined in Section 3.2.4. The combined evapotranspiration and lateral losses derived from the GoldSim model were then applied to each reach in the TUFLOW model as time-varying “negative” rainfall for the second iteration. For the pulsed scenarios, these losses accumulated during the “dry” periods and the reach had capacity to accept increased infiltration when the flow restarted.

4.3 Calibration

The calibration of the TUFLOW model centred around matching the timing of the wetting front associated with the 2020 discharge trial from Ophthalmia Dam reaching the Fortescue River Downstream Gauging Station (GS). As outlined by Rea (2021), the discharge event in question involved the release of water from Ophthalmia Dam at a rate of 130 ML/day from 23 January to 10 August 2020. The wetting front arrived at the Fortescue River Downstream GS after 129 days with a relatively constant flow rate of 22 ML/day observed between 1 June and 14 August 2020. This implies that a steady state loss rate of 108 ML/d occurred over the distance between the dam and the gauging station (i.e., 90 mm/day based on average flow widths from aerial imagery).

The infiltration rate for the base of Fortescue River is a key parameter in determining the timing of the wetting front of any water release. An initial infiltration rate of 450 mm/d (18.75 mm/h) was adopted in the Fortescue River reaches. It must be noted that infiltration rates in the Fortescue River during natural flow events were found be as high as 580 mm/day (Rea, 2021). These two values represent the lower and upper bounds of infiltration rates tested during the calibration process.

The OB32 Surplus Water SPS independent peer review (IPR) team identified that a reduction in the depth to the groundwater table correlated to a considerable increase in the wetting front timing/extent predicted by the 2D hydraulic modelling, which showed the importance of adopting a reasonable and accurate depth to groundwater value.

As outlined in Section 4.1.3, the cell size and number of wet cells serve to limit the available alluvial storage in the TUFLOW model. In reality, there is a far greater potential storage volume available (see green shading in Figure 4-2). In order to ensure that the TUFLOW model reflected the true available alluvial storage, a factor was applied to the depth to groundwater parameter. Applying this factor served to increase the available alluvial storage in the model.

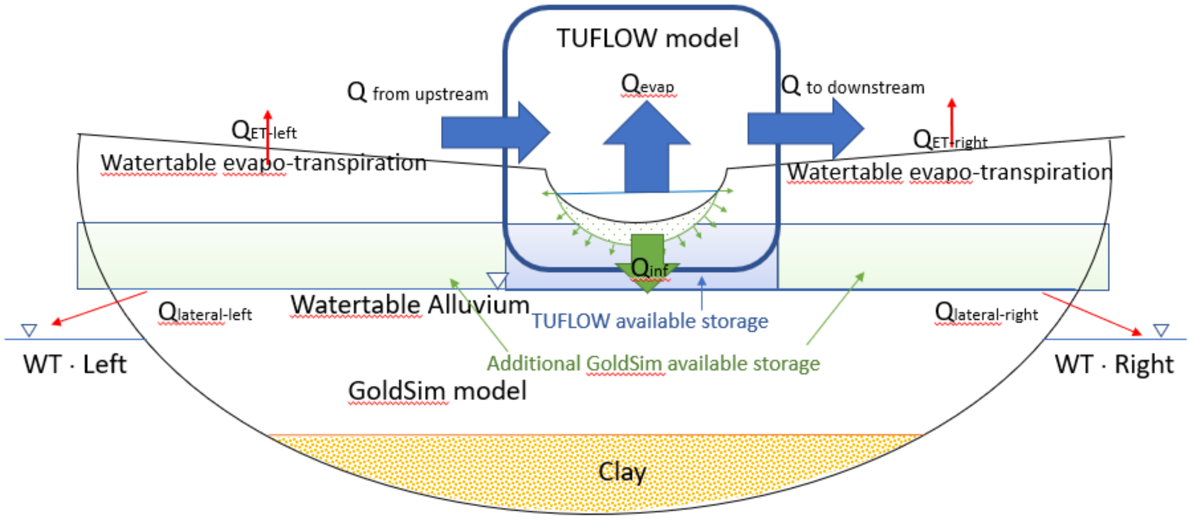

Figure 4-2: Model cross-section (blue zone shows unfactored available alluvial storage)

TUFLOW calibration runs, and their associated wetting front timings are summarised in Table 4-2. The scenario applying 450 mm/d infiltration rate with a depth to groundwater factor of 2.5 took exactly 129 days to reach the Fortescue River Downstream GS. The same result was achieved by adopting 580 mm/d infiltration rate, with a depth to groundwater factor of 2.35.

Table 4-2: Wetting front timing calibration (Ophthalmia dam – 130 ML/d for 200 days)

Run No.	Infiltration rate (mm/d)	Depth to groundwater factor	Days to reach Fortescue River Downstream GS
1	580	1	66
2	450	2	112
3	**450**	**2.5**	**129**
4	450	3	147
5	450	3.2	150
6	580	2.3	127
7	**580**	**2.35**	**129**
8	580	2.5	134

The next step of the calibration process was to replicate the steady state losses occurring between Ophthalmia Dam and the Fortescue River Downstream GS during the 2020 discharge event. To expedite this process, the effect of alluvial storage was removed from the equation by setting the depth to groundwater in the model to zero. A range of loss rates were tested in an attempt to replicate the 22 ML/d of remaining flow at the Fortescue River Downstream GS. The results are summarised in Table 4-3. A loss rate of 55 mm/d for the area between Ophthalmia Dam and the Fortescue River Downstream GS resulted in a steady state loss of approximately 108 ML/d.

Table 4-3: Steady state loss calibration runs (130 ML/d discharge for 200 days)

Run No.	Loss rate (mm/d)	Flow at Fortescue River Downstream GS (ML/d)
1	8.5	111
2	20	87
3	40	48
4	53	25
5	**55**	**22**
6	60	14
7	70	0.01
8	90	0

The TUFLOW model required a lower steady state loss rate (55 mm/d instead of 90 mm/d proposed by Rea [2021]) to reproduce the flow rate observed at the Fortescue River Downstream GS during the 2020 discharge trial. Although Rea (2021) did not outline the average flow width associated with the 2020 discharge event, average flow widths associated with natural flow events were listed between 21-30 m. These natural flow events are likely to have had flows orders of magnitude greater than the 130 ML/d discharge trial. It is therefore reasonable to assume that the average flow width associated with the 2020 discharge trial would've been in the order of 10-15 m.

Given that the TUFLOW model cell size was 25 m, this equates to the minimum flow width in the model. A larger wet area for losses to act on necessitated a lower loss rate to achieve the same flows at the Fortescue River Downstream GS.

5 PREDICTIVE MODELLING

5.1 Scenarios

The surplus water discharge location on Homestead Creek was modelled in the 2D hydraulic model. The flows from Kalgan Creek and Ophthalmia Dam were considered to investigate the impact of the proposed OB32 creek discharge combined with the existing operational dewatering practices on the timing and extent of the potential wetting front. The respective discharge locations are depicted in

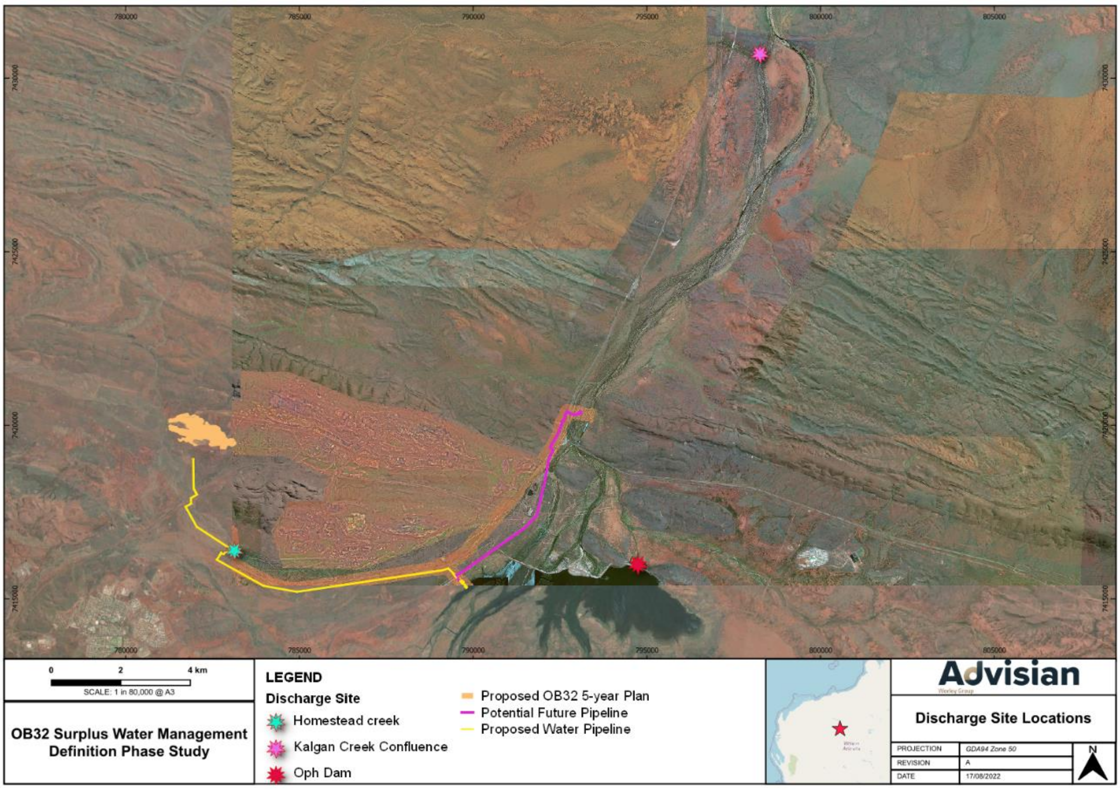

Figure 5-1, and the modelled scenarios are outlined in Table 5-1.

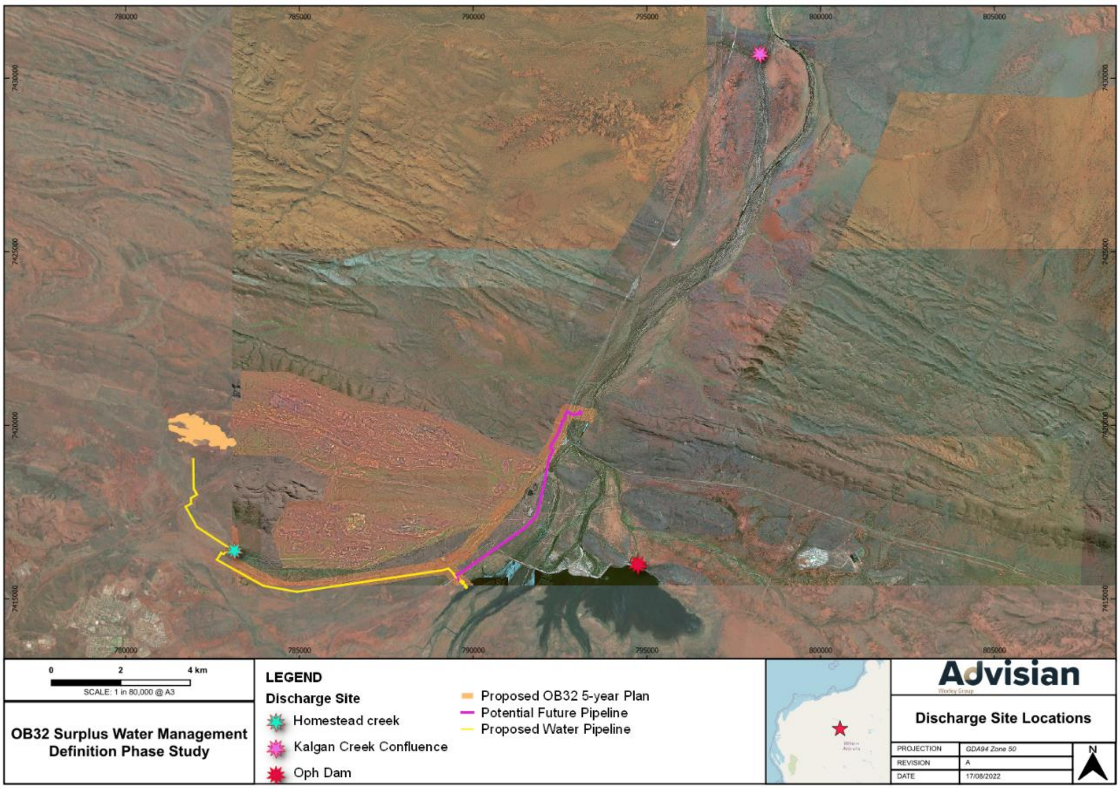

Figure 5-1: Discharge site locations.

The modelling approach differed depending on the scenario being modelled. The scenarios with the specified discharge rates included the factored depth to groundwater as a representation of the available alluvial storage. Given the long model runtimes, it was decided to fast-track the scenarios requiring steady state conditions. To do so, the depth to groundwater in the TUFLOW model was reduced to zero. This allowed the model to reach steady state in a matter of days rather than years.

The maximum discharge + natural event scenario stipulated that the 1-in-2 year, 72-hour rainfall event be included as an additional inflow after the model had reached steady state. The inflow hydrograph representing the flow generated from this rainfall event in the Homestead Creek catchment was derived from an existing RORB model (see Figure 5-2 for the model schematisation). Flow for the 1-in-10 year, 72-hour event was extracted downstream of the sub-catchment AB (upstream of the creek discharge model domain) and indexed via the application of a decay factor of 0.214 to obtain a hydrograph representing the 1-in-2 year, 72-hour event.

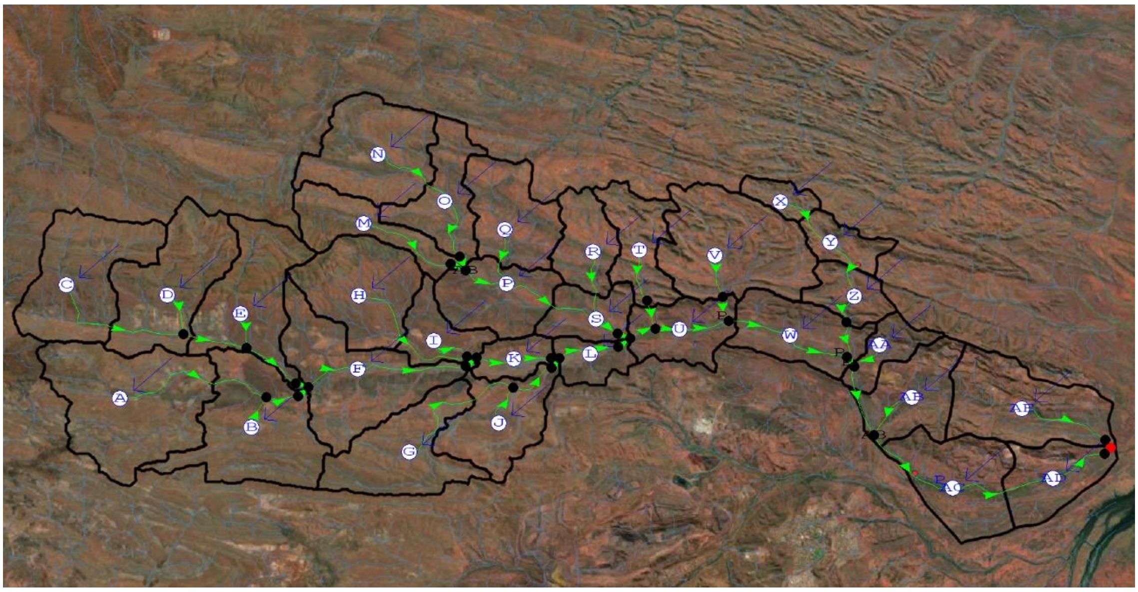

Figure 5-2: RORB model schematisation of Homestead Creek catchment

Table 5-1: Discharge modelling scenarios

Model type	Scenario	Discharge rate(s)
Infiltration loss model including alluvial storage	Continuous	Continuous 60 ML/d
	Pulse	60 ML/d for 4 months, off for 2 months, repeat
	Kalgan Creek	Continuous 60 ML/d + 27 ML/d inflow from Kalgan Creek confluence
	Oph Dam Release 1	Continuous 60 ML/d + 120ML/d for 3 months from Oph Dam
	Oph Dam Release 2	Continuous 60 ML/d + 250 ML/d for 3 months from Oph Dam
	Kalgan Creek + Oph Dam Release 1	Continuous 60 ML/d + 27 ML/d inflow from Kalgan Creek confluence + 120 ML/d for 3 months from Oph Dam
	Kalgan Creek + Oph Dam Release 2	Continuous 60 ML/d + 27 ML/d inflow from Kalgan Creek confluence + 250 ML/d for 3 months from Oph Dam
Steady state model with no alluvial storage	Maximum discharge optimisation	Maximum continuous discharge that can be released without reaching (i) Jigalong Road and (ii) Nullagine Rd

Model type	Scenario	Discharge rate(s)
	Maximum discharge + natural event	Maximum continuous discharge that can be released without reaching (i) Jigalong Road and (ii) Nullagine Rd, in combination with 1-in-2 year, 72 hour rain event (included as additional inflow after steady state has been reached). Model run time extended until steady conditions achieved.
	Pulse optimisation	Optimise pulse sequence to (i) Jigalong and (ii) Nullagine Roads

5.2 Modelling results

The TUFLOW model was run for the scenarios outlined in Section 5.1 using the iterative process outlined in Sections 3.5 and 4.2.3. Initial model scenarios were set to run for a duration of one year, with the duration being extended for some scenarios. All model scenarios involved output of results on a daily basis. The downstream points of interest and the flow distances associated with each discharge location are shown in Table 5-2 (noting that the end of the TUFLOW model domain was limited by the available elevation data).

Table 5-2: Approximate potential flow distances associated with each discharge location and downstream point of interest

Discharge Location	Distance to Jigalong Road (km)	Distance to Nullagine Road (km)	Distance to End of TUFLOW Model (km)
Homestead Creek	75	130	140
Ophthalmia Dam	68	123	132
Kalgan Creek	50	105	114

The base case of 60 ML/day over 365 days was run for two iterations. Figure 5-3 shows the change in wetting front distance over the first year for the two iterations. The shorter distance in the second iteration is a result of including the additional storage in and losses from the alluvium calculated in the GoldSim model.

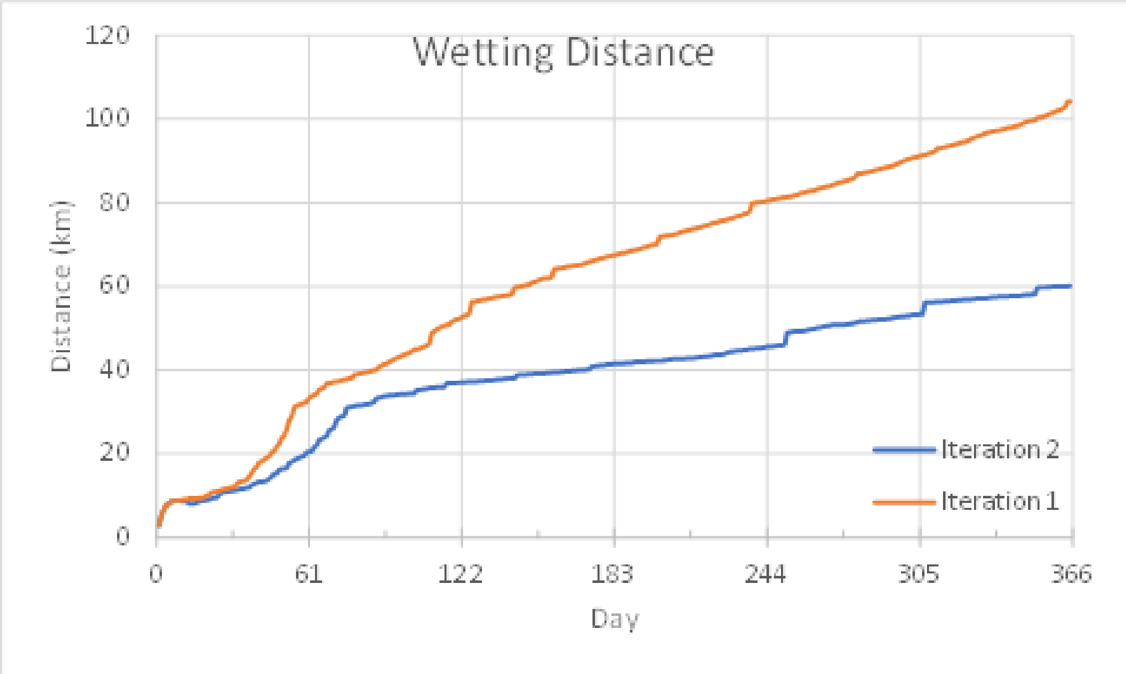

Figure 5-3: Wetting front distance for 60 ML/day discharge from Homestead Creek

Figure 5-4 shows the simulated water table levels in selected reaches in the GoldSim model. The water tables initially rise fast as the surface water infiltration fills the immediate volume under the reach, and then slows as the water flows into the outer parts of the alluvium. It then flattens as the reach alluvium becomes full (Reaches 12, 23 and 30).

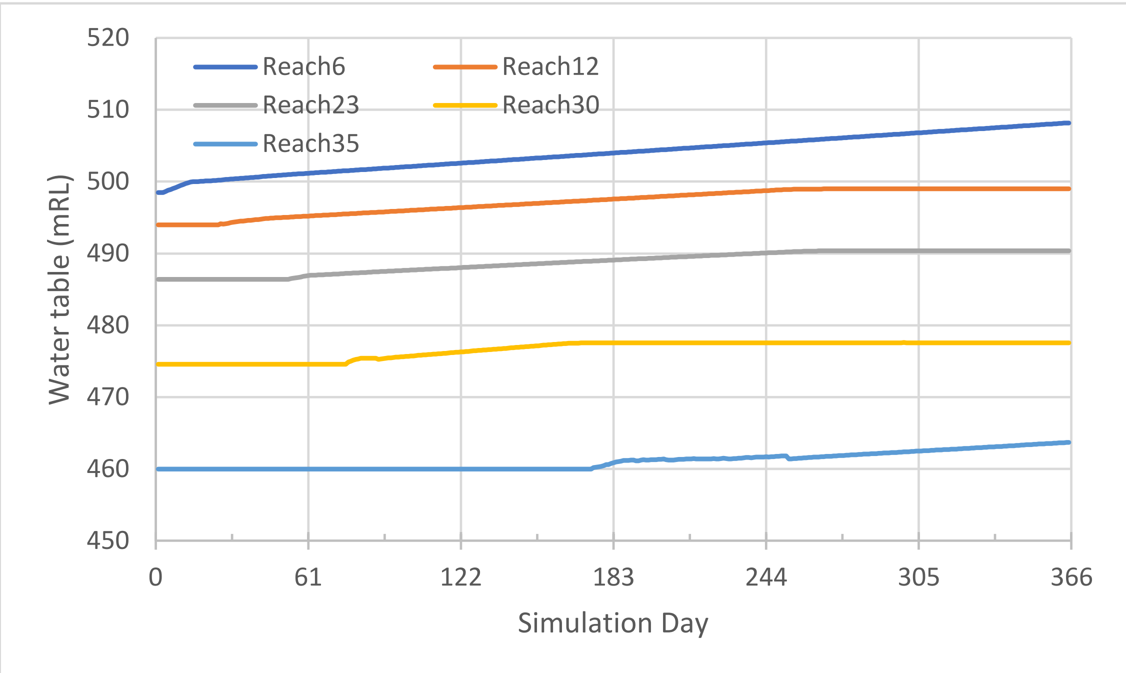

Figure 5-4: Simulated water level in selected reaches for 60 ML/day discharge

Evapotranspiration from the water table for selected reaches is shown in Figure 5-5. Reaches 6 and 12 had only small rates of evapotranspiration compared with the other reaches. The evapotranspiration rates became constant once the water table reached the base of the creek.

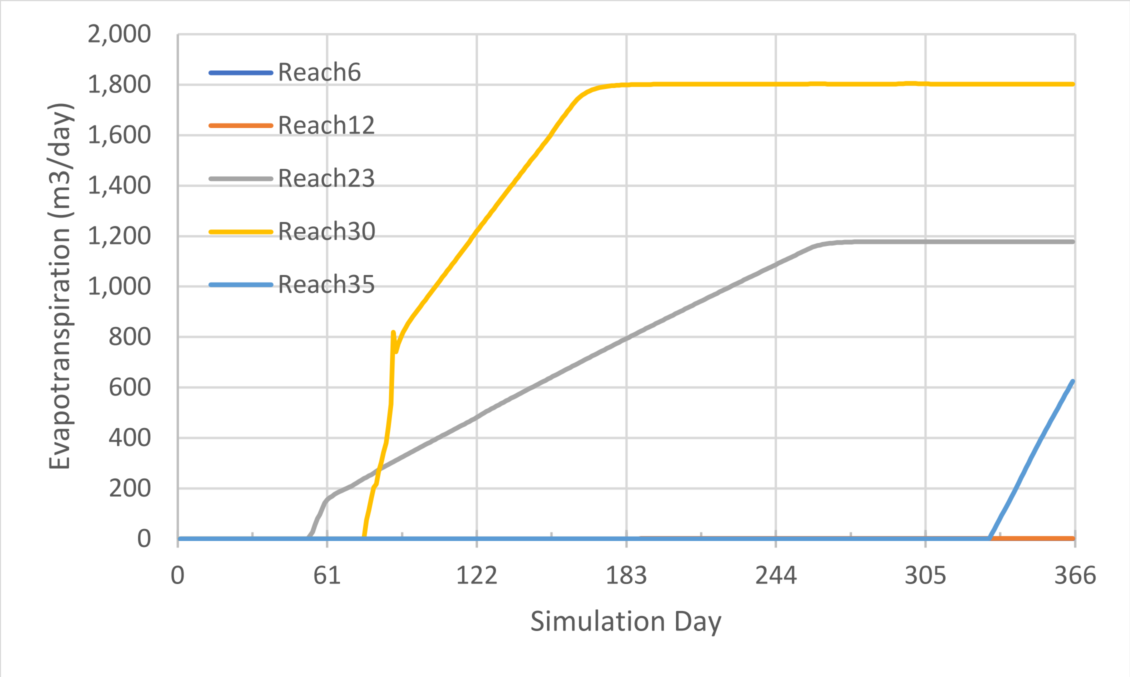

Figure 5-5: Simulated water table evapotranspiration for selected reaches for 60 ML/day discharge

The lateral losses for selected reaches are shown in Figure 5-6. The only reach with substantial lateral leakage from the alluvium is Reach 6, with both left and right fluxes peaking at around 4.5 m^3/day. These fluxes are substantially less than those associated with evapotranspiration.

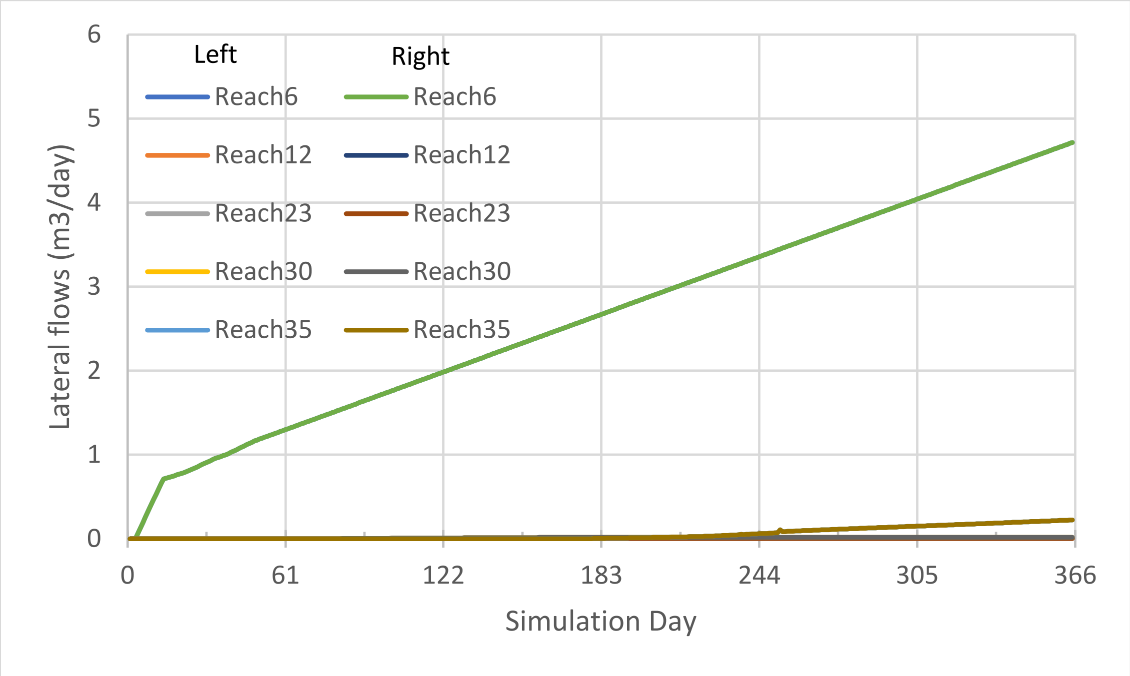

Figure 5-6: Lateral flow from selected reaches for 60 ML/day discharge

5.2.1 Steady state

Steady state modelling was conducted by removing the influence of alluvial storage to determine the maximum continuous and pulsed discharge rates which could be adopted without the wetting front reaching Jigalong Road and Nullagine Road. Without removing the influence of alluvial storage, it would have taken many years of model runtime to reach steady state. Given that it took ~12 hours per year of run time, it was not feasible to persist with this approach.

A continuous discharge rate of 47.5 ML/d resulted in the TUFLOW model (with no available alluvial storage) reaching steady state before the wetting front arrived at Jigalong Road. A continuous discharge rate of 82 ML/d resulted in the same TUFLOW model reaching steady state before the wetting front arrived at Nullagine Road.

After applying the 1-in-2 year, 72 hour rain event, it took another 15 days for the scenario with a discharge rate of 47.5 ML/d to reach steady state again. For the scenario with a discharge rate of 82 ML/d, it took another 27 days to reach steady state after applying the rainfall event as an inflow boundary condition.

The optimised continuous discharge scenarios were used as a starting point to determine the optimal pulsed discharge timing without the wetting front reaching Jigalong Road and Nullagine Road. Firstly, the Homestead Creek discharge was run at a rate of 47.5 ML/d for 80 days to reach steady state. The discharge was then stopped for 30 days, and the surface water levels in the reaches reduced over time to either a dry reach or a smaller number of wetted cells (presumably isolated pools in the reach).

It is noted that the available surface water underwent evaporation during this period, and the ongoing infiltration balanced the losses (lateral flow to adjacent formations and evapotranspiration from the alluvium) until the reach (surface water) became dry. If the surface water became dry in a reach, then no more infiltration took place, and the water table began to fall due to ongoing lateral flow to adjacent formations and evapotranspiration.

It was evident that the rates of evapotranspiration and lateral flow from the alluvium decreased as the water table declined. Once the discharge recommenced (at a rate of 60 ML/d – greater than the steady-state rate), then flow resumed along the reaches, filling the alluvium, and eventually reaching Jigalong Road again. The modelling found that this would occur if the discharge continued for 13 days or more. Therefore a cycle of 30 days of no-discharge followed by 12 days of discharge would prevent surface flow over Jigalong Road.

The optimised pulse sequence for Nullagine Road was found to involve the same timing (30 days off, 12 days on), however the discharge rate during the pulse was 120 ML/d instead of 60 ML/d.

For the 60 ML/day pulsed discharge, the reaches that became dry during or immediately after the dry period were 12, 20-23, 25-29, 31-32, 34-38 and 40-42. Pools that could continue to supply infiltration to the alluvium remained in all other reaches.

An example using Reach 32 is shown in the figures below. Figure 5-7 shows the number of wet cells in the reach. The number of wet cells decreased to zero by Day 104 in the first off period (24 days after the cessation of discharge) and Day 147 in the second off period (14 days after the cessation of discharge). The rewetting of the reach occurs in Day 117 and Day 159 in first and second 60 ML/day discharge periods, respectively. In the off periods, the water table initially declines slowly until the reach becomes dry, and then the rate of decline increases until the reach rewets, when the water table rises back towards the base elevation of the creek.

The rate of evapotranspiration from the reach (see Figure 5-9) increases as the number of wetted cells (and thus the width of the waterway) decrease, increasing the area available for evapotranspiration. The evapotranspiration reaches a maximum as the number of wetted cells goes to zero, and then starts to decline slowly with the lowering of the water table. It stays low as the reach rewets because the waterway flow covers a larger area and then increases again as the flow recedes during the no-flow phase. There are very slight decreases in the lateral loss rates proportional to the dropping of the water table in the reach, but these are relatively small changes (<0.1%).

An examination of the period of no wet cells between Ophthalmia Dam (Reach 19) and where the Fortescue River turns east (Reach 32) is shown in Table 5-3. Note that the reaches not included have wet cells through the dry period. It is dry for a maximum of 25 days in Reach 29 (which includes 3 days until the restarted discharge rewets the reach). The drop in water table in the reaches is up to 20 cm and drops at rates between 0.6 cm/day and 1.4 cm/day prior to the restart. Note that the rate of water table decrease becomes smaller with time as the water table falls.

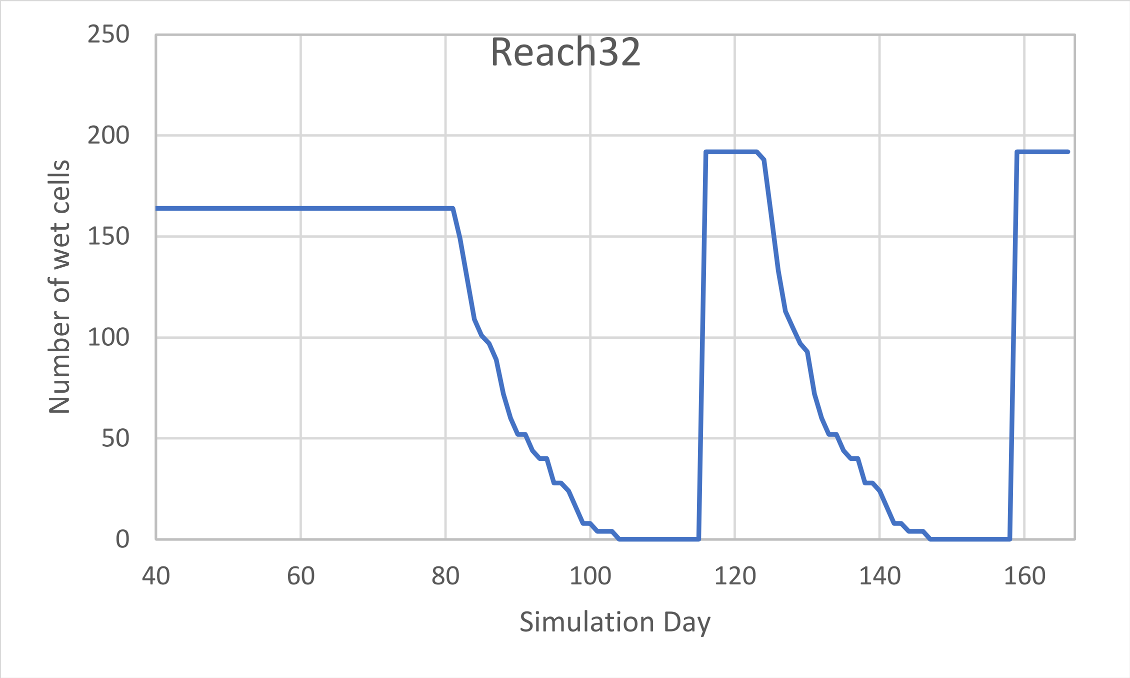

Figure 5-7: Number of wet cells in Reach 32 for 60 ML/day pulsed scenario

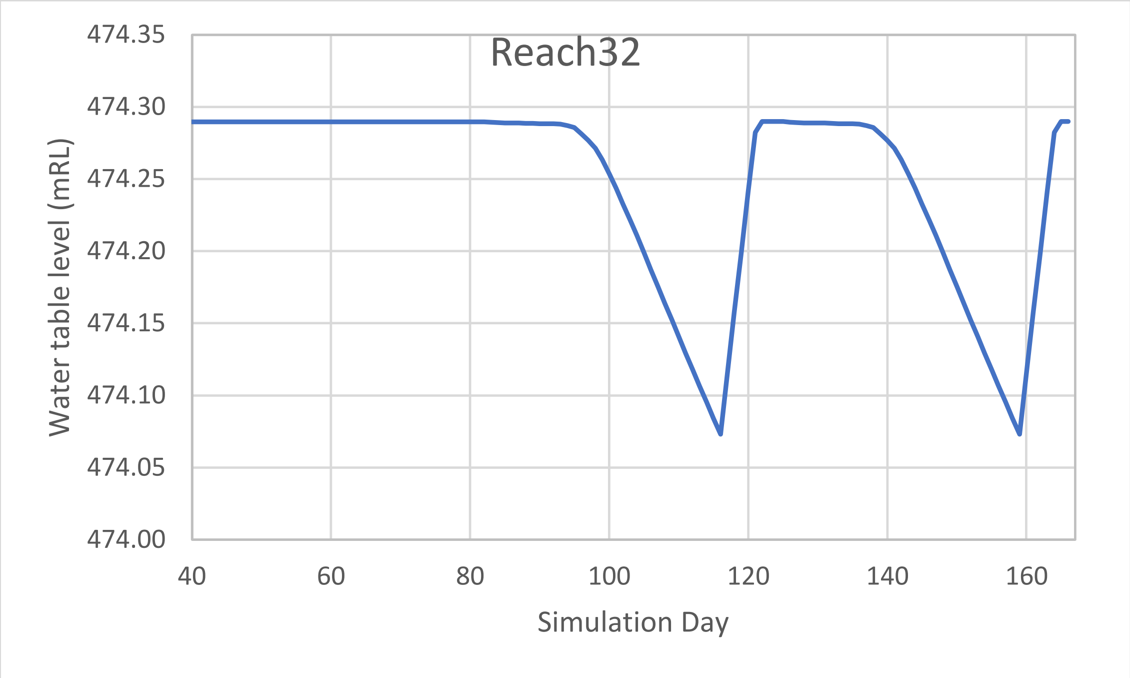

Figure 5-8: Water table level in Reach 32 for 60 ML/day pulsed scenario

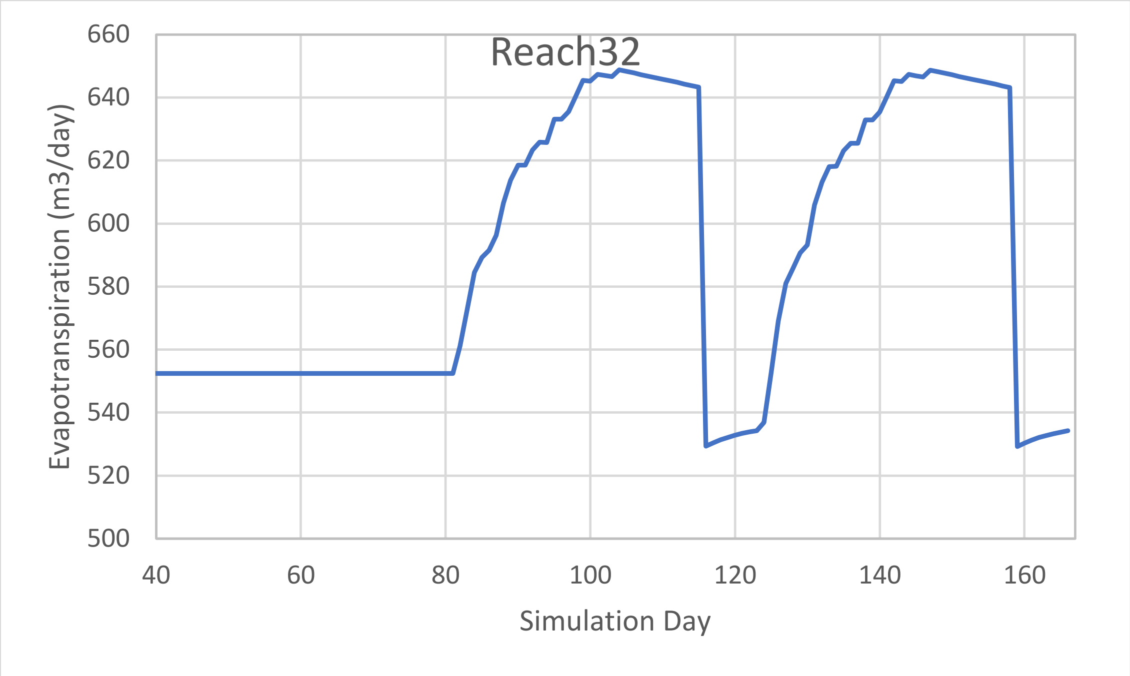

Figure 5-9: Evapotranspiration from Reach 32 for 60 ML/day pulsed scenario

Table 5-3: Water table drop in alluvium during period of no discharge for 60 ML/day pulse

Reach	Drop total (m)	Drop before restart (m)	Dry days	Dry days before restart	Daily drop (m/day)	Daily drop before restart (m/day)
20	0.1192	0.1114	15	13	0.0079	0.0086
21	0.1760	0.1561	17	14	0.0104	0.0111
22	0.2052	0.1857	20	17	0.0103	0.0109
23	0.0624	0.0417	6	3	0.0104	0.0139
25	0.0882	0.0738	12	9	0.0073	0.0082
26	0.1124	0.0994	17	14	0.0066	0.0071
27	0.0710	0.0603	13	10	0.0055	0.0060
28	0.1173	0.1038	17	14	0.0069	0.0074
29	0.1698	0.1569	25	22	0.0068	0.0071
31	0.0222	0.0071	3	0	0.0074	-
32	0.0906	0.0744	11	8	0.0082	0.0093

Similar results were found for the pulsed discharge of 120 ML/day to Nullagine Road. The reaches that became dry during or immediately after the dry period were 12, 20-23, 25-29, 31-32, 34-38, 40, 42-47 and 49-50. An examination of the period of no wet cells between Ophthalmia Dam (Reach 19) and where the Fortescue River turns east (Reach 32) is shown in Table 5-4. Note that the reaches not included have wet cells through the dry period. It is dry for a maximum of 23 days in Reach 29 (which includes 3 days until the restarted discharge rewets the reach). The drop in water table in the reaches is up to 20 cm and drops at rates between 0.6 cm/day and 1.6 cm/day.

Table 5-4: Water table drop in alluvium during period of no discharge for 120 ML/day pulse

Reach	Drop total (m)	Drop before restart (m)	Dry days	Dry days before restart	Daily drop (m/day)	Daily drop before restart (m/day)
20	0.1192	0.1036	14	12	0.0085	0.0086
21	0.1571	0.1368	14	12	0.0112	0.0114
22	0.2048	0.1842	18	16	0.0114	0.0115
23	0.0535	0.0320	4	2	0.0134	0.0160
25	0.0813	0.0668	10	8	0.0081	0.0083
26	0.1084	0.0951	15	13	0.0072	0.0073
27	0.0658	0.0549	11	9	0.0060	0.0061
28	0.1216	0.1007	16	13	0.0076	0.0077
29	0.1678	0.1477	23	20	0.0073	0.0074
31	0.0222	0.0000	2	0	0.0111	-
32	0.0927	0.0677	10	7	0.0093	0.0097

Table 5-5 and NB: Given that the Homestead Continuous scenario eventually reached Jigalong Rd, it is expected that the other scenarios would also reach Jigalong Rd with longer model runtimes.

Table 5-6 summarise the results of the specified discharge and steady state modelling scenarios, respectively. Appendix A shows the wetting front extent associated with the Homestead, Ophthalmia Dam and Kalgan Creek discharge locations for the Design and Optimisation scenarios.

Table 5-5: Summary of specified discharge modelling results

Scenario Name	Model run time (days)	Wetting Front Distance (km)	Days to reach Jigalong Rd
Homestead Continuous	1,806	76	1,806
Homestead Pulse	365	41	N/A*
Kalgan Creek	365	61	N/A*
Oph Dam Release 1	365	58	N/A*
Oph Dam Release 2	365	86	84
Kalgan Creek + Oph Dam Release 1	365	71	N/A*
Kalgan Creek + Oph Dam Release 2	365	93	70

NB: Given that the Homestead Continuous scenario eventually reached Jigalong Rd, it is expected that the other scenarios would also reach Jigalong Rd with longer model runtimes.

Table 5-6: Summary of steady state modelling results

Scenario	Discharge rate (ML/d)	No. of days to reach steady state
Maximum continuous discharge that can be released without reaching Jigalong Road	47.5	70
Maximum continuous discharge that can be released without reaching Nullagine Rd	82	182
Maximum continuous discharge that can be released without reaching Jigalong Road and, in combination with 1-in-2 year, 72 hour rain event (to be included as additional inflow after steady state in the model has been reached)	47.5	85 (15 days after natural rainfall event)
Maximum continuous discharge that can be released without reaching Nullagine Rd and, in combination with 1-in-2 year, 72 hour rain event (to be included as additional inflow after steady state in the model has been reached)	82	209 (27 days after natural rainfall event)
Optimise pulse sequence to Jigalong Road	Discharge at 47.5 ML/day for 80 days, off for 30 days, on at 60 ML/day for 12 days, off for 30 days, on at 60 ML/day for 12 days.	N/A
Optimise pulse sequence to Nullagine Road	Discharge at 80 ML/day for 182 days, turn off flow for 30 days, turn on flow at 120 ML/day for 12 days, turn off flow for 30 days, turn on flow at 120 ML/day for 12 days.	N/A

5.3 Sensitivity analysis

5.3.1 TUFLOW model

Sensitivity analysis was conducted on several parameters to determine their impact on the timing and extent of the estimated wetting front. A summary of the parameters tested, the models in which they were tested and the sensitivity of the modelling results to each parameter is presented in Table 5-7.

Table 5-7: Parameters tested in sensitivity analysis

Parameter	Units	Values Tested	Model Tested	Comment
Porosity	%	0.1, 0.2	Alluvial storage	Slightly sensitive
Evapotranspiration	mm/h	6.5, 10.5	Steady state	Very sensitive
Hydraulic Conductivity	mm/h	18.75, 9.375	Alluvial storage	Very sensitive
Depth to water table factor	-	1 - 3.2	Alluvial storage	Very sensitive

During the SPS (report No. PREP-1210-C-12057), the parameters Manning's n and Suction were tested as 'not sensitive' or 'slightly sensitive', hence they were excluded for the sensitivity analysis in the DPS.

The porosity fraction is a measure of the void space in a material. In the context of the 2D hydraulic modelling conducted during this project, it can be seen as the volume available for water storage within the soil.

Porosity was reduced from 0.2 (20%) to 0.1 (10%) and resulted in a small increase in how far and fast the wetting front travelled in the 2D model domain. Table 5-8 shows the difference between the timing of wetting front reaching the Jigalong Road for the different porosity values tested:

Table 5-8: Wetting front timing sensitivity to porosity

Downstream Location	Days to arrive (Porosity = 0.2)	Days to arrive (Porosity = 0.1)
Jigalong Rd	1,806	1,736

Evapotranspiration affects the predicted extent of the wetting front in the TUFLOW model. The steady state model (i.e., without alluvial storage) was used to test the sensitivity of the predicted wetting front distance to variations in evapotranspiration. Table 5-9 shows the steady state results with different adopted evapotranspiration values applied:

Table 5-9: Wetting front extent sensitivity to evapotranspiration

Evapotranspiration rate (mm/d)	Wetting Front Distance (km)
6.5	83
8.5	75
10.5	71

Hydraulic conductivity is a key parameter in determining the timing of the wetting front of any water release. Variations in the hydraulic conductivity affect the infiltration rate and therefore the time taken to fill the available alluvial storage. Halving the hydraulic conductivity from 18.75 to 9.375 mm/h resulted in a significant increase in how far and fast the wetting front travelled in the 2D model domain. This indicates the potential impact that could occur should there be a reduction in hydraulic conductivity due to the formation of precipitate. Table 5-10 shows the difference between the timing of wetting front reaching the downstream points of interest for the different values tested:

Table 5-10: Wetting front timing sensitivity to Hydraulic Conductivity

Downstream Location	Weeks to reach (Hydraulic Conductivity = 18.75)	Weeks to reach (Hydraulic Conductivity = 9.375)
Jigalong Rd	1,806	707

The TUFLOW model's sensitivity to groundwater depth was tested during the calibration process (see Section 4.3). The results indicate that there is a proportional relationship between the depth to groundwater and the time taken for the wetting front to reach the downstream locations of interest.

5.3.2 GoldSim model

Sensitivity of the interaction with adjacent formations was tested for hydraulic conductivity, adjacent head values and distance to the adjacent head. The hydraulic head was altered by orders of magnitude, the adjacent head was increased and decreased by 2 m and the distance to the adjacent head was halved and doubled. It is noted that for the reaches adjacent to existing pits, the distance and adjacent hydraulic heads were not changed. The greatest effect was associated with the hydraulic conductivity to the adjacent formations with commensurate changes in the calculated fluxes. Increased and decreased water table levels in the adjacent formations also affected the flow, with the greatest effects occurring where the initial water table was close to the surface. The distance to the adjacent head increased the flux with shorter distance and vice versa. However, the changes in lateral fluxes had very little influence on the amount of infiltration into the alluvium aquifer (< 1%) and thus little influence on the wetting front.

The sensitivity of the evapotranspiration extinction depth was also small, with an increase of 2 m to 6 m below ground level and a decrease to 2 m below ground level.

The halving of the extinction depth led to less simulated evapotranspiration and deeper extinction depths led to greater evapotranspiration, with the overall changes in each reach dependent on the provided slope away from the waterway. The overall changes were less than percentage changes in the extinction depth and had less than 3% effect on the overall infiltration rate, and thus again little influence on the extent of the wetting front.

6 LIMITATIONS

Infiltration of surface water into the soil is a one-way process in TUFLOW. Once the void space in the subsurface is filled with water there is no mechanism for additional infiltration or reduction of the groundwater table. This is particularly pertinent for the pulse scenarios. During the drying period the groundwater depth won't reduce to the level that it was at the start of the model run, and in the next wetting period no infiltration will occur in the previous wet area. As such, the entire volume of creek discharge water travelling over the "pre-wet" areas will continue down the creek as runoff, with infiltration only occurring in areas that the wetting front did not reach in the previous discharge pulse. This has been included in the modelling system within the GoldSim water balance. The losses from the alluvium were calculated within GoldSim and a revised evaporation rate provided for the next TUFLOW iteration which included any additional storage in the alluvium and alluvial losses. This adaption to the modelling method served to reduce the TUFLOW model's tendency to overpredict the wetting front progression in areas that had previously had the alluvial storage filled.

The GoldSim water balance modelling was limited in that it is based on average conditions in a reach. Although the modelling does include a representation of the extent of the wetting front within a reach and a component of lateral flow within a reach, it is assumed in the model that the water table remains flat within a reach. In reality the water table is likely to be mounded under the waterway due to the creek discharge with lower levels towards the lateral extents. Similarly, the evapotranspiration calculation for the reach is based on a constant slope from the creek bed to the edge of the alluvium, whereas it is likely to be consist of low flow and/or braided channels with banks and flood-plains for greater flows.

The GoldSim water balance modelling also assumed that the lateral groundwater flow from the alluvium to the surrounding formations was outward only (i.e., no groundwater inflow to the alluvium). It is also based on calculating losses in excess of any pre-existing losses based on the initial conditions in a reach.

The modelling storage capacity for infiltration is based on specified initial conditions. As found in the data provided for the calibration, large rainfall events can result in large rises in the water table levels within the alluvium that may substantially reduce the available storage. The modelling procedure is also based on average evaporation. Evaporation varies seasonally and as such the extent of creek discharge may vary with the prevailing climatic conditions.

7 REFERENCES

Advisian. (2020). Identification Phase Study WAIO Project – Central Pilbara Hub Surplus Water Identification Phase Study Report. PREP-1220-G-12164, 156pp.

Advisian. (2021). *Selection Phase Study WAIO Project Ore Body 32 Surplus Water Creek Discharge Modelling Report PREP-1210-C-12057.* Perth: BHP.

BHP. (2018). *Eastern Pilbara Water Resource Management Plan.* Perth, Australia: BHP.

BMT. (2021). *TUFLOW*. Retrieved from TUFLOW: https://www.tuflow.com/

Bureau of Meteorology. (2021, June 1). *Average annual & monthly evapotranspiration*. Retrieved from Bureau of Meteorology: http://www.bom.gov.au/jsp/ncc/climate_averages/evapotranspiration/index.jsp?maptype=6&period=an#maps

DMIRS. (2021, May 25). *DataWA*. Retrieved from Geological Series Maps: https://catalogue.data.wa.gov.au/org/department-of-mines-industry-regulation-and-safety

ESRI. (2021). World Imagery.

GoldSim Technology Group LLC. (2021). *GoldSim*. Retrieved from GoldSim: https://www.goldsim.com/Web/Products/GoldSim/Overview/

Green, W., & Ampt, G. (1911). Studies on Soil Physics. *The Journal of Agricultural Science*, 1-24.

Horton, R. E. (1933). The role of infiltration in the hydrologic cycle. *Transactions, American Geophysical Union, 14*(1), 446-460.

Rea, I. (2021). *Selection of Infiltration Rate for Fortescue River Discharge.* Perth: BHP.

APPENDIX A – CREEK DISCHARGE WETTING FRONT EXTENT MAPS

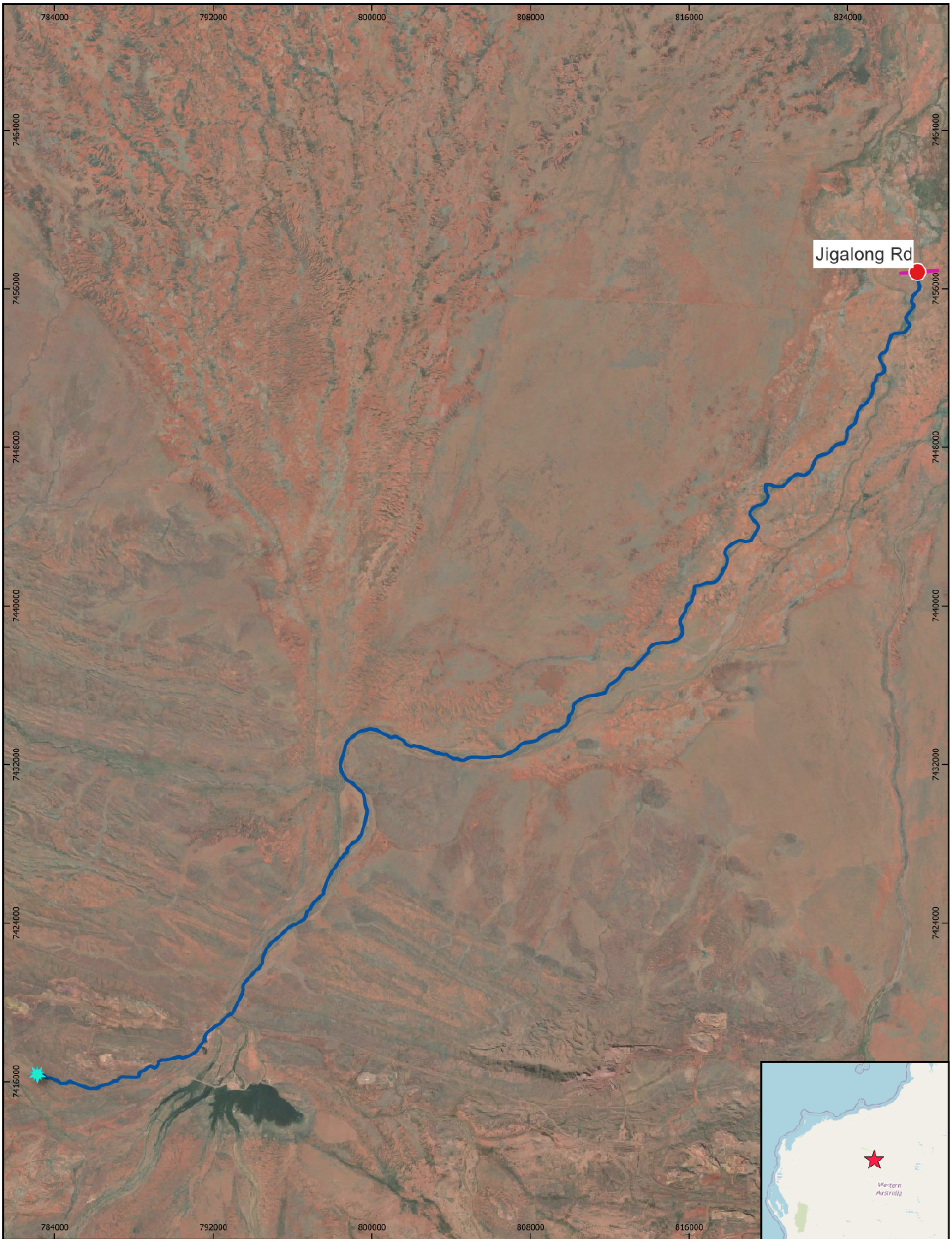

0 5 10 km

SCALE: 1 in 170,000 @ A3

OB32 Surplus Water Management Definition Phase Study

LEGEND

- Homestead Creek
- Jigalong Rd
- Expected Flow Path
- Wetting Front

Continuous 60 ML/d

PROJECTION	*GDA94 Zone 50*
REVISION	A
DATE	17/08/2022

N

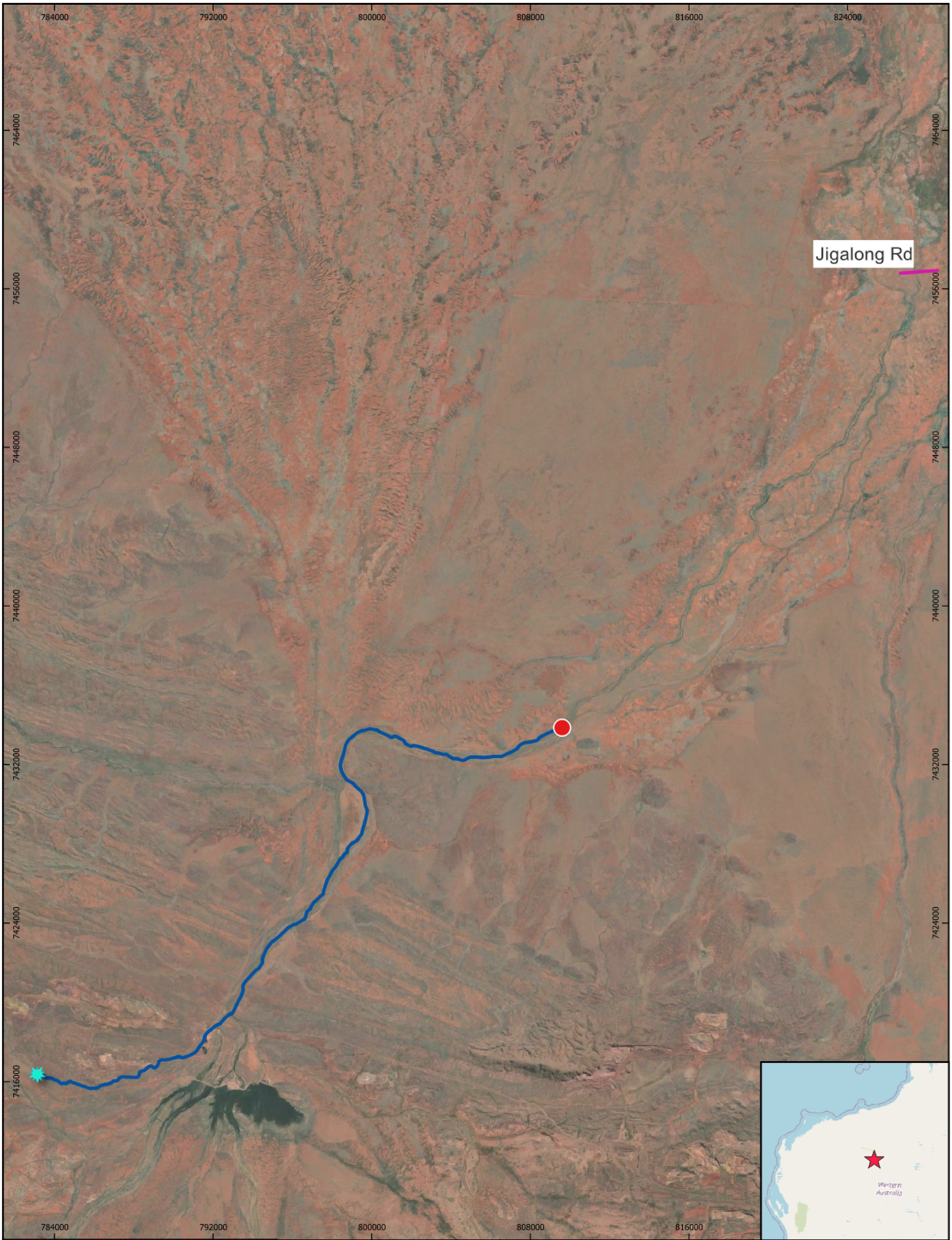

0 5 10 km

SCALE: 1 in 170,000 @ A3

LEGEND

- Homestead Creek
- Jigalong Rd
- Expected Flow Path
- Wetting Front

OB32 Surplus Water Management Definition Phase Study

Pulse 60 ML/d

PROJECTION	GDA94 Zone 50
REVISION	A
DATE	17/08/2022

N

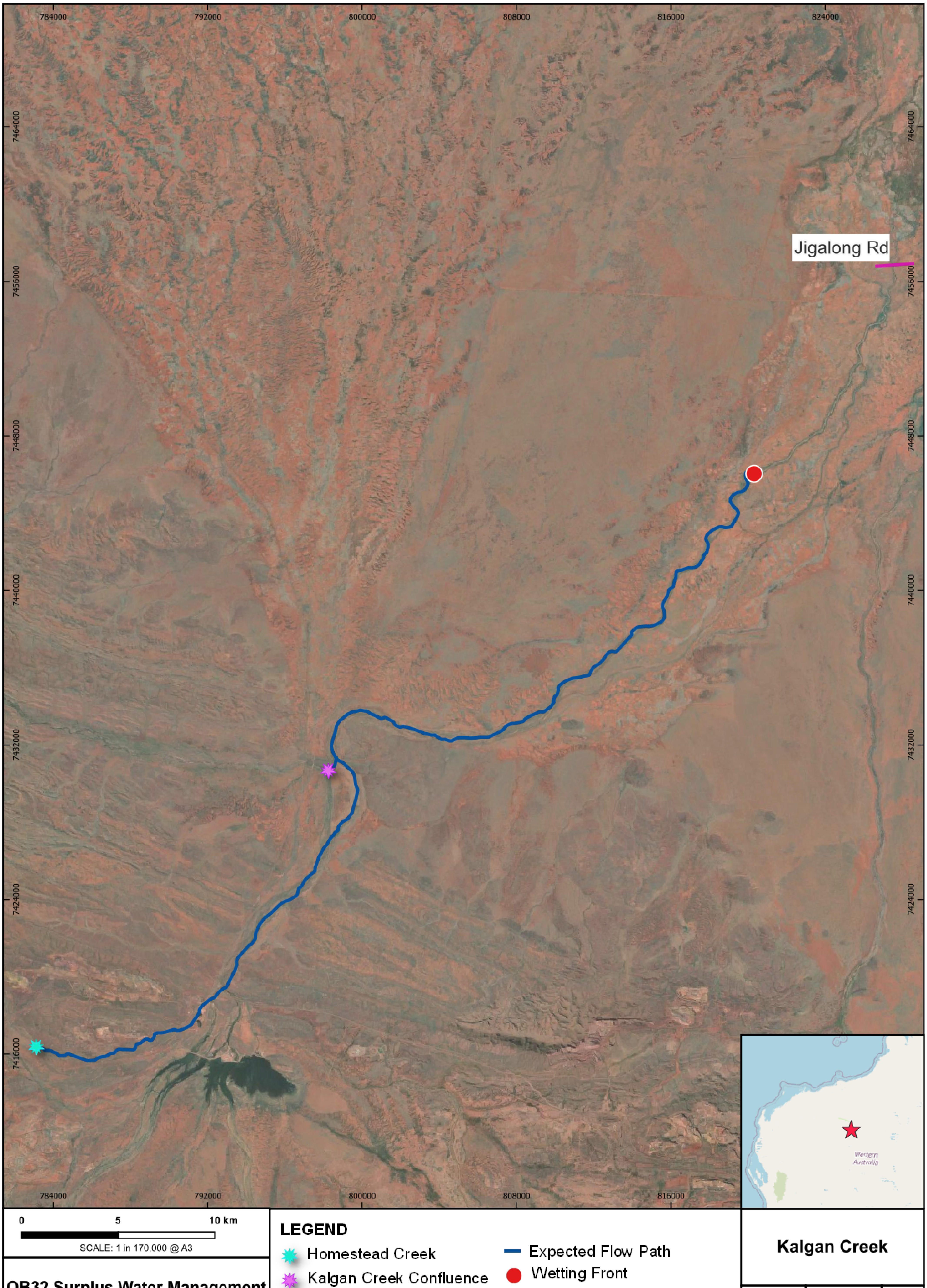

OB32 Surplus Water Management Definition Phase Study

Kalgan Creek

PROJECTION	GDA94 Zone 50
REVISION	A
DATE	17/08/2022

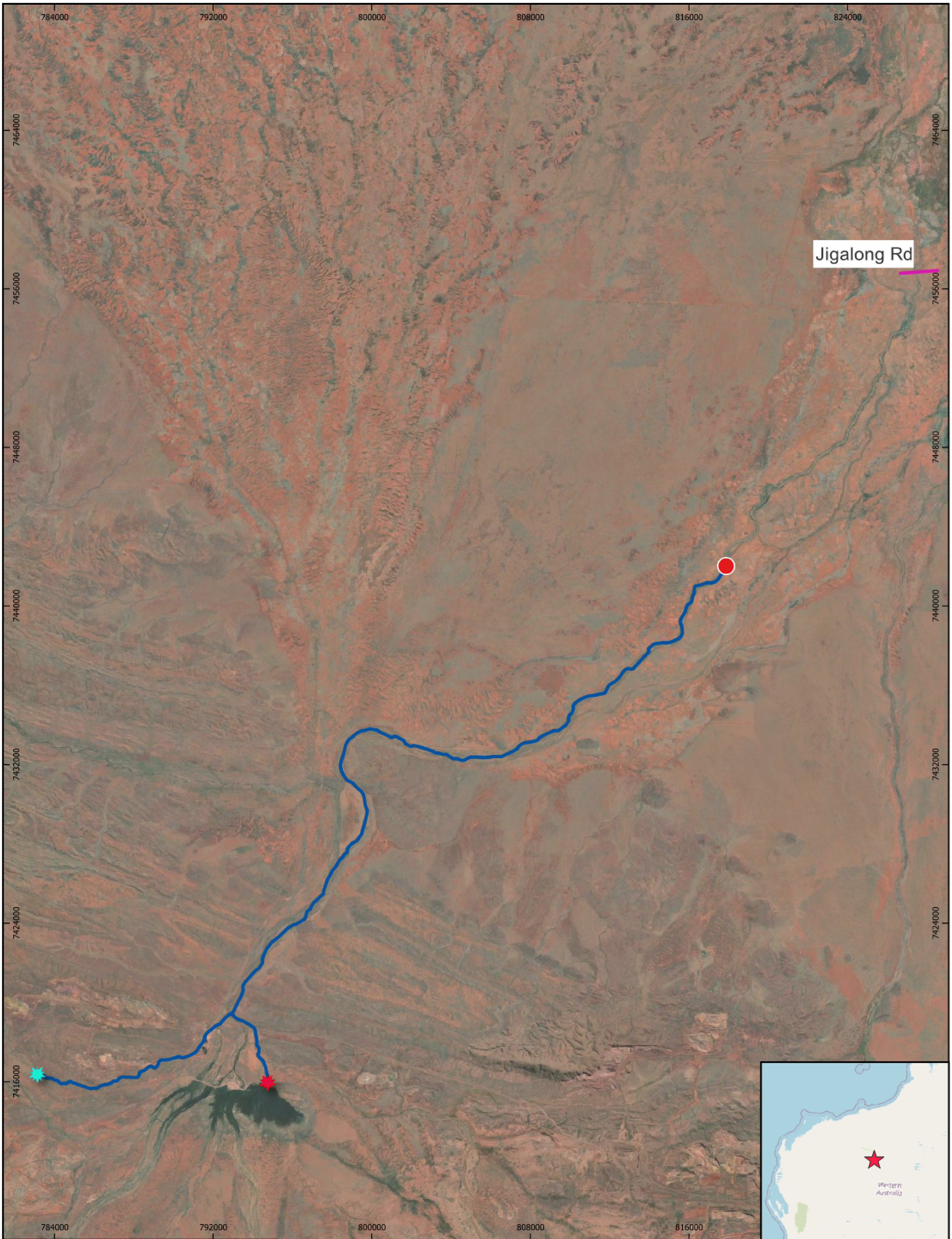

0 5 10 km

SCALE: 1 in 170,000 @ A3

OB32 Surplus Water Management Definition Phase Study

LEGEND

- Homestead Creek
- Oph Dam
- Jigalong Rd
- Expected Flow Path
- Wetting Front

Oph Dam Release 1

PROJECTION	GDA94 Zone 50
REVISION	A
DATE	17/08/2022

N

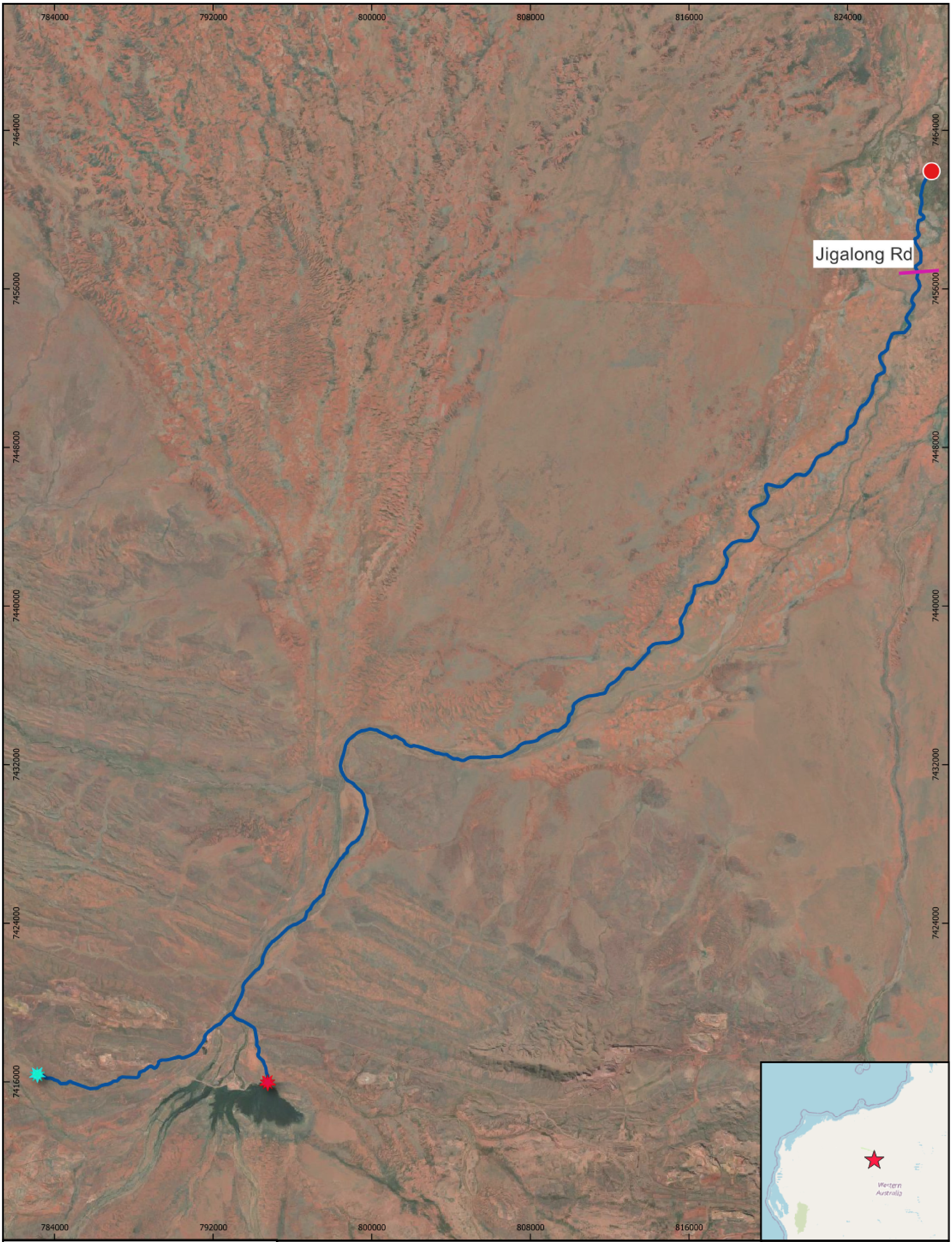

0 5 10 km

SCALE: 1 in 170,000 @ A3

OB32 Surplus Water Management Definition Phase Study

LEGEND

- Homestead Creek
- Oph Dam
- Jigalong Rd
- Expected Flow Path
- Wetting Front

Oph Dam Release 2

PROJECTION	GDA94 Zone 50
REVISION	A
DATE	17/08/2022

N

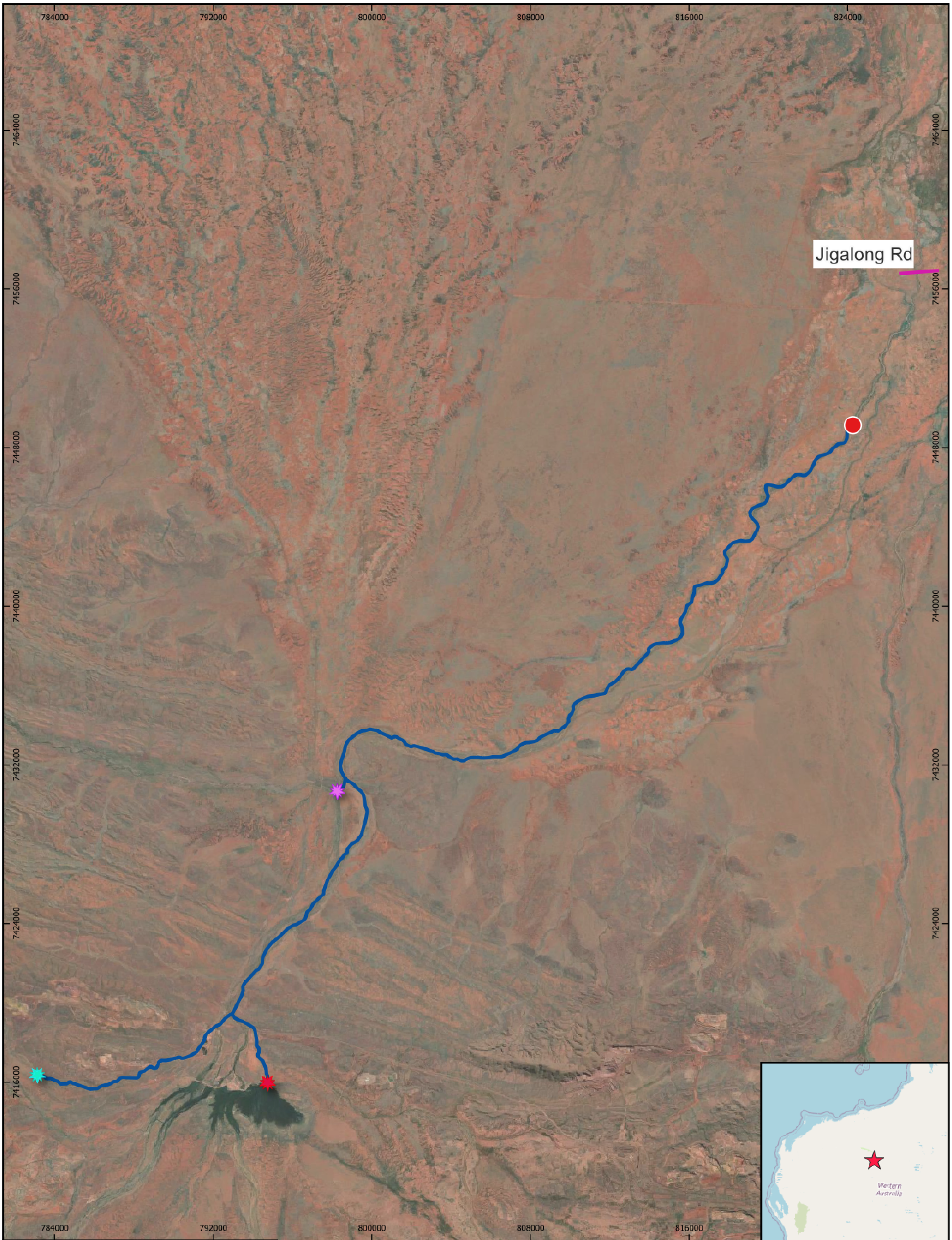

0 5 10 km

SCALE: 1 in 170,000 @ A3

OB32 Surplus Water Management Definition Phase Study

LEGEND

- Homestead Creek
- Kalgan Creek Confluence
- Oph Dam
- Jigalong Rd
- Expected Flow Path
- Wetting Front

Kalgan Creek + Oph Dam Release 1

PROJECTION	GDA94 Zone 50
REVISION	A
DATE	17/08/2022

N

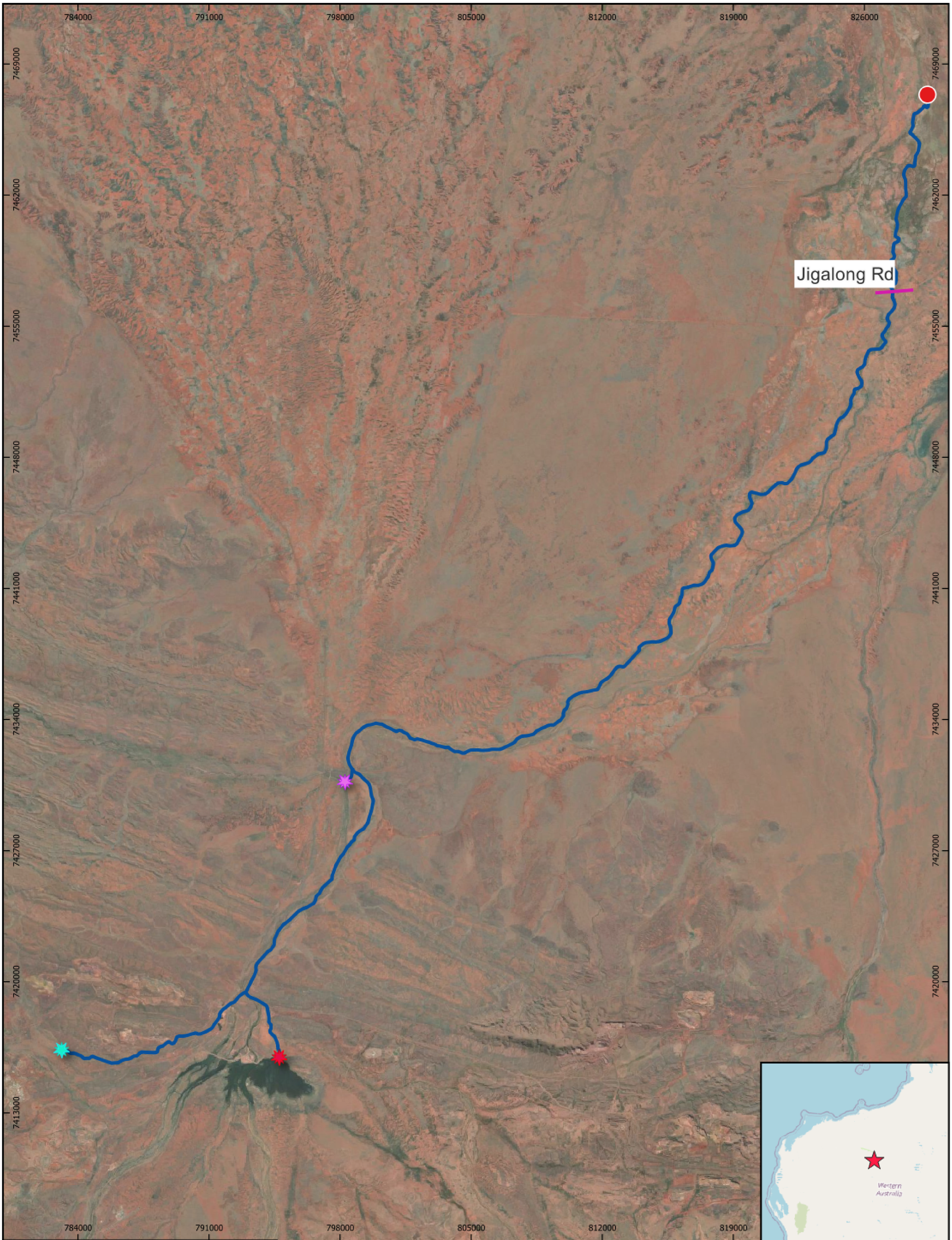

0 5 10 km

SCALE: 1 in 180,000 @ A3

OB32 Surplus Water Management Definition Phase Study

LEGEND

- Homestead Creek
- Kalgan Creek Confluence
- Oph Dam
- Jigalong Rd
- Expected Flow Path
- Wetting Front

Kalgan Creek + Oph Dam Release 2

PROJECTION	*GDA94 Zone 50*
REVISION	A
DATE	17/08/2022

N

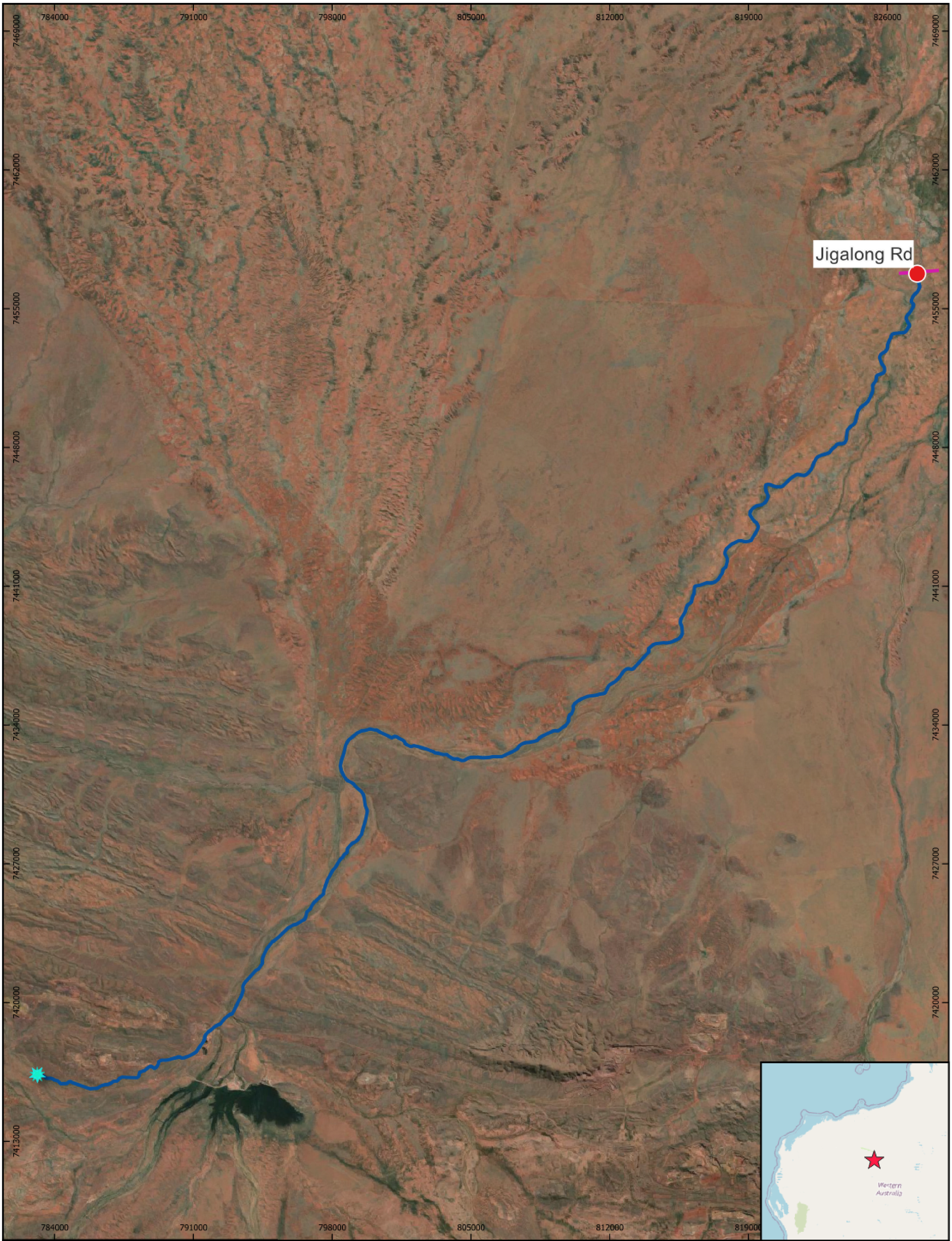

0 5 10 km

SCALE: 1 in 170,000 @ A3

LEGEND

- Homestead Creek
- Jigalong Rd
- Expected Flow Path
- Wetting Front

OB32 Surplus Water Management Definition Phase Study

Maximum Discharge rates 47.5 ML/d

PROJECTION	GDA94 Zone 50
REVISION	A
DATE	17/08/2022

N

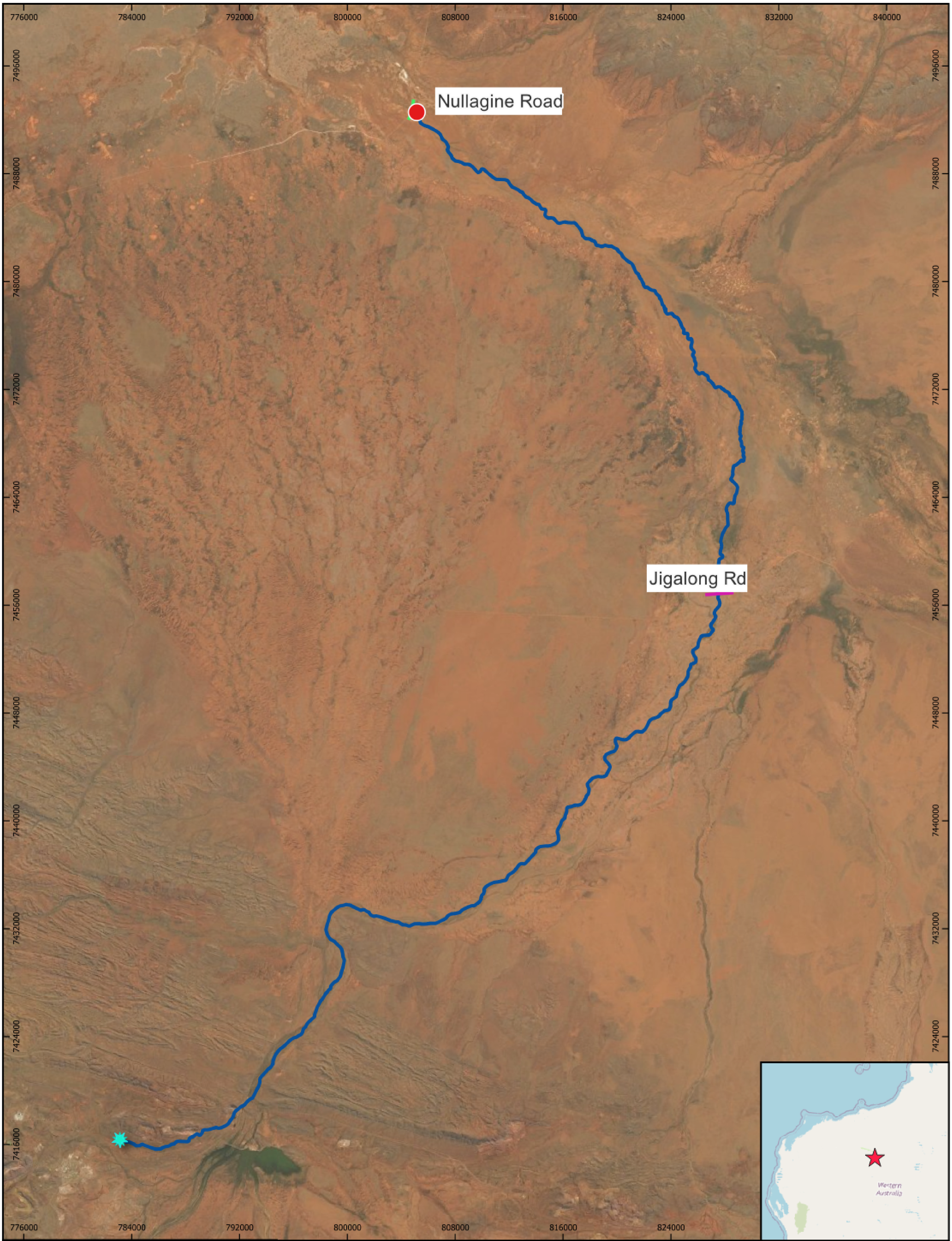

0 5 10 km

SCALE: 1 in 250,000 @ A3

OB32 Surplus Water Management Definition Phase Study

LEGEND

- Homestead Creek
- Jigalong Rd
- Nullagine Road
- Expected Flow Path
- Wetting Front

Maximum Discharge rates 82 ML/d

PROJECTION	*GDA94 Zone 50*
REVISION	A
DATE	17/08/2022

N

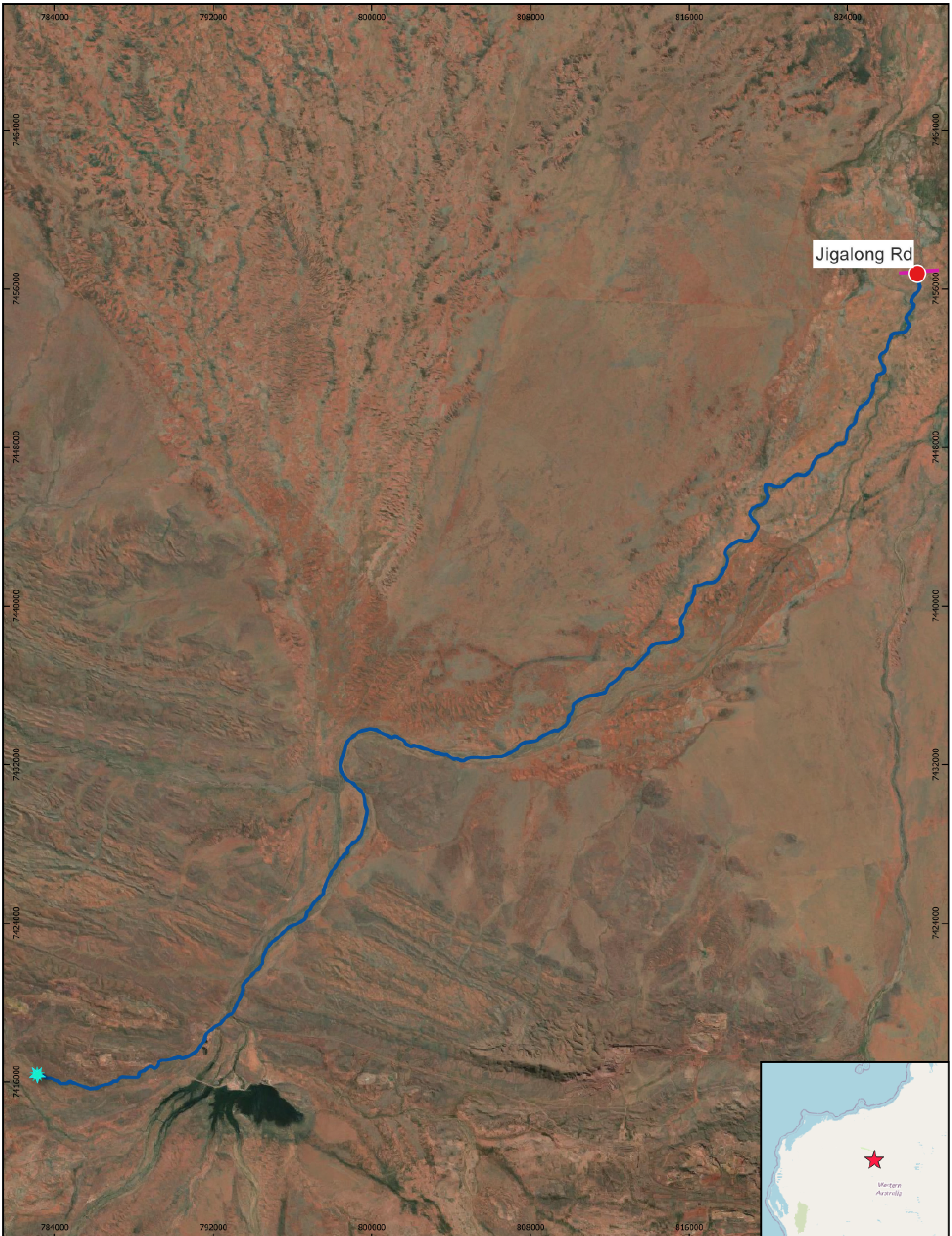

0 5 10 km

SCALE: 1 in 170,000 @ A3

OB32 Surplus Water Management Definition Phase Study

LEGEND

- Homestead Creek
- Jigalong Rd
- Expected Flow Path
- Wetting Front

Pulse Optimisation to Jigalong Road

PROJECTION	GDA94 Zone 50
REVISION	A
DATE	17/08/2022

N

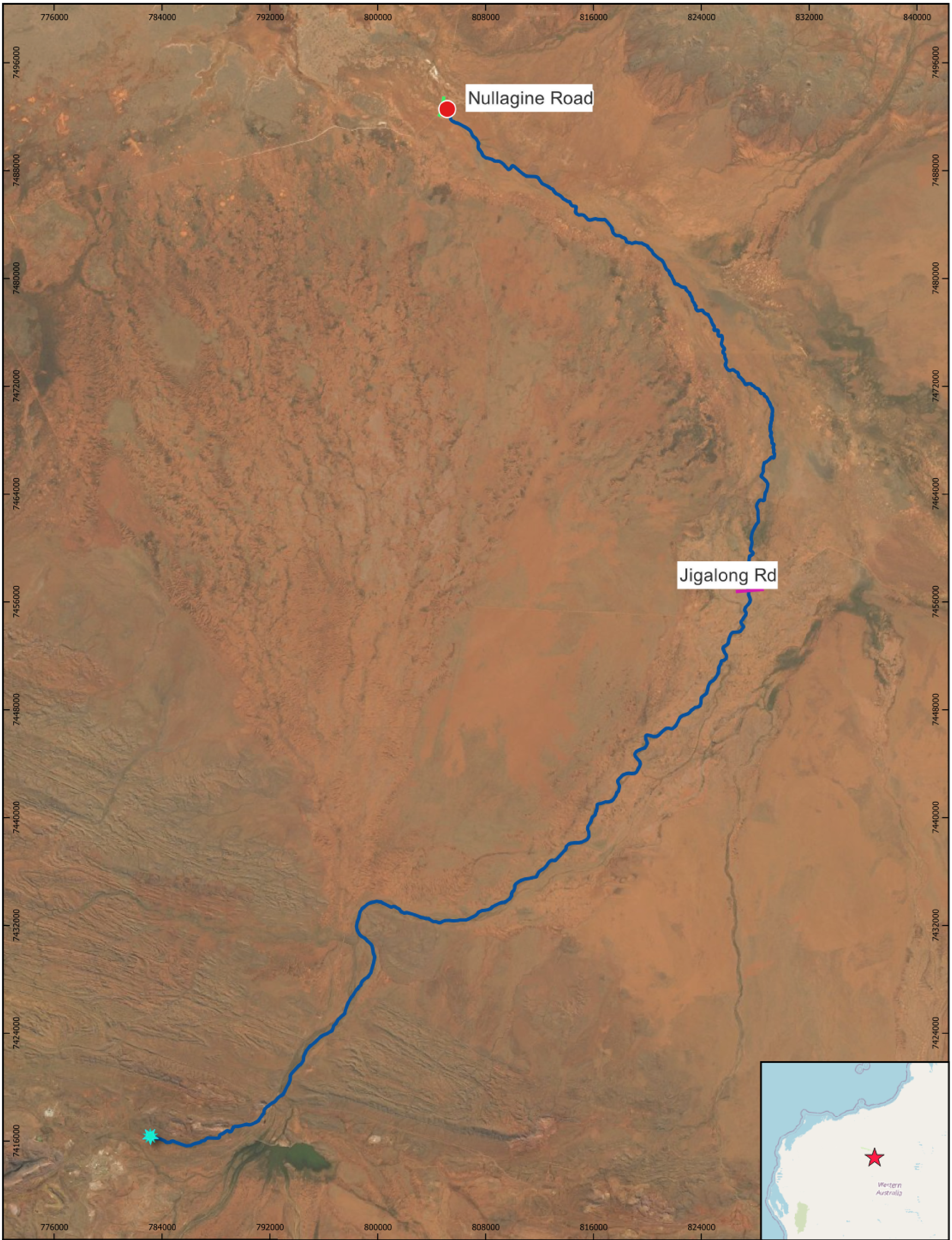

0 5 10 km

SCALE: 1 in 250,000 @ A3

OB32 Surplus Water Management Definition Phase Study

LEGEND

- Homestead Creek
- Jigalong Rd
- Nullagine Road
- Expected Flow Path
- Wetting Front

Pulse Optimisation to Nullagine Road

PROJECTION	GDA94 Zone 50
REVISION	A
DATE	17/08/2022

N